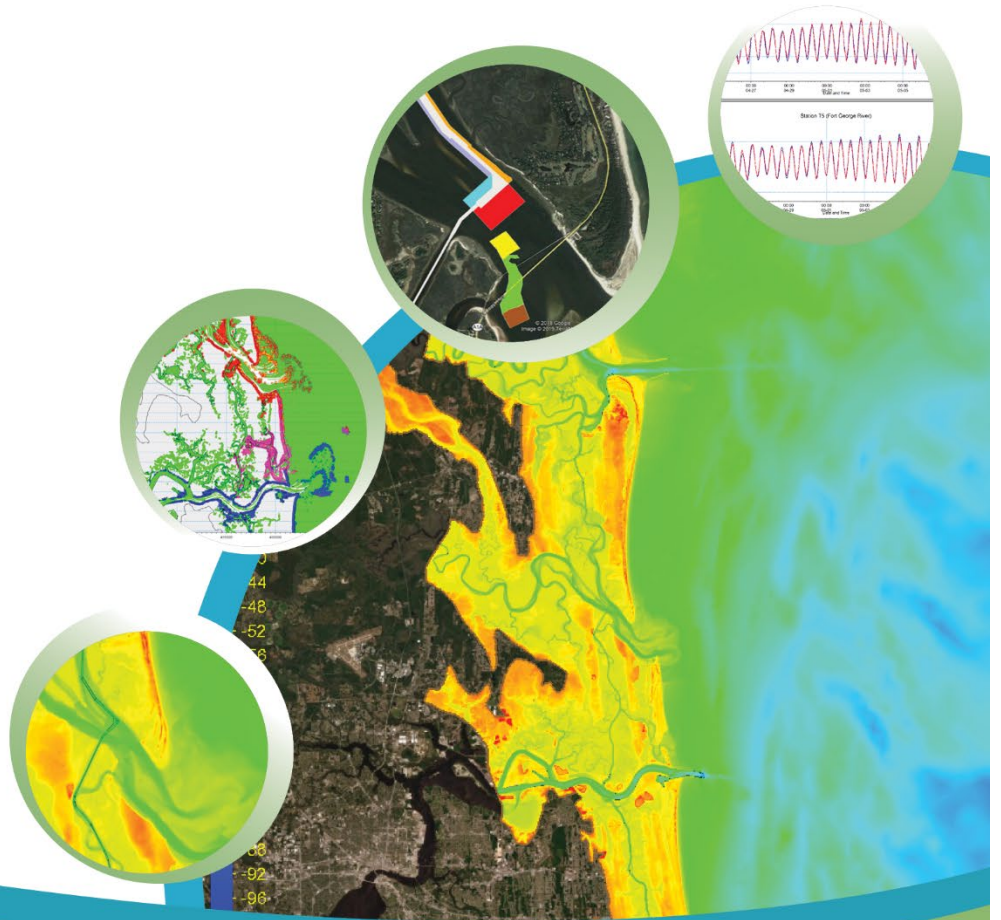




# Sawpit Creek Sediment Impoundment Basin Feasibility Study — Data Collection, Model Development, and Evaluation of Performance of Basin Alternatives



Sawpit Creek Sediment Basin Feasibility Study —  
Data Collection, Model Development, and  
Evaluation of Performance of Basin Alternatives  
Duval and Nassau Counties

Draft Report

Prepared for  
Florida Inland Navigation District

by

Taylor Engineering, Inc.  
10199 Southside Blvd., Ste 310  
Jacksonville, FL 32256  
(904) 731-7040

October 2019

C2019-009

## TABLE OF CONTENTS

<b>EXECUTIVE SUMMARY .....</b>	<b>vii</b>
<b>1.0 INTRODUCTION .....</b>	<b>1</b>
<b>2.0 DATA COLLECTON AND ANALYSIS .....</b>	<b>2</b>
2.1 Tide Data .....	2
2.1.1 NOAA Tide Data .....	2
2.1.2 Field Measurement of Inshore Tide Level.....	2
2.2 Wind Data .....	6
2.3 Wave Data.....	7
2.4 Flow Velocity Data .....	14
2.5 Bathymetric and Topographic Data .....	14
2.5.1 FEMA East Coast 2012 ADCIRC Model Mesh Data.....	14
2.5.2 AIWW and St. Johns River Bathymetry Update .....	14
2.5.3 Nassau Sound and Nassau River Bathymetry Update .....	14
2.5.4 Bathymetry Update Near Sawpit Creek.....	15
2.6 Sediment and Other Geotechnical Data .....	15
2.6.1 Sediment Grab Sampling.....	15
2.6.2 Sediment Characteristics .....	15
<b>3.0 MODEL DEVELOPMENT AND MODEL VALIDATION .....</b>	<b>23</b>
3.1 Hydrodynamic Model (HD) .....	23
3.1.1 Hydrodynamic Model Setup .....	23
3.1.2 Hydrodynamic Model Calibration .....	25
3.1.1 Hydrodynamic Model Verification .....	36
3.1.1 Hydrodynamic Model Parameter Sensitivity Analysis .....	37
3.2 Wave Model (SW) .....	46
3.2.1 Wave Model Setup.....	46
3.2.2 Wave Model Parameters .....	46
3.3 Sediment Transport Model (ST).....	46
3.4 Sediment Particle Tracking Model (PT).....	47
3.4.1 Empirical Estimation of Sediment Settling Velocity.....	47
3.4.2 Estimation of Critical Velocity for Sediment Erosion and Re-suspension.....	50

<b>4.0 EVALUATION OF PERFORMANCE OF SHOALING-REDUCTION DESIGNS .....</b>	<b>52</b>
4.1 Representative Hydraulic Condition .....	52
4.2 Sediment Sources, Transport Pathways, and Proposed Basins .....	53
4.2.1 Discarded Sediment Basin/Structures Alternatives .....	56
4.2.2 Proposed Basin Alternatives for In-Channel Shoaling Reduction .....	62
4.3 Shoaling Rates in Navigation Channel .....	64
4.4 Sediment Transport Model Parameter Sensitivity Analysis .....	64
4.5 Cost Comparison of Basin Alternatives .....	66
4.6 Hydraulic Impacts of Basin Alternatives .....	72
4.6.1 Peak Flow Velocities .....	72
4.6.2 Peak Wave Heights .....	74
<b>5.0 DREDGING, DESIGN, AND PERMITTING CONSIDERATIONS .....</b>	<b>83</b>
5.1 Dredging Method .....	83
5.2 Engineering Design and Submerged Aquatic Vegetation Survey Considerations .....	83
5.3 Permitting Considerations .....	84
5.3.1 Overview .....	84
5.3.2 Permit Application .....	84
5.3.3 Pre-Application Meetings .....	85
5.3.4 Responses to request for Additional Information (RAI) .....	85
5.4 Other Considerations .....	85
<b>6.0 CONCLUSIONS AND RECOMMENDATIONS .....</b>	<b>87</b>
6.1 Conclusions .....	87
6.2 Recommendations .....	88
<b>REFERENCES.....</b>	<b>89</b>
<b>APPENDIX A</b>	WIS Stations 63402 Monthly Hindcasted Wave Rose for 1980 – 2014
<b>APPENDIX B</b>	Measured Depth-Averaged Flow Velocity
<b>APPENDIX C</b>	Coordinates of Proposed Basins Bottom Corners

## LIST OF FIGURES

Figure ES.1	Locations of the AIWW Cuts, Sawpit Creek, and Nassau Sound .....	vii
Figure ES.2	Locations of Proposed Sediment Basins In-Channel Shoaling Reduction.....	x
Figure 2.1	Locations of Select NOAA Tide Stations and Wind Stations .....	3
Figure 2.2	Locations of the Tide Level and Velocity Measurement Stations.....	5
Figure 2.3	Measured Wind Speed and Direction in April 2019 .....	8
Figure 2.4	Measured Wind Speed and Direction in May 2019.....	9
Figure 2.5	Wind Roses at Fernandina Beach Municipal Airport, Jacksonville International Airport, and Mayport Pilot Station (April 1, 2019 – May 31, 2019) .....	10
Figure 2.6	Location of WIS Station 63402.....	11
Figure 2.7	Hindcasted Wave Rose at WIS Station 63402 for 1980 – 2017 (Source: U.S. Army Engineer Research and Development Center).....	12
Figure 2.8	WIS Station 63402 Wave Height Return Period (Source: U.S. Army Engineer Research and Development Center) .....	13
Figure 2.9	FEMA Northeast Florida-Georgia Version 12b ADCIRC Model Mesh .....	16
Figure 2.10	FEMA Northeast Florida-Georgia Version 12b ADCIRC Model Bed Elevation Points .....	17
Figure 2.11	Areas of Bathymetry Data Update in AIWW and St. Johns River .....	18
Figure 2.12	Areas of Arc Surveying & Mapping, Inc. June 22, 2018 Bathymetry Data Update in Nassau Sound and Nassau River .....	19
Figure 2.13	Areas of USACE-SAJ January – April 2019 Bathymetry Data Update in AIWW Cuts 24, 25, 26, 27, 27A, and 27C.....	20
Figure 2.14	Locations of Surface Sediment Sampling Stations.....	21
Figure 3.1	Model Domain and Bed Elevations.....	25
Figure 3.2	Comparison of Modeled and Measured Water Levels at Stations T3 and T5 (Calibration Period).....	29
Figure 3.3	Comparison of Modeled and Measured Water Levels at Stations T6 and NOAA 8720218 (Calibration Period) .....	30
Figure 3.4	Comparison of Modeled and Measured Velocity and Components at Station V1E (Calibration Period).....	31
Figure 3.5	Comparison of Modeled and Measured Velocity and Components at Station V2E (Calibration Period).....	32

Figure 3.6	Comparison of Modeled and Measured Velocity and Components at Station V2W (Calibration Period).....	33
Figure 3.7	Comparison of Modeled and Measured Velocity and Components at Station V3E (Calibration Period).....	34
Figure 3.8	Comparison of Modeled and Measured Velocity and Components at Station V3W (Calibration Period).....	35
Figure 3.9	Comparison of Modeled and Measured Water Levels at Stations T3 and T5 (Verification Period).....	38
Figure 3.10	Comparison of Modeled and Measured Water Levels at Stations T6 and NOAA 8720218 (Verification Period).....	39
Figure 3.11	Comparison of Modeled and Measured Velocity and Components at Station V1E (Verification Period).....	40
Figure 3.12	Comparison of Modeled and Measured Velocity and Components at Station V1W (Verification Period).....	41
Figure 3.13	Comparison of Modeled and Measured Velocity and Components at Station V2E (Verification Period).....	42
Figure 3.14	Comparison of Modeled and Measured Velocity and Components at Station V2W (Verification Period).....	43
Figure 3.15	Comparison of Modeled and Measured Velocity and Components at Station V3E (Verification Period).....	44
Figure 3.16	Comparison of Modeled and Measured Velocity and Components at Station V3W (Verification Period).....	45
Figure 3.17	Settling Velocity Diagram for $1 < Re < 2000$ .....	49
Figure 3.18	Shield's Diagram .....	51
Figure 4.1	Locations of Profiles for Littoral Gross Transport Calculation .....	54
Figure 4.2	Monthly Gross Longshore Transport for the Year with Average Annual Gross Transport .....	55
Figure 4.3	Particle Track and Deposition from Various Sediment Sources in Nassau County, FL and Camden County, GA.....	57
Figure 4.4	Particle Track and Deposition from Various Sediment Sources in Nassau and Duval Counties, FL .....	58

Figure 4.5	Sediment Basin near Cut-27F to Cut-27J (not recommended due to locally-limited effect) .....	59
Figure 4.6	Locations of Sediment Basin, Groynes, and Reef near Sawpit Creek (Structures not recommended due to substantially increased shoaling in Cut-27) .....	60
Figure 4.7	Location of Sediment Basin near Cut-11 (not recommended due to rapid basin shoaling and poor in-channel reduction performance) .....	61
Figure 4.8	Locations of Proposed Sediment Basins to Reduce In-Channel Shoaling .....	63
Figure 4.9	Modeled Baseline Peak Flood Velocity .....	75
Figure 4.10	Modeled Baseline Peak Ebb Velocity .....	75
Figure 4.11	Difference in Modeled Alternative A and Baseline Peak Flood Velocities .....	76
Figure 4.12	Difference in Modeled Alternative A and Baseline Peak Ebb Velocities .....	76
Figure 4.13	Difference in Modeled Alternative B and Baseline Peak Flood Velocities .....	77
Figure 4.14	Difference in Modeled Alternative B and Baseline Peak Ebb Velocities .....	77
Figure 4.15	Difference in Modeled Alternative C and Baseline Peak Flood Velocities .....	78
Figure 4.16	Difference in Modeled Alternative C and Baseline Peak Ebb Velocities .....	78
Figure 4.17	Difference in Modeled Alternative D and Baseline Peak Flood Velocities .....	79
Figure 4.18	Difference in Modeled Alternative D and Baseline Peak Ebb Velocities .....	79
Figure 4.19	Difference in Modeled Alternative E and Baseline Peak Flood Velocities .....	80
Figure 4.20	Difference in Modeled Alternative E and Baseline Peak Ebb Velocities .....	80
Figure 4.21	Difference in Modeled Alternative F and Baseline Peak Flood Velocities .....	81
Figure 4.22	Difference in Modeled Alternative F and Baseline Peak Ebb Velocities .....	81
Figure 4.23	Baseline Modeled Peak Wave Heights and Directions .....	82

## LIST OF TABLES

Table ES.1	Combinations of Basins in Proposed Alternatives .....	x
Table ES.2	Estimated Equivalent Uniform Annual Cost for Baseline and Alternatives .....	xi
Table ES.3	Ranking of Alternatives for In-Channel Shoaling Reduction .....	xii
Table 2.1	NOAA Tide Datums and Locations of Select Stations near the Area of Interest (1983 – 2001 Tidal Epoch) .....	4
Table 2.2	Coordinates, Period of Record, and Time Interval of Measured Tide Level and Velocity Stations .....	6
Table 2.3	WIS Station 63402 Hindcasted Wave Height and Return Period (1980 – 2017) (Source: U.S. Army Engineer Research and Development Center) .....	13
Table 2.4	Properties of Sediment Samples at Project Area.....	22
Table 3.1	Mean Error, RMSE, and Correlation Coefficients for Water Levels for Various Manning’s n Values at Select Stations during Hydrodynamic Model Calibration .....	27
Table 3.2	Mean Error, RMSE, and Correlation Coefficients for Water Levels for Various Manning’s n Values at Select Stations during Hydrodynamic Model Verification .....	37
Table 4.1	Proposed Basins Characteristics .....	63
Table 4.2	Basins in Proposed Alternatives.....	63
Table 4.3	Modeled Shoaling Rates as a Percentage of Baseline Shoaling Rates ( $D_{50} = 0.16$ mm, Grading Coefficient = 2.5).....	65
Table 4.4	Modeled Shoaling Rates as a Percentage of Baseline Shoaling Rates ( $D_{50} = 0.20$ mm, Grading Coefficient = 1.5).....	66
Table 4.5	Summary of Historical Maintenance Dredging in Sawpit Creek Area (2006 – 2018) <i>Source: USACE-SAJ</i> .....	67
Table 4.6	Summary of Offers for 2018 Dredging of Sawpit Creek Area <i>Source: USACE-SAJ</i> .....	67
Table 4.7	Other Costs Associated with Dredging Projects .....	67
Table 4.8	Details of Equivalent Uniform Annual Cost Estimates.....	70
Table 6.1	Summary of Ranking of Alternatives for In-Channel Shoaling Reduction .....	88

## EXECUTIVE SUMMARY

The Atlantic Intracoastal Waterway (AIWW) near Sawpit Creek lies 2.5 mi northwest of the intensely-morphologically active Nassau Sound ebb shoal. At Nassau Sound, wave- and tide-generated currents entrain and transport river and littoral sediments westward. These currents move sediments until flow velocities decrease below a critical value, at which point sediments fall out of suspension and form shoals in Cuts 24 – 27A in Duval County and Cuts 27A – Cut 27N in Nassau County (see Figure ES.1). Among these cuts, Cut-27A often experiences the largest shoaling as it lies nearest to Nassau Sound and lies across Nassau River and thereby in the direct path of large sediment transport from the Nassau Sound ebb shoal. Historically, the U.S. Army Corps of Engineers Jacksonville District (USACE-SAJ) conducts maintenance dredging at Cut-27A on average once every six years to maintain the authorized AIWW navigation depth of -12 ft-MLLW. These maintenance dredging events often include an over dredge of 2 ft and can extend to the other cuts (e.g., Cut-24 to Cut-27N) to remove smaller amounts of shoaling. Past dredging events in 2006, 2013, and 2018 yielded dredge volumes of 429,163 cy, 519,556 cy, and 599,785 cy each at a total cost of \$4.058, \$3.992, \$5.329 million, respectively.

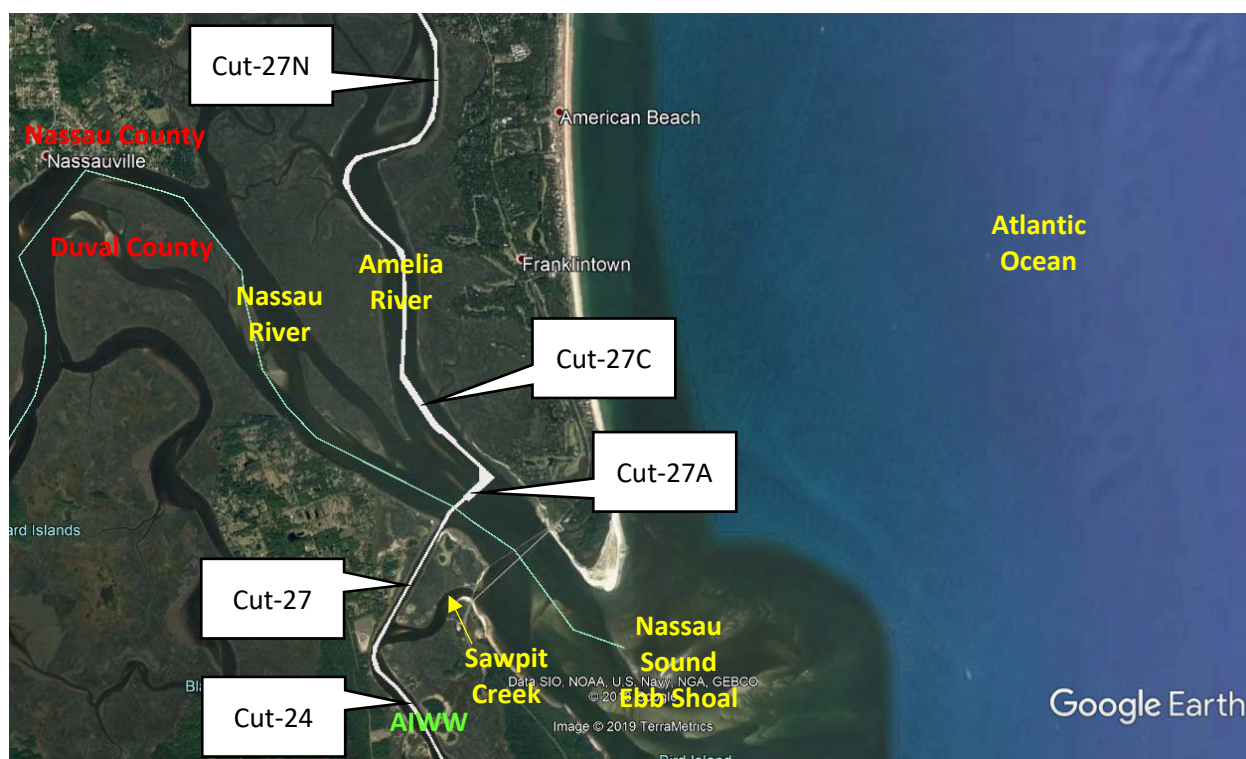


**Figure ES.1** Locations of the AIWW Cuts, Sawpit Creek, and Nassau Sound

Experience at several Florida inlets and waterways shows a deposition (impoundment) basin, by providing an area of deep water, can effectively decrease flow velocities and cause sediments to settle in a designated area. An effective deposition basin on or near a waterway can capture sediments, reduce sediment deposition in navigable waterways, reduce maintenance dredging requirements within navigation channels, and serve as a sand source for inlet sand bypassing operations. At Sawpit Creek and/or nearby waterways, construction of deposition basins and/or removal of nearby shoal sediment sources could, with periodic dredging, provide these benefits. The prospect of this cost-saving outcome encouraged the Florida Inland Navigation District (FIND) to request Taylor Engineering perform a

sediment deposition basin study in the Sawpit Creek area. The FIND requested Taylor Engineering provide a feasibility study to evaluate up to three sediment impoundment basin design alternatives in or near Sawpit Creek to increase the interval period between AIWW maintenance dredging.

To analyze the effect of sediment basins, this study developed a two-dimensional depth-averaged MIKE21 FM hydrodynamic model mesh using available mesh and elevation data from the 2013 FEMA Northeast Florida-Georgia Version 12b ADCIRC model mesh. Various recent bathymetric surveys of the AIWW and St. Johns River including Arc Surveying & Mapping, Inc. June 22, 2018 survey of Nassau Sound and Nassau River; and the USACE-SAJ January – April 2019 bathymetric survey along AIWW Cuts 24, 25, 26, 27, 27A, and 27C provided updated bed elevation information to the model mesh. The MIKE21 FM hydrodynamic model mesh extends approximately from Fort George Inlet to approximately 21.1 miles (mi) east (offshore boundary), 29.6 mi north (ocean north boundary), and 16.6 mi south (ocean south boundary); and includes more than 50 mi of the AIWW from south of Satilla River to the Atlantic Blvd. Bridge (in Jacksonville), 14.5 mi of St. Marys River, 20.8 mi of Nassau River, 4.6 mi of Fort George River, and 10.6 mi of St. Johns River. At the area of interest—at Sawpit Creek, AIWW, and nearby waterways—small elements provided the means to evaluate in more detail the hydraulic sediment transport conditions. The wave model, sediment transport, and sediment particle tracking models use the same model mesh as the hydrodynamic model.

Hydrodynamic (HD) model validation consisted of comparisons of modeled water level and flow velocity at select locations in the project area during model calibration and verification. Specifically, measured water levels in April – May 2019 at Stations T3 (Nassau Sound), T5 (Fort George River), T6 (near St. Marys River entrance), and NOAA-measured water level at Mayport Bar Pilot Dock (NOAA 8720218); and measured flow velocities in the AIWW at Stations W1E, W1V, W2E, W2W, W3E, and W3W provided the HD model validation data. This study used visual inspection and statistical parameters (mean error, root mean square error, and correlation coefficient) to compare modeled and measured water levels and visual inspection to compare modeled and measured flow velocities at select locations. Given the generally good visual comparisons and favorable statistics, this study considered the hydrodynamic model's water level and flow velocity calculation well validated to transport sediment from nearby inshore and nearshore areas to Sawpit Creek and the AIWW.

In lieu of model calibration, this study applied wave model parameters recommended from literature. This study also developed a two-dimensional sediment transport model that can estimate total sediment transport from bed load and suspended sediment transport. This study applied a morphological model with the sediment transport model to estimate shoaling rates (deposition and erosion) in channels and proposed basins. Comparisons of inshore morphological model results with observed historical sedimentation patterns shows the modeled sedimentation patterns are consistent with observed historical sedimentation patterns. These sedimentation patterns include (a) large deposition along Fort George River; (b) large sediment transport from the Nassau Sound ebb shoal through Nassau River, Amelia River, and the AIWW; (c) AIWW shoaling between Cut-24 to Cut-27M; and (d) very large shoaling rates at Cut-27A and Cut-27C. The general good agreement between modeled and observed sedimentation patterns at inshore and nearshore locations makes the sediment transport and morphological model validated to transport sediment from nearby inshore areas to the areas of interest in Sawpit Creek and the AIWW.

This study also developed a two-dimensional depth-averaged particle tracking model that can simulate the fate of the dredged material sediment plume; and simulate the transport, erosion, and deposition of multi-class sediments from stationary or moving sources and sinks to identify potential

sources of sediment erosion and locations of deposition. The particle tracking model requires as model input sediment properties including sediment settling rate, critical shear stress for erosion, and mass rate of dredged material release into the water column (for analysis of fate of dredged material plume). As these data from past dredging events at Sawpit Creek area are not presently available, in lieu of particle tracking model validation, this study used established data and equations in literature to estimate the required particle tracking model input data that includes sediment properties, settling rate, and critical shear stress for erosion. The particle tracking model provides the means to locate sediment transport pathways, deposition areas, and proposed in-channel shoaling reduction sediment basins.

In general, given that (1) the hydrodynamic model is calibrated and verified to provide good estimates of hydraulics in the inshore, inlet, and nearshore areas; (2) the wave model provided wave heights, periods, and direction that can generate longshore transport; (3) the sediment transport was validated to provide good estimates of sediment transport patterns in the area of interest; and (4) the particle tracking model applies established data and equations in literature for model input, this study considers the hydrodynamic, wave, sediment transport, and particle tracking models validated for evaluating the tide and wave hydraulics; and sediment transport in Sawpit Creek area and AIWW to nearby inshore areas. The results from these models provided input hydraulic information to the sediment transport and particle tracking models to allow evaluation of the sediment trapping performance of basins in near the AIWW and nearby inshore areas.

To evaluate the performance of various combinations of basins in trapping sediments and reducing in-channel shoaling, this study evaluated and compared with the Baseline (no basins) conditions the shoaling volumes calculated for basin Alternatives A – F using the hydraulic conditions of the representative month. Table ES.1 lists the basins included in each alternative and Figure ES.2 shows the locations of each basin.

Comparisons of the model simulations for Baseline and the Alternatives A – F provide longer dredging intervals of 9 years (Alternative A), 11 years (Alternative B), 9 years (Alternative C), 10 years (Alternative D), 10 years (Alternative E), and 9 years (Alternative F). This study evaluated the Baseline and Alternatives A – F equivalent uniform annual cost using a project life of 45 – 55 years (i.e., multiples of dredging intervals); the new federal annual interest rate of 2.750% for 2020; and an assumption that the next dredging event occurs in 2024. Table ES.2 provides the details of the cost analysis. Compared to the Baseline maintenance dredging annual cost (i.e., the current annualized dredging cost), the cost analysis ranks Alternative A first for offering the largest savings of \$788,000/year; Alternative F second for offering savings of \$720,000/year; Alternative C third for offering savings of \$569,000/year; Alternative D fourth for offering savings of \$491,000/year; Alternative B fifth for offering savings of \$294,000/year; and Alternative E sixth for offering small savings of \$14,000/year. This study does not recommend Alternative E for further consideration because it provides only a small estimated annual savings which is well within uncertainties in dredge volume calculations and dredge maintenance cost estimation. Model results show Alternative A would likely have the least hydraulic impact; Alternative F will likely have the second least hydraulic impact; Alternative C will likely have the third least hydraulic impact; and Alternative D will likely have the fourth least hydraulic impact. Alternatives B and E can divert more flood flows from the north tidal channel to the south tidal channel and will likely impact larger areas. Model results show Alternative B will likely have the fifth least hydraulic impact and Alternative E will likely have the largest hydraulic impact among the alternatives. However, for all alternatives, velocity differences from Baseline conditions are too small to affect navigation safety and too small to increase shoreline erosion. Table ES.3 summarizes the rankings of Alternative A – F based on their performance to reduce in-channel shoaling, cost savings, and extent of hydraulic impact.

**Table ES.1** Combinations of Basins in Proposed Alternatives

Alternatives	Included Basin						
	1	2	3	4	5	6	7
Baseline (no basins)							
Alternative A				X	X		
Alternative B	X	X	X	X	X		
Alternative C	X		X	X	X		
Alternative D	X		X	X	X	X	X
Alternative E	X	X	X	X	X	X	X
Alternative F				X	X	X	



**Figure ES.2** Locations of Proposed Sediment Basins In-Channel Shoaling Reduction

Based on the overall ranking, this study recommends proceeding with the permitting, engineering, and design of Basin 4, 5, and 6 of Alternative F. Design of Basins 4, 5, and 6 should include finding more efficient in-channel shoaling-reduction performance through adjustments of basin sizes. The engineering design for the final channel and basin modifications should also evaluate long-term (e.g., year-long) shoaling rate variation for better estimation of the variation of the sediment trapping performance of channels and basins and to better account for more potential variations of waves and water levels. The engineering design should also account for the construction of future borrow areas on the Nassau Sound ebb shoal that maybe constructed to provide beach material for the Amelia Island southern shoreline beach nourishment. Future bathymetric surveys should include the areas of Basins 4, 5, and 6 to establish baseline shoaling rates at these locations.

**Table ES.2** Estimated Equivalent Uniform Annual Cost for Baseline and Alternatives

	<b>Parameter</b>	<b>Baseline</b>	<b>Alt. A</b>	<b>Alt. B</b>	<b>Alt. C</b>	<b>Alt. D</b>	<b>Alt. E</b>	<b>Alt. F</b>
<b>A.</b>	Dredging Frequency (years)	6	9	11	9	10	10	9
<b>B.</b>	Project Life (years)	48	45	55	45	50	50	45
<b>C.</b>	Number of Dredging Events	8	5	5	5	5	5	5
<b>D.</b>	Quantity (cubic yards per event)	516,168	566,728	874,536	660,248	740,463	954,751	595,868
<b>E.</b>	Total Yardage (cubic yards)	4,129,344	2,833,640	4,372,680	3,301,240	3,702,315	4,773,755	3,575,208
<b>F.</b>	Yardage Cost (Per Dredging Event)	\$5,399,876	\$5,928,808	\$9,148,933	\$6,907,165	\$7,746,332	\$9,988,100	\$6,233,656
<b>G.</b>	Mobilization/Demobilization Cost	\$2,032,279	\$2,032,279	\$2,032,279	\$2,032,279	\$2,032,279	\$2,032,279	\$2,032,279
<b>H.</b>	Total Dredging Cost (F+G)	\$7,432,155	\$7,961,087	\$11,181,212	\$8,939,444	\$9,778,611	\$12,020,379	\$8,265,935
<b>I.</b>	Permitting Cost (initial \$50,000 and \$15,000 at every dredging event)	n/a	\$15,000	\$15,000	\$15,000	\$15,000	\$15,000	\$15,000
<b>J.</b>	Environmental Study Cost (initial \$20,000 and \$5,000 per acre at every dredging event)	\$0	\$0	\$0	\$0	\$0	\$0	\$0
<b>K.</b>	E&D Cost (initial \$110,000 and 5% of Total Dredging Cost at every dredging event)	\$371,608	\$398,054	\$559,061	\$446,972	\$488,931	\$601,019	\$413,297
<b>L.</b>	Construction Administration Cost (10% of Total Dredging Cost)	\$743,216	\$796,109	\$1,118,121	\$893,944	\$977,861	\$1,202,038	\$826,593
<b>M.</b>	Total Cost (H + I + J + K + L)	\$8,546,979	\$9,170,250	\$12,873,393	\$10,295,361	\$11,260,403	\$13,838,435	\$9,520,825
<b>N.</b>	Total Cost (Rounded to Nearest Thousand)	\$8,547,000	\$9,170,000	\$12,873,000	\$10,295,000	\$11,260,000	\$13,838,000	\$9,521,000
<b>O.</b>	Equivalent Uniform Annual Cost	\$2,583,000	\$1,795,000	\$2,289,000	\$2,014,000	\$2,092,000	\$2,569,000	\$1,863,000
<b>P.</b>	<b>Annual Savings</b>	<b>n/a</b>	<b>\$788,000</b>	<b>\$294,000</b>	<b>\$569,000</b>	<b>\$491,000</b>	<b>\$14,000</b>	<b>\$720,000</b>

Notes:

1. The estimated materials and unit costs represent Taylor Engineering's best judgment as a professional design firm familiar with the

type of construction proposed. Taylor Engineering has no control over the availability or cost of labor, equipment or materials, market conditions, or the contractor’s methods of pricing. Accordingly, Taylor Engineering makes no warranty, express or implied, that the actual bids or negotiated prices will not vary from the cost shown in the table.

2. All quantities estimated as in-place approximate quantities.
3. Construction cost may change due to fluctuations in the prices of materials and petroleum.
4. This project does not anticipate encountering hazardous materials nor require special handling.
5. Equivalent uniform annual cost represents total of initial and annual maintenance costs and associated dredging costs. Cost estimation assumes a 45- to 55-year project life and an interest rate of 2.750%.
6. Total dredging cost includes typical Sawpit Creek area and proposed basin shoal dredging maintenance costs.
7. Maintenance dredging occurs when Cut-27A shoals to bed elevations at or shallower than authorized project depth.

**Table ES.3** Ranking of Alternatives for In-Channel Shoaling Reduction

Alternatives	Basis for Ranking			Overall Ranking
	Performance	Cost Savings	Hydraulic Impact	
Alternative F	3	2	2	1
Alternative A	4	1	1	2
Alternative D	1	4	4	3
Alternative C	5	3	3	4
Alternative B	6	5	5	5
Alternative E	2	6	6	6

## 1.0 INTRODUCTION

Navigation channels, especially those located near tidal inlets and rivers, require maintenance dredging to remove shoals that impede navigation. In the case of Nassau Sound, flood currents can entrain and transport river and littoral sediments along Nassau River and cause shoaling in Nassau River, Amelia River, Sawpit Creek, and the AIWW. These currents move sediments until flow velocities decrease below a critical value, at which point sediments fall out of suspension onto the waterway bed and form shoals.

Experience at several Florida inlets and waterways shows a deposition (impoundment) basin, an area of deep water, can effectively decrease flow velocities and cause sediments to settle in a designated area. An effective deposition basin on or near a waterway can capture sediments, reduce sediment deposition in navigable waterways, reduce maintenance dredging requirements within navigation channels, and serve as a sand source for inlet sand bypassing operations. At the AIWW near Sawpit Creek, construction of deposition basins and/or removal of nearby shoal sediment sources could, with periodic dredging, provide these benefits. The prospect of this cost-saving outcome encouraged Florida Inland Navigation District (FIND) to request Taylor Engineering perform a sediment deposition basin study in Sawpit Creek and adjacent waterways. FIND requested Taylor Engineering provide a feasibility study to evaluate up to three sediment impoundment basin design alternatives in or near Sawpit Creek to increase the interval between AIWW maintenance dredging events.

This study employed numerical models to evaluate the performance of various sediment impoundment basin design alternatives. Data collection and field measurements provided the input data for model development, validation, and model boundary conditions for production runs to evaluate sediment impoundment basin performance.

Following this introduction, Chapter 2 of this report presents details of the data collection, field measurements, and data analyses. Chapter 3 describes the development of the hydrodynamic, wave, sediment transport, and particle tracking model including model mesh and model boundary condition setup. Chapter 4 describes the evaluation of the performance of various sediment basin designs and provides cost comparisons for the sediment impoundment basin design alternatives. Chapter 5 summarizes dredging, design, and permitting considerations. Finally, Chapter 6 concludes the report with a summary of the findings and recommendations.

## 2.0 DATA COLLECTON AND ANALYSIS

The study area spans portions of the Atlantic Ocean, Fancy Bluff Creek, Cumberland River, St. Marys River, Amelia River, Nassau River, Nassau Sound, Sawpit Creek, Clapboard Creek, Fort George River, Fort George Inlet, Sisters Creek, St. Johns River, and Pablo Creek to Atlantic Blvd. Bridge in Jacksonville, FL. These areas are influenced daily by tides, waves, and winds and occasionally by storm surge. The paragraphs below describe the data collection to support model development, validation, and application.

### 2.1 Tide Data

Semi-diurnal tides—two high and two low per day—and mixed tides during neap period characterize the astronomical tides in the study area. Collection and review of published tide records as well as field measurements of tides contributed to a comprehensive set of tide data for this study. The following sections describe published tidal data and measured tide data.

#### 2.1.1 NOAA Tide Data

Figure 2.1 and Table 2.1 show the locations of the National Oceanic and Atmospheric Administration (NOAA) tidal datum stations near the area of interest. Tidal data from these stations indicate an ocean mean tidal range of approximately 6.62 ft (NOAA 8677344 at St. Simons Island) to 5.07 ft (NOAA 8720291 at Jacksonville Beach). Inshore mean tidal range varies at 4.84 ft in St. Marys River (NOAA 8720004 at Crandall), 6.02 ft in Amelia River (NOAA 8720030 at Fernandina Beach), 4.16 ft in Nassau River (NOAA 8720093 at Halfmoon Island), 5.16 ft at Nassau River Entrance (NOAA 8720135), 4.78 ft in Fort George River (NOAA 8720186 at Fort George Island), 4.52 ft in St. Johns River (NOAA 8720218 at Mayport Bar Pilot Dock), 3.37 ft in St. Johns River (NOAA 8720219 at Dames Point), 3.77 ft in Pablo Creek (NOAA 8720267 at Atlantic Blvd. Bridge); 5.08 ft in Sawpit Creek (NOAA 8720143 at one mile south of entrance), and 4.29 ft in Sisters Creek (NOAA 8720196). Table 2.1 presents tidal datums for these stations based on the 1983 – 2001 tidal epoch. In the absence of tide datum data in some of these stations, NOAA’s VDATUM software provided approximate mean tide level relative to NAVD88.

#### 2.1.2 Field Measurement of Inshore Tide Level

Taylor Engineering installed eight tide gages (Stations T1 – T8) on April 16, 17, and 22, 2019 to provide water level data for hydrodynamic model validation. Figure 2.2 shows the locations of the tide measurement stations and Table 2.2 provides the locations, periods of record, and interval of the tide measurements. Inspection of the measured tides show measurements reflect mean tide ranges consistent with tidal ranges from NOAA stations. Notably, the measured water level data reflects wind setup that caused non-tidal fluctuations in the measured tides.

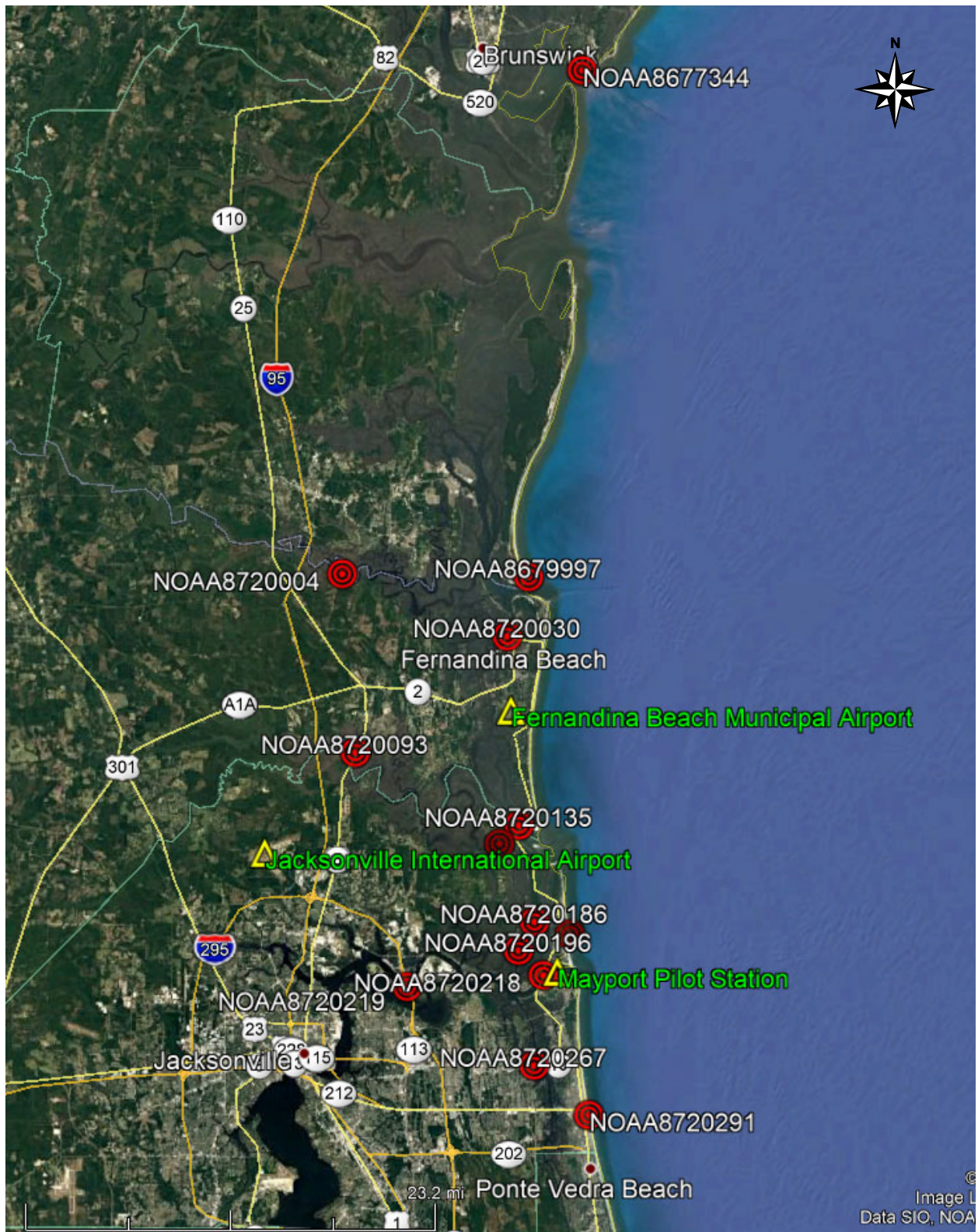


**Figure 2.1** Locations of Select NOAA Tide Stations and Wind Stations

**Table 2.1** NOAA Tide Datums and Locations of Select Stations near the Area of Interest (1983 – 2001 Tidal Epoch)

<b>Tide Datums, Mean Tide Range, and Coordinates</b>	<b>NOAA 8677344 St. Simons Island, GA  (ft-NAVD)</b>	<b>NOAA 8720004 St. Marys River, Crandall, FL  (ft-NAVD)</b>	<b>NOAA 8720030 Fernandina Beach, FL  (ft-NAVD)</b>	<b>NOAA 8720093 Nassau River, Halfmoon Island, FL (ft-NAVD)</b>	<b>NOAA 8720135 Nassau River Entrance, FL  (ft-NAVD)</b>	<b>NOAA 8720143 Sawpit Creek (1 mi South of Entrance), FL (ft-NAVD)</b>
Mean Higher High Water (MHHW)	2.97	2.46	2.74	1.94	2.50	2.37
Mean High Water (MHW)	2.60	2.20	2.39	1.76	2.16	2.03
Mean Tide Level (MTL)	-0.72	-0.22	-0.62	-0.32	-0.42	-0.51
Mean Low Water (MLW)	-4.03	-2.64	-3.64	-2.41	-3.00	-3.05
Mean Lower Low Water (MLLW)	-4.23	-2.83	-3.82	-2.61	-3.19	-3.19
Mean Tide Range (ft)	6.62	4.84	6.02	4.16	5.16	5.08
Latitude	31°7.9'N	30°43.3'N	30°40.3'N	30°34.6'N	30°31.1' N	30°30.2'N
Longitude	81°23.8'W	81°37.3'W	81°27.9'W	81°36.5'W	81°27.2' W	81°28.3'W
<b>Tide Datums, Mean Tide Range, and Coordinates</b>	<b>NOAA 8720196 Sisters Creek, FL  (ft-NAVD)</b>	<b>NOAA 8720186 Fort George Island, Fort George River, FL (ft-NAVD)</b>	<b>NOAA 8720218 Mayport (Bar Pilots Dock), FL  (ft-NAVD)</b>	<b>NOAA 8720219 Dames Point, FL  (ft-NAVD)</b>	<b>NOAA 8720267 Pablo Creek, Atlantic Blvd. Bridge, FL (ft-NAVD)</b>	<b>NOAA 8720291 Jacksonville Beach, FL  (ft-NAVD)</b>
Mean Higher High Water (MHHW)	1.85	2.25	1.96	1.42	1.49	2.48
Mean High Water (MHW)	1.60	1.95	1.69	1.27	1.29	2.10
Mean Tide Level (MTL)	-0.54	-0.44	-0.57	-0.42	-0.60	-0.44
Mean Low Water (MLW)	-2.69	-2.83	-2.83	-2.10	-2.48	-2.97
Mean Lower Low Water (MLLW)	-2.81	-2.97	-2.99	-2.21	-2.63	-3.14
Mean Tide Range (ft)	4.29	4.78	4.52	3.37	3.77	5.07
Latitude	30°25' N	30°26.4'N	30°23.8'N	30°23.2'N	30°19.4'N	30°17.0'N
Longitude	81°27.2' W	81°26.3'W	81°25.8'W	81°33.5'W	81°26.3'W	81°23.2'W

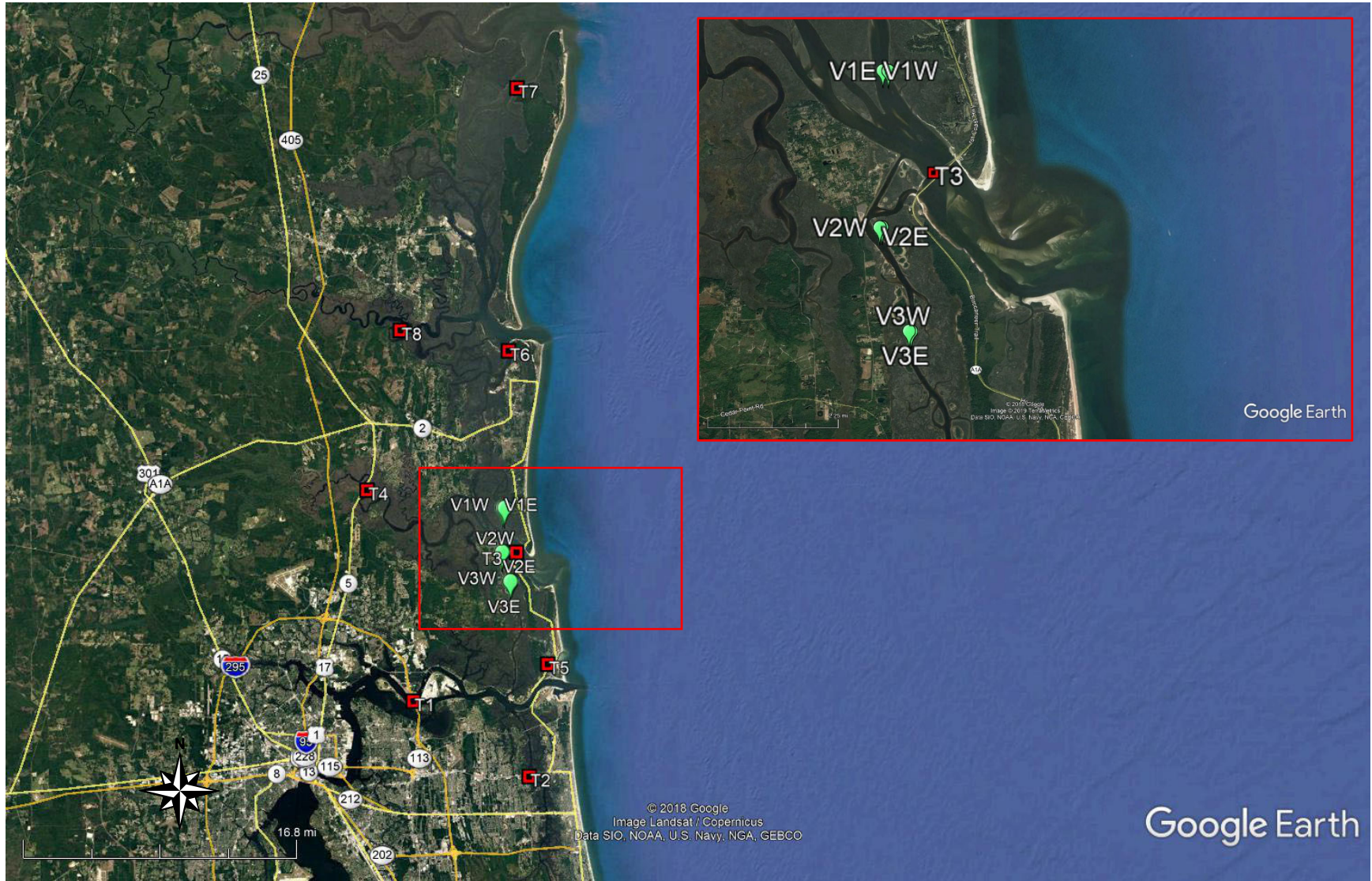


Figure 2.2 Locations of the Tide Level and Velocity Measurement Stations

**Table 2.2** Coordinates, Period of Record, and Time Interval of Measured Tide Level and Velocity Stations

Station	Coordinates		Water Depth (ft)	Period of Record	Time Interval	Location/Remarks
	N Latitude	W Longitude				
T1	30°55'48.00"N	81°26'48.00"W	n/a	4/22/2019 – 05/29/2019	15 minutes	Near NOAA 8678688
T2	30°43'18.00"N	81°37'18.00"W	n/a	4/22/2019 – 05/29/2019	15 minutes	Near NOAA 8720004
T3	30°43'12.00"N	81°26'42.00"W	n/a	4/22/2019 – 05/29/2019	15 minutes	Near NOAA 8679997
T4	30°34'36.00"N	81°36'30.00"W	n/a	4/22/2019 – 05/29/2019	15 minutes	Near NOAA 8720093
T5	30°31'06.00"N	81°27'12.00"W	n/a	4/22/2019 – 05/29/2019	15 minutes	Near NOAA 8720135
T6	30°25'48.00"N	81°24'18.00"W	n/a	4/22/2019 – 05/29/2019	15 minutes	Near NOAA 8720194
T7	30°19'24.00"N	81°26'18.00"W	n/a	4/22/2019 – 05/29/2019	15 minutes	Near NOAA 8720267
T8	30°23'12.00"N	81°33'30.00"W	n/a	4/22/2019 – 05/29/2019	15 minutes	Near NOAA 8720219
V1E	30°32'22.08"N	81°27'54.84"W	12.5	05/10/2019 & 05/17/2019	60 – 90 minutes	Nassau Cut-27C
V1W	30°32'22.39"N	81°28'00.56"W	15.3	05/10/2019 & 05/17/2019	60 – 90 minutes	Nassau Cut-27C
V2E	30°30'02.23"N	81°28'01.47"W	11.5	05/10/2019 & 05/17/2019	60 – 90 minutes	Duval Cut-24
V2W	30°30'02.04"N	81°28'03.76"W	11.0	05/10/2019 & 05/17/2019	60 – 90 minutes	Duval Cut-24
V3E	30°28'29.12"N	81°27'30.96"W	13.4	05/10/2019 & 05/17/2019	60 – 90 minutes	Duval Cut-18
V3W	30°28'29.30"N	81°27'33.26"W	14.0	05/10/2019 & 05/17/2019	60 – 90 minutes	Duval Cut-18

## 2.2 Wind Data

Characterizing an estuarine and coastal site typically requires wind measurements. Fortunately, wind data and other meteorology data (rainfall) is available at three nearby locations (see Figure 2.1)—Fernandina Beach Municipal Airport (coordinates 30°36'42.60"N, 81°27'40.30"W), Jacksonville International Airport (coordinates 30°29'42.00"N, 81°41'36.96"W), and Mayport Pilot Station

(coordinates 30°24'00.00"N, 81°25'00.01"W). These locations lie approximately 5.9 mi north (Fernandina Beach Municipal Airport), 14.2 mi west (Jacksonville International Airport), and 9.1 mi south (Mayport Pilot Station) from AIWW Cut-27A. Figure 2.3 and Figure 2.4 show the April and May 2019 measured winds at these stations and Figure 2.5 shows the prevailing wind roses for April – May, 2019. Wind roses show the distribution of the measured wind data when sorted into 16 direction angle bands and 20 wind speed bins. The roses show winds mostly originate from the east and southeast directions. About 4 – 18% of winds were near 0 mph. Because of their sufficiently long record and proximity to the project area and the ocean, this study chose the wind data from Fernandina Beach Municipal Airport and Mayport Pilot Station as the best indicators of the project site-specific winds.

### 2.3 Wave Data

Collection and review of hindcasted waves provided offshore wave characterization data for this study. Figure 2.6 shows the locations of U.S. Army Corps of Engineers (USACE) Wave Information Study (WIS) Station 63402 that provide hourly hindcasted wave data from January 1, 1980 to December 31, 2017. Station 63402 is located at 30°34'48"N and 81°04'48"W or approximately 20 mi east of Nassau Sound at water depth of approximately 65.6 ft. Hindcasted wave data consist of significant wave height, peak wave period, mean wave direction, and wave directional spread.

The USACE Engineer Research and Development Center (ERDC) analyzed the 1980 – 2017 hindcasted wave data at WIS Station 63402. Figure 2.7 shows the wave rose generated by ERDC from all 1980 – 2017 hindcasted waves at the station. The figure shows most waves originate from the east-southeast, east, and east-northeast directions. Figure A.1 to Figure A.12 in Appendix A1 shows WIS Station 63402 wave rose for each month. These figures show the seasonal variation of the nearshore wave climate—large easterly waves in September to December, east and east-southeasterly waves predominate in January to March, and small east-southeasterly waves in April to August characterize the wave conditions. These figures characterize the seasonal wave conditions and provide information on potential wave conditions during dredging operations in the AIWW near Sawpit Creek.

Figure 2.8 and Table 2.3 show ERDC's estimation of the significant wave height from the zero moment (integral) of the power spectrum. In Figure 2.8, the blue circle indicates hindcasted significant wave height data points. The solid red line indicates the best fit line (up to the available annual maximum wave height data) and the dash-dot red line indicates the extrapolation of the best fit line (to estimate wave height beyond the available data) of the distribution of the hindcasted significant wave height. The green and pink asterisks indicate estimates of the 50-yr and 100-yr significant wave height. The list in the enclosure provides the hindcasted significant wave height, peak period, and mean direction (origin) of the top ten hindcasted wave events—e.g., Event 1 to Event 10 indicate the ten rightmost blue dots in Figure 2.8. Table 2.3 shows that in any given year, there is a 100% chance that a 13.9-ft wave, a 20% chance that a 17.4-ft wave, and a 1% chance that a 23.8-ft wave will occur offshore at Station WIS 63402.

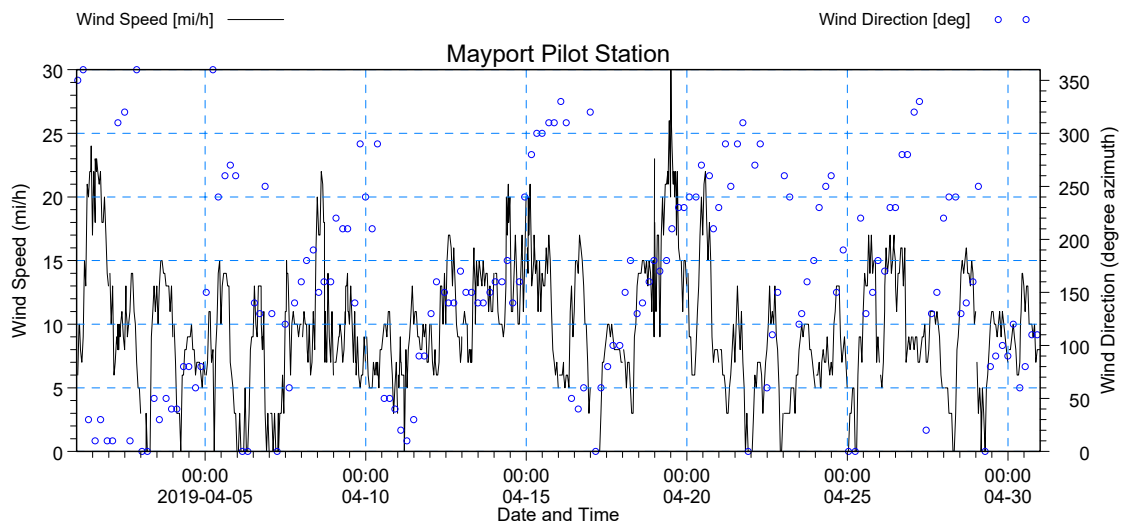
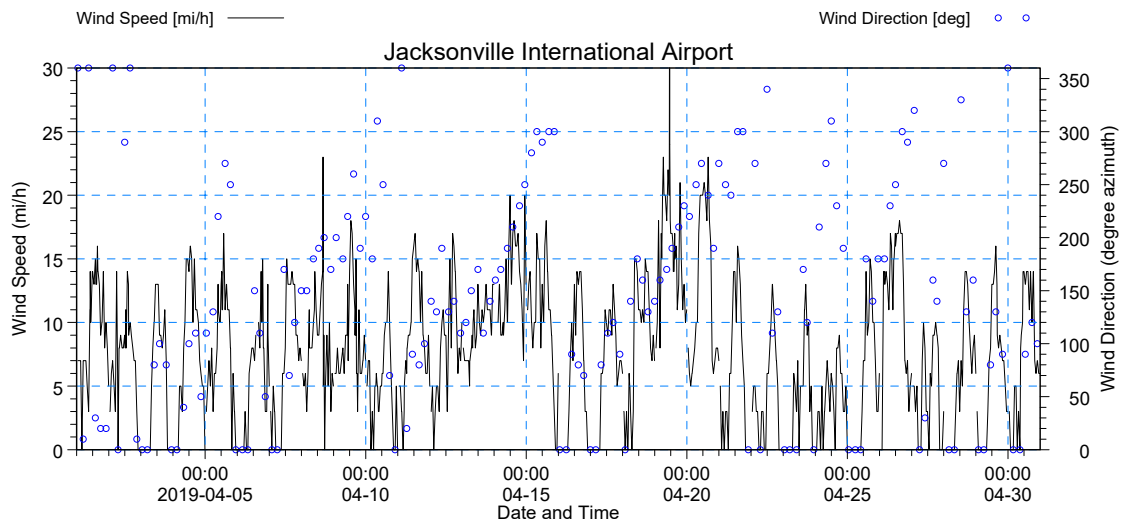
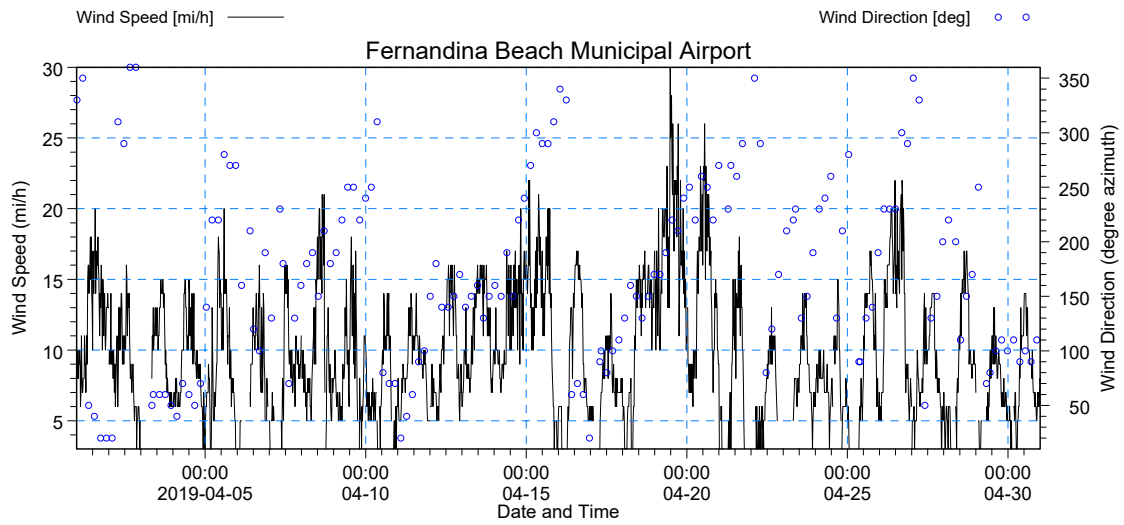


**Figure 2.3** Measured Wind Speed and Direction in April 2019

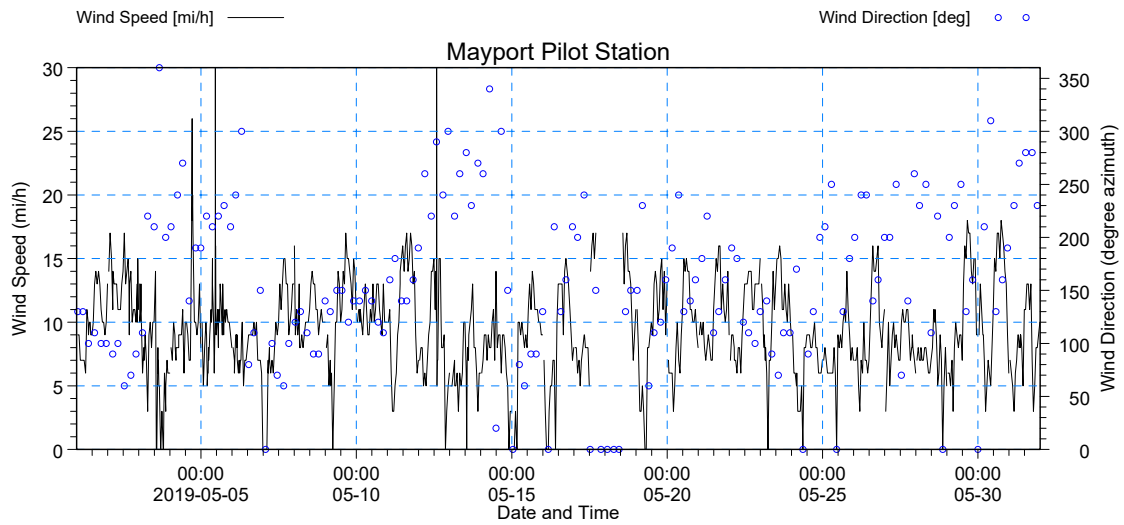
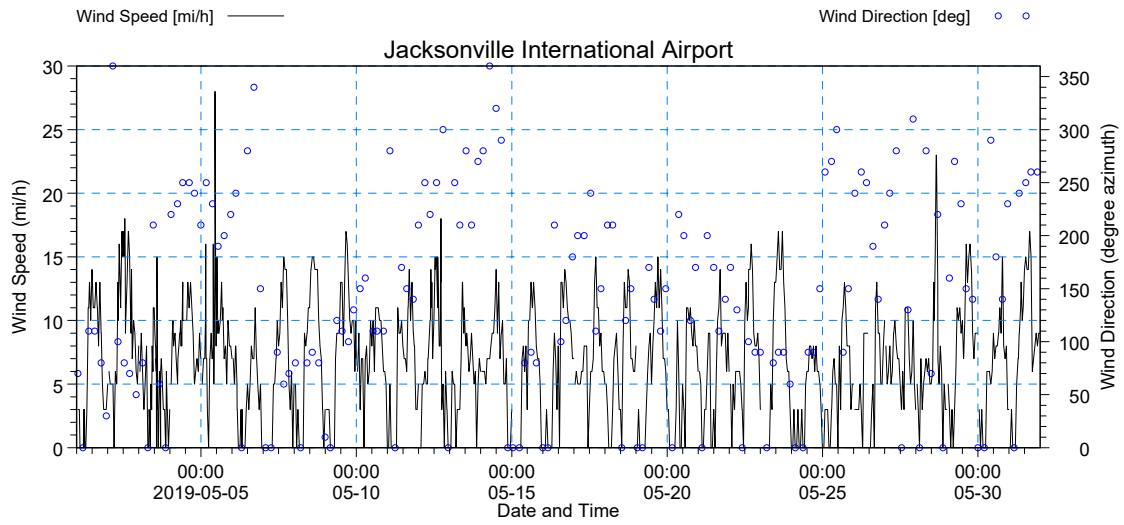
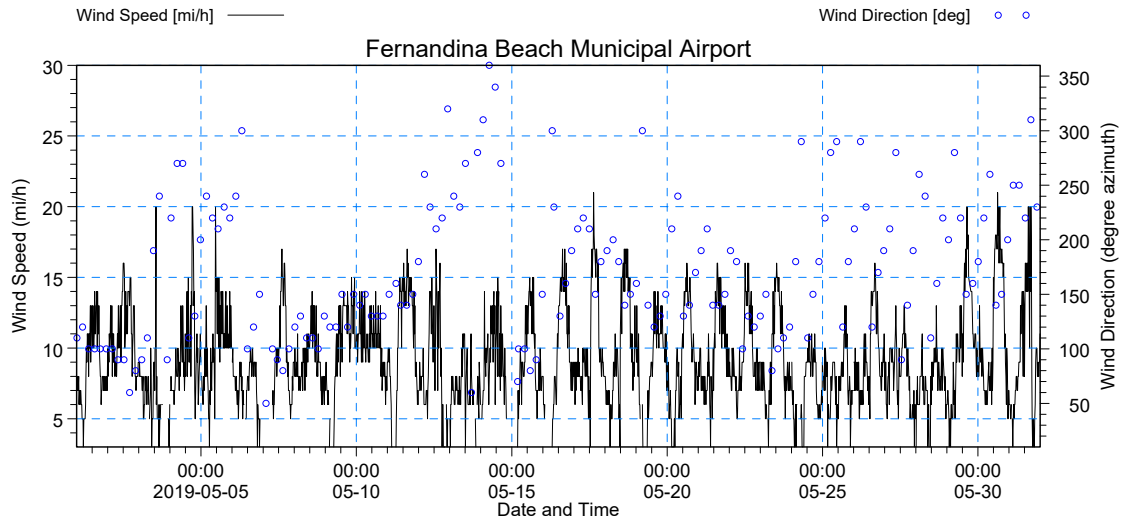


**Figure 2.4** Measured Wind Speed and Direction in May 2019

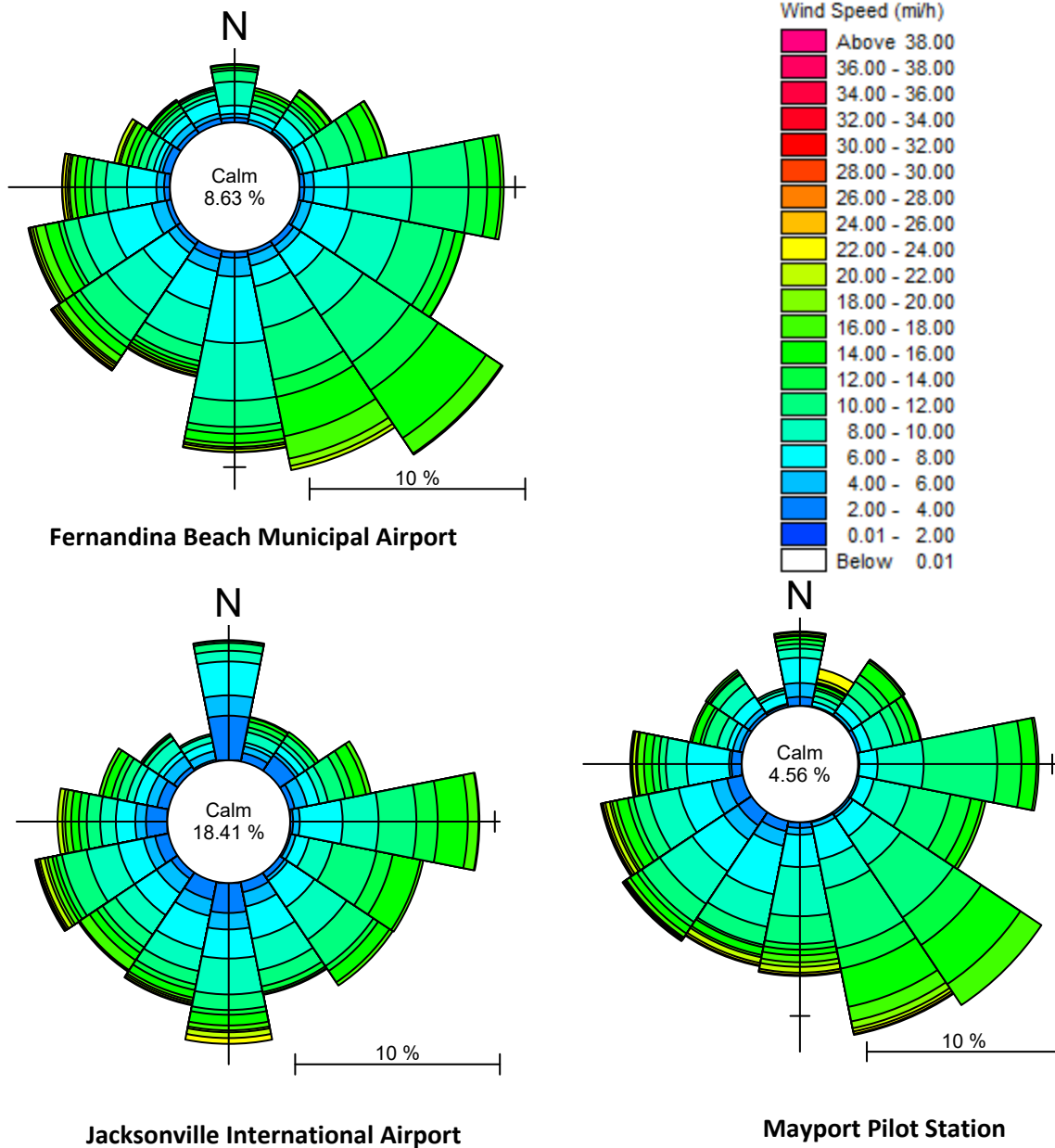


**Figure 2.5** Wind Roses at Fernandina Beach Municipal Airport, Jacksonville International Airport, and Mayport Pilot Station (April 1, 2019 – May 31, 2019)

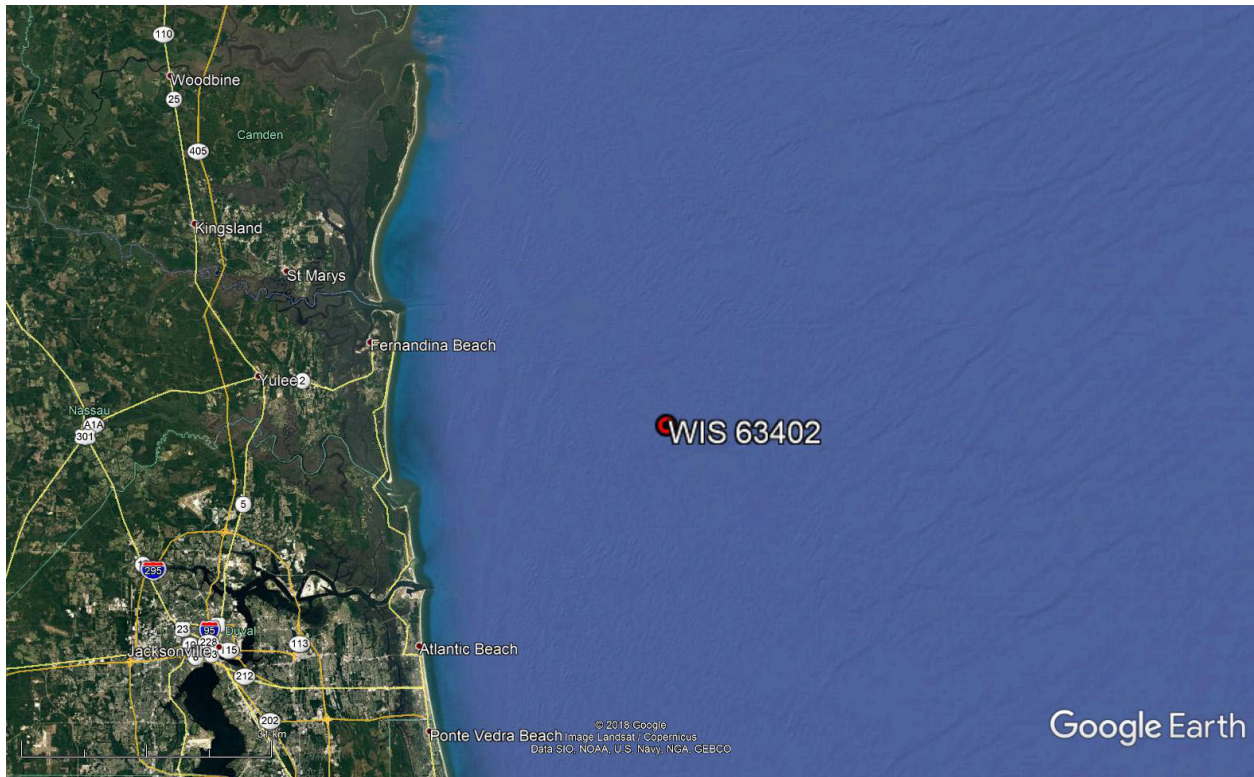
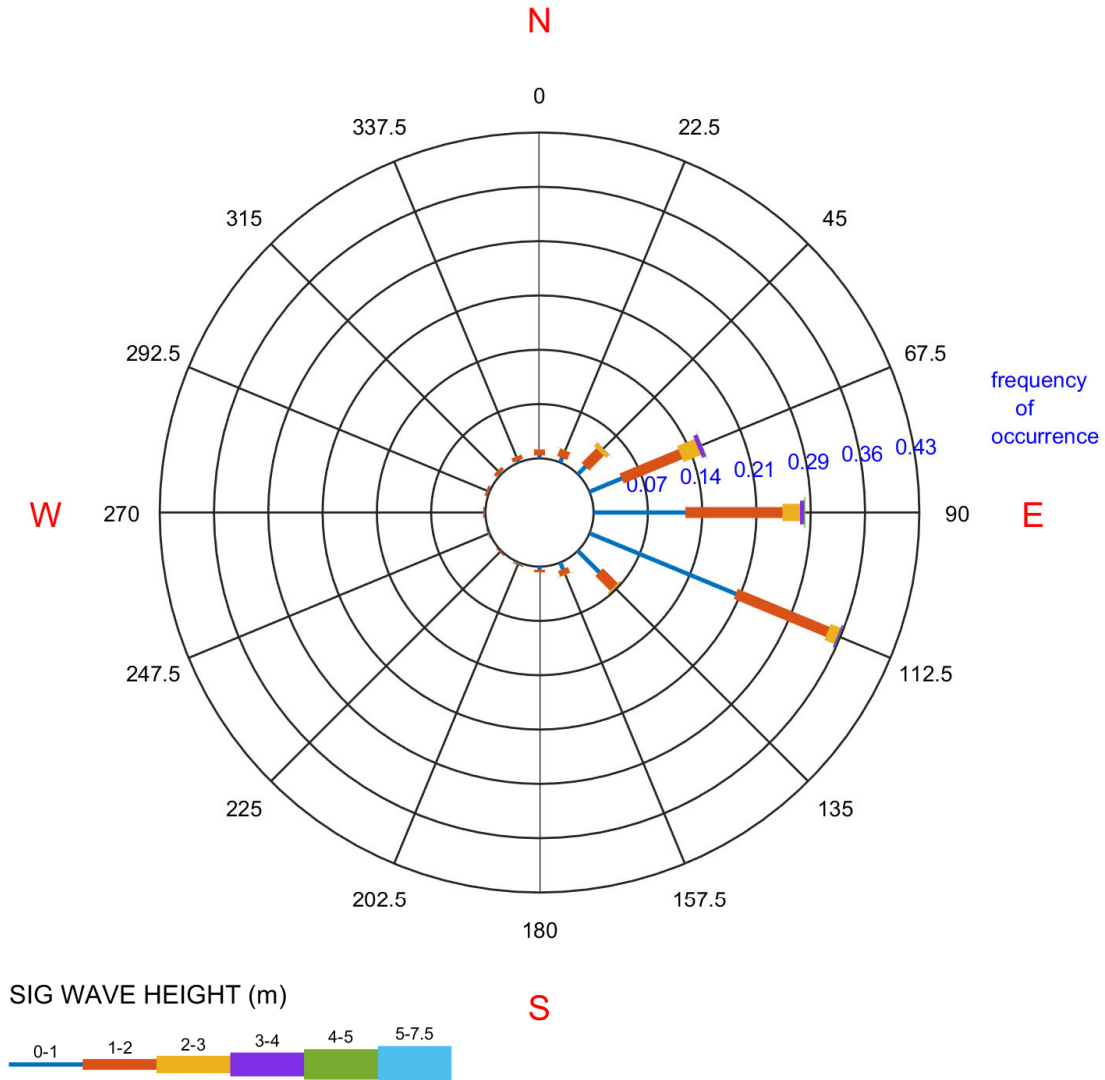


**Figure 2.6** Location of WIS Station 63402



Atlantic WIS Station 63402  
01-Jan-1980 thru 31-Dec-2017  
Long: -81.08° Lat: 30.58° Depth: N/A m  
Total Obs : 333119

### WAVE ROSE



US Army Engineer Research & Development Center

ST63402\_v03

**Figure 2.7** Hindcasted Wave Rose at WIS Station 63402 for 1980 – 2017  
(Source: U.S. Army Engineer Research and Development Center)

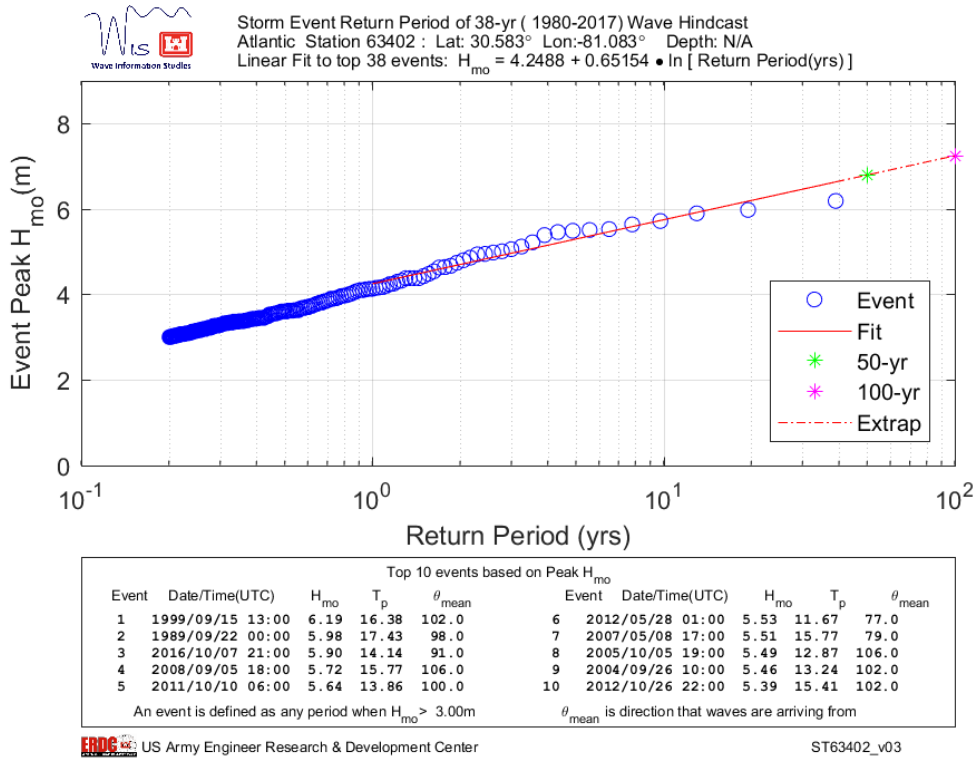


**Figure 2.8** WIS Station 63402 Wave Height Return Period  
 (Source: U.S. Army Engineer Research and Development Center)

**Table 2.3** WIS Station 63402 Hindcasted Wave Height and Return Period (1980 – 2017)  
 (Source: U.S. Army Engineer Research and Development Center)

Return Period (year)	Annual Exceedance Probability	Wave Height (ft)
1	100%	13.9
2	50%	15.4
5	20%	17.4
10	10%	18.9
25	4%	20.8
50	2%	22.3
100	1%	23.8

## 2.4 Flow Velocity Data

To increase understanding of the flow velocity patterns that will drive sediment transport in the AIWW, this study used a boat-mounted down-looking Aquadopp on May 10, 2019 (neap tides) and May 17, 2019 (spring tides) to measure currents at 60 – 90-minute intervals at each of the flow velocity measurement Stations V1E (Cut-27), V1W (Cut-27), V2E (Cut-24), V2W (Cut-24), V3E (Cut-18), and V3W (Cut-18). Figure 2.2 shows the locations of the current measurement stations. Table 2.2 provides the locations, periods of record, and number of measurements along the water depth. Appendix B provides the May 10 and 17, 2019 depth-averaged flow velocity measurements from four to ten 1.6-ft thick vertical layers. The number of vertical layers depended on the water depth at the time of the measurements.

## 2.5 Bathymetric and Topographic Data

This section discusses the collection of the bathymetric and topographic data. Survey data include bathymetric survey data of the AIWW, Nassau Sound, Sawpit Creek, Clapboard Creek, Sisters Creek, and St. Johns River and topographic survey data at the beaches of Nassau and Duval Counties and at other locations where the model mesh extends above the mean highwater level. This study sourced its bathymetric and topographic data from four main sources—(a) the Federal Emergency Management Agency (FEMA) Northeast Florida–Georgia ADCIRC model Version 12b mesh; (b) various recent bathymetric surveys of AIWW and St. Johns River; (c) 2018 Nassau Sound and Nassau River bathymetric survey; and (d) 2019 USACE-SAJ AIWW bathymetric survey. The ADCIRC mode Version 12b mesh provided the base bathymetric data in the Atlantic Ocean, St. Marys River, Nassau River, Fort George River, and at many waterways adjacent to Sawpit Creek and the other survey data provided updated bed elevation data in Nassau Sound, Nassau River, and AIWW.

### 2.5.1 FEMA East Coast 2012 ADCIRC Model Mesh Data

Figure 2.9 shows the FEMA Northeast Florida–Georgia ADCIRC model Version 12b mesh and domain. It includes the Gulf of Mexico, Caribbean Sea, and a portion of the Atlantic Ocean. As shown in Figure 2.10, the mesh provided bed elevation data in the Atlantic Ocean and inshore areas.

### 2.5.2 AIWW and St. Johns River Bathymetry Update

This study compiled bathymetric surveys completed since the development of the June 6, 2013 FEMA Northeast Florida–Georgia ADCIRC model Version 12b mesh to update the bathymetry along the AIWW and St. Johns River. Figure 2.11 shows the coverage areas of the compiled bathymetric survey which are referenced to ft-NAVD88. For the model mesh development, the compiled bathymetric surveys data replaced the ADCIRC model mesh bathymetry data in their common coverage area to apply recent updates on the bathymetry data.

### 2.5.3 Nassau Sound and Nassau River Bathymetry Update

This study applied the Nassau Sound bed elevation data from the June 22, 2018 Arc Surveying & Mapping, Inc. (ARC) to replace the ADCIRC model mesh bathymetry data in their common coverage area to apply more recent updates on the Nassau Sound and Nassau River bathymetry data. Figure 2.12 shows the coverage areas of the compiled ARC bathymetric surveys which are referenced to ft-NAVD88.

#### 2.5.4 Bathymetry Update Near Sawpit Creek

This study compiled January – April 2019 bathymetric surveys completed by the USACE-SAJ to update the bathymetry along AIWW Cuts 24, 25, 26, 27, 27A, and 27C. Figure 2.13 shows the coverage areas of the compiled bathymetric surveys which are referenced to ft-MLLW. For the model mesh development, this study converted the compiled bathymetric surveys data by using Table 2.1 tidal datum from NOAA 8720143 (Sawpit Creek 1 mi South of Entrance) to reference ft-NAVD88; and replaced the ADCIRC model mesh bathymetry data in their common coverage area to apply recent updates on the bathymetry data.

### 2.6 Sediment and Other Geotechnical Data

#### 2.6.1 Sediment Grab Sampling

On May 19, 2019, Taylor Engineering performed surface sediment grab sampling at several locations (Figure 2.14). The sample locations are at or near the potential pathways of sediment transport. Red marked stations are characterized by very fine sediments and white marked stations are characterized by fine grained sediments.

#### 2.6.2 Sediment Characteristics

Geotechnical analyses and standard sieve analyses of the samples provided sediment classification and grain size distribution. In general, the analyses suggest mostly fine sand at the project area with only four samples indicating very fine sediments (marked in red). This study estimated the sediment median grain size and gradation from the grain size distribution curves. Table 2.4 summarizes the sediment grain sizes of the samples taken from the project area. Median grain sizes  $D_{50}$  and grading coefficients vary 0.09 – 0.21 mm and 1.3 – 6.6. Based on the data from Table 2.4, this study estimated the average median grain size at  $D_{50} = 0.16$  mm and the average grading coefficient at 2.5 for the project area.



Figure 2.9 FEMA Northeast Florida-Georgia Version 12b ADCIRC Model Mesh

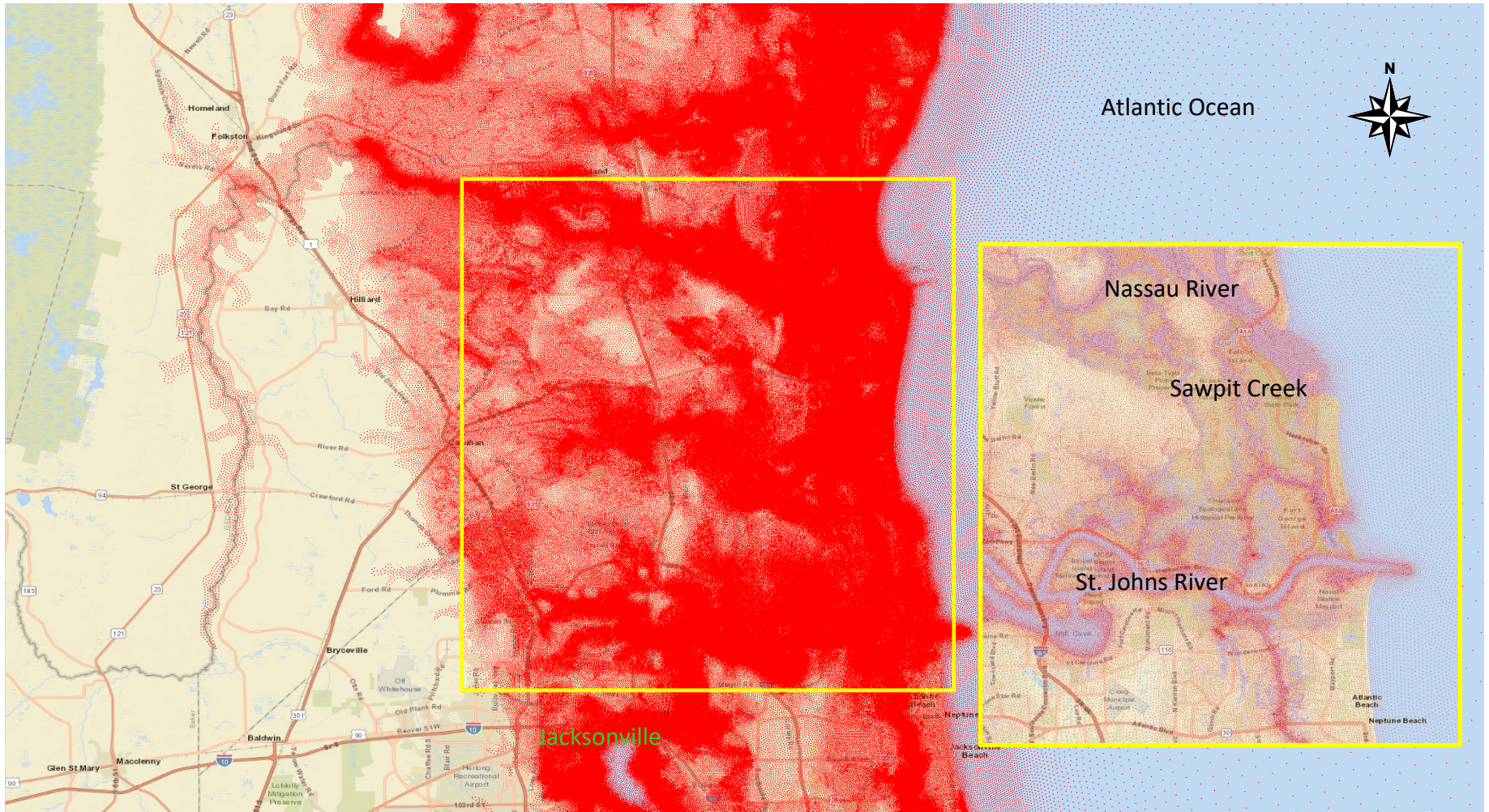


Figure 2.10 FEMA Northeast Florida-Georgia Version 12b ADCIRC Model Bed Elevation Points

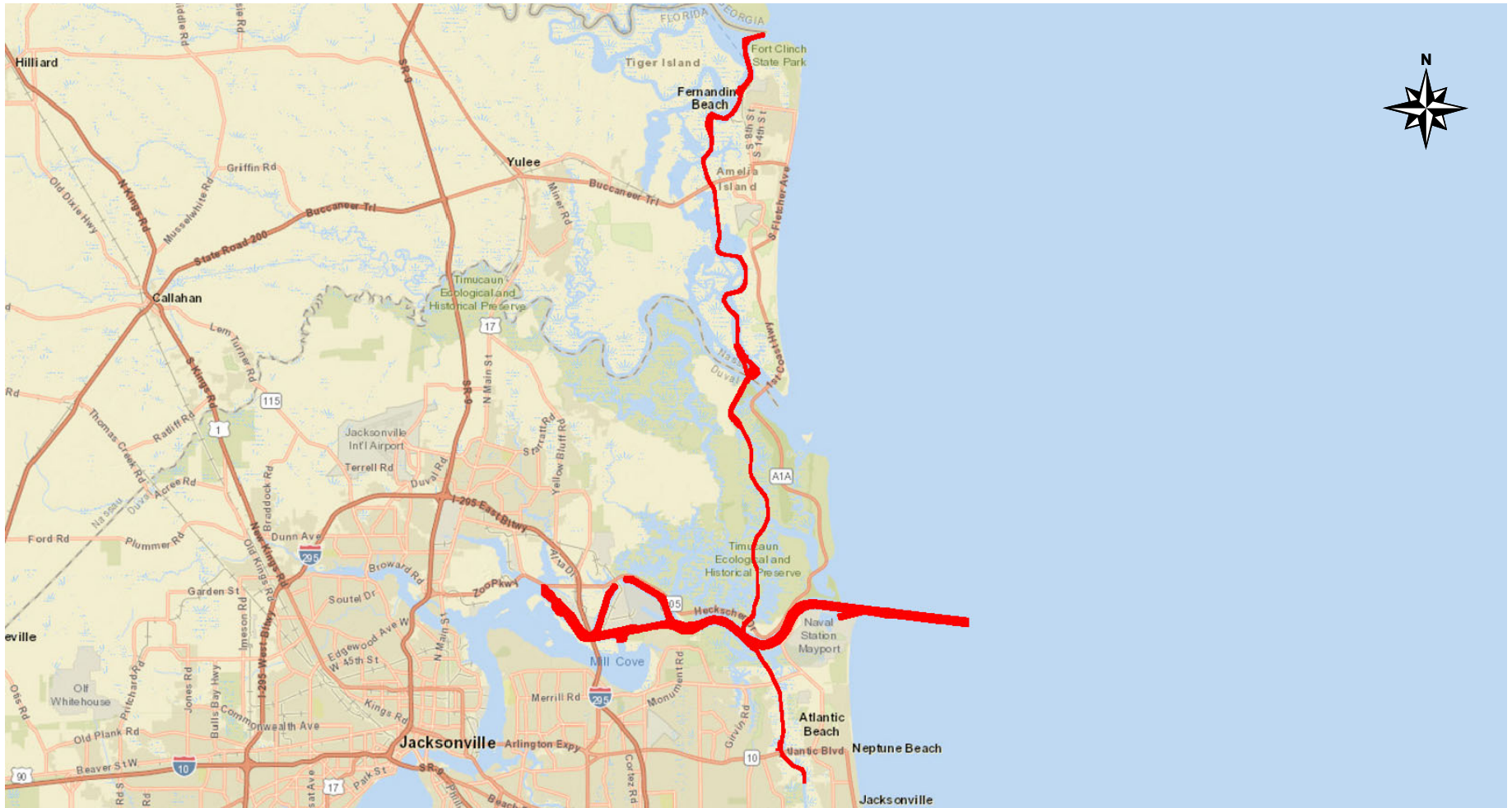
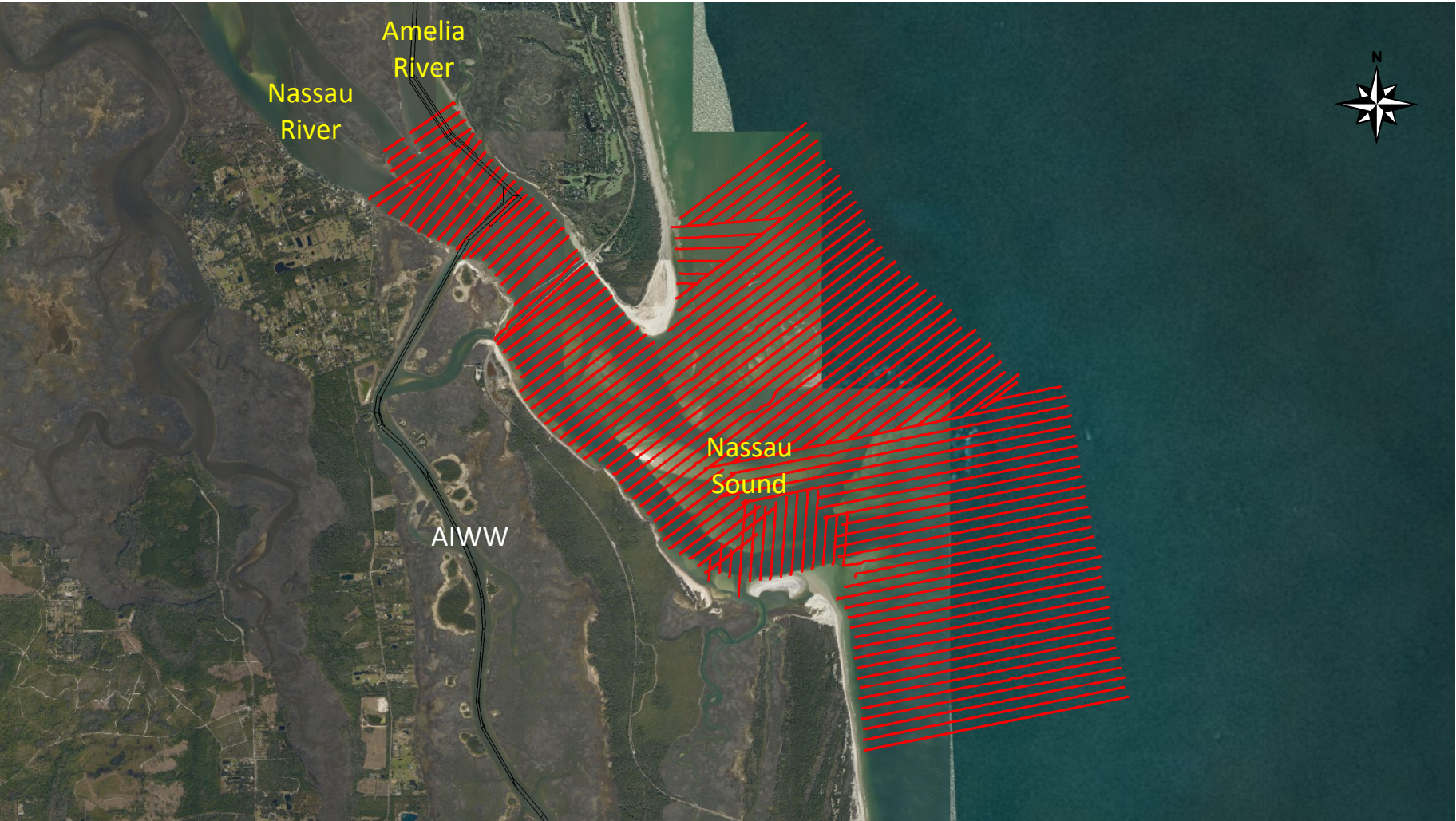


Figure 2.11 Areas of Bathymetry Data Update in AIWW and St. Johns River



**Figure 2.12** Areas of Arc Surveying & Mapping, Inc. June 22, 2018 Bathymetry Data Update in Nassau Sound and Nassau River



20

**Figure 2.13** Areas of USACE-SAJ January – April 2019 Bathymetry Data Update in AIWW Cuts 24, 25, 26, 27, 27A, and 27C

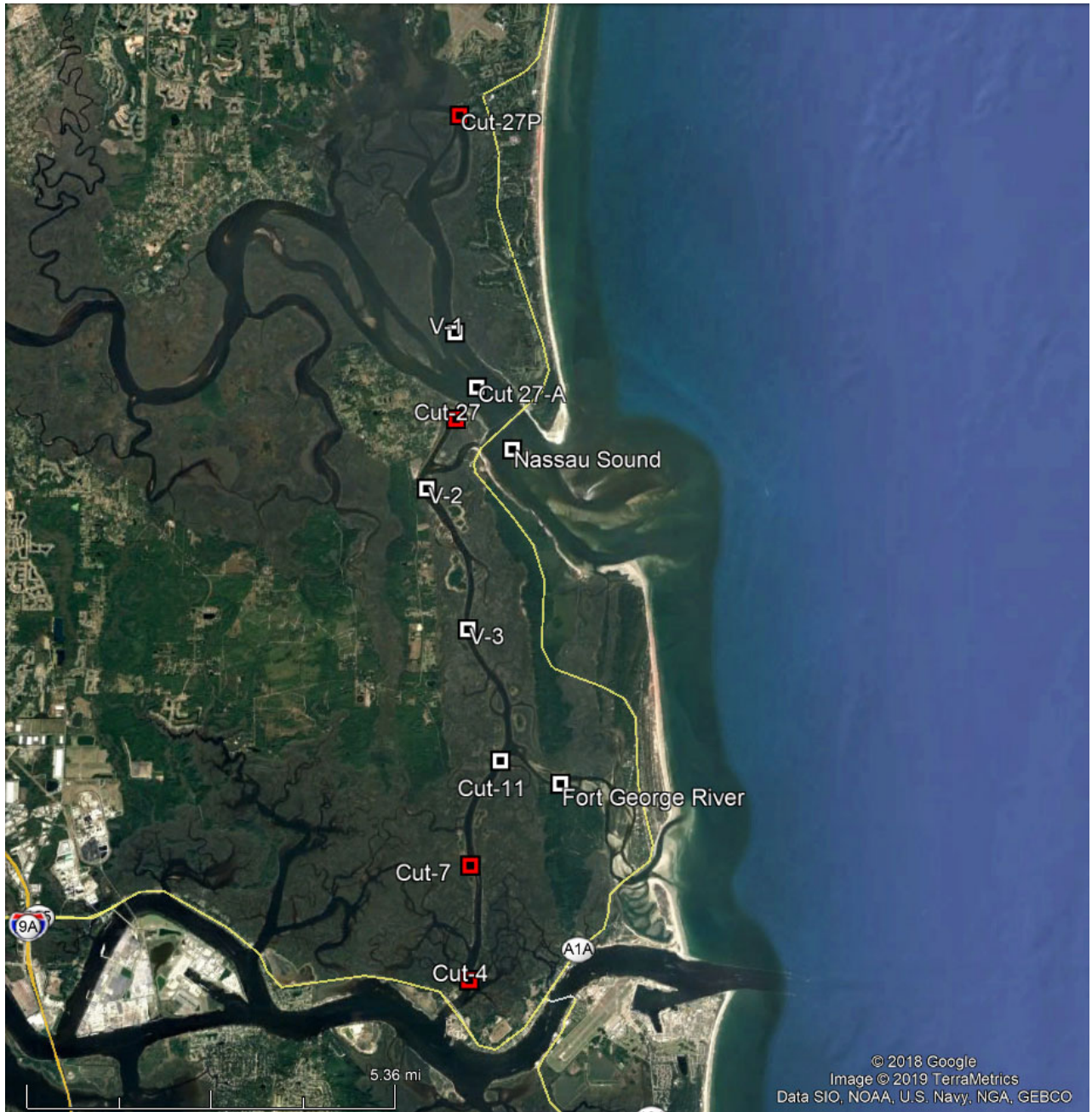


**Figure 2.14** Locations of Surface Sediment Sampling Stations

**Table 2.4** Properties of Sediment Samples at Project Area

Location	Lat (°N)	Long (°W)	Mean (mm)	Sorting (φ)	D <sub>14</sub> (mm)	D <sub>50</sub> (mm)	D <sub>86</sub> (mm)	D <sub>90</sub> (mm)	D <sub>95</sub> (mm)	Estimated Grading Coefficient
Nassau Sound	30.512752	81.448225	0.26	1.1	0.140	0.21	0.49	0.71	1.62	1.9
Cut-27A	30.526502	81.457654	0.22	0.91	0.140	0.20	0.31	0.34	0.52	1.5
Cut-27P	30.587847	81.464069	n/a	n/a	0.005	0.14	0.22	0.24	0.30	6.6
V-1	30.538658	81.463571	0.16	0.49	0.120	0.15	0.21	0.23	0.28	1.3
Cut-27	30.519431	81.462678	n/a	n/a	0.009	0.10	0.15	0.18	0.21	4.1
Cut-4	30.399173	81.455466	n/a	n/a	0.008	0.09	0.15	0.18	0.21	4.3
Cut-7	30.423115	81.455966	n/a	n/a	0.065	0.13	0.25	0.40	0.90	2.0
Cut-11	30.445294	81.449185	0.22	0.59	0.150	0.21	0.31	0.34	0.46	1.4
Fort George River	30.440435	81.434133	0.16	0.47	0.130	0.16	0.22	0.24	0.31	1.3
V-3	30.473474	81.458204	0.19	0.58	0.140	0.19	0.25	0.28	0.35	1.3
V-2	30.504085	81.46956	0.20	0.69	0.140	0.19	0.30	0.34	0.56	1.5
<b>Average</b>			<b>0.20</b>	<b>0.69</b>	<b>0.100</b>	<b>0.16</b>	<b>0.26</b>	<b>0.32</b>	<b>0.52</b>	<b>2.5</b>

### 3.0 MODEL DEVELOPMENT AND MODEL VALIDATION

This chapter describes the two-dimensional hydrodynamic, wave, sediment transport and morphology (bed change), and particle tracking models. These models simulate water surface elevation, flow velocity, sediment (sand) transport, bed change, sediment particle tracing, erosion, and deposition at the area of interest. The numerical models represent portions of Atlantic Ocean, Fancy Bluff Creek, Cumberland River, St. Marys River, Amelia River, Nassau River, Nassau Sound, Sawpit Creek, Clapboard Creek, Sisters Creek, Fort George River, Fort George Inlet, St. Johns River, and other waterways as two-dimensional waterways.

This study applied the MIKE21 Flexible Mesh (FM) Version 2019 hydrodynamic (HD), wave (SW), sediment transport and morphology (ST), and particle tracking (PT) models. In MIKE21 FM, these models link dynamically—(1) the SW model computes and feeds back wave radiation stresses to the HD model to affect the HD model flow computation; (2) the HD model computes the tide- and wave-generated flow velocities that drive sediment transport; (3) the ST model-calculated sediment movement results in either erosion or deposition that changes bed elevations or shoreline location; and (4) bed or shoreline changes affect the subsequent SW and HD model computations (i.e., ST model feedbacks bed level changes to the SW and HD models). The fully dynamic integration of the wave calculation, flow calculation, sediment transport, and bed changes makes the MIKE21 FM a state-of-the-art modeling system that can simulate nearshore, inlet, and estuarine hydraulics and morphological process. The sections below focus on the model description, model setup including mesh generation, development of boundary conditions, calibration, and verification of the models to estimate shoaling rates in the AIWW cuts and proposed sediment basin.

#### 3.1 Hydrodynamic Model (HD)

The MIKE21 FM HD model applies the time-dependent mass and momentum conservation equations to compute transient flows and water surface elevations. The HD model requires flows, velocities, or stage hydrographs at its boundaries. Given the hydraulic conditions at the boundaries, MIKE21 FM HD—a two-dimensional, transient, and depth-averaged model—employs finite volume methods to compute flows and water surface elevations inside the model domain. The governing equations treat conservation of mass, conservation of momentum in the x- and y-directions and turbulence closure. Model capabilities include wetting and drying, Coriolis acceleration, wind stress, bed friction assignment, eddy viscosity or Smagorinsky definition of turbulent exchange coefficients, choices for boundary conditions (including flow, velocity, or elevation), and inclusion of flow sources (inflows or outflows).

##### 3.1.1 Hydrodynamic Model Setup

The application of the MIKE21 FM HD model to an area requires development of a finite volume mesh to map the bathymetry and topography into the model's input format. The mesh divides the model domain into triangular and/or quadrilateral elements. The size of the elements usually varies from large sizes (e.g., model mesh element side length at 3,000 ft) in regions far from the area of interest to very small sizes (e.g., model mesh element side length at 30 ft) at the area of interest. The next step of model setup after mesh development consists of defining the model boundaries. Measured, hindcasted, or predicted data provide the hydraulic conditions at the model boundaries. The following paragraphs describe the development of the model mesh and application of the model boundary data.

### Model Schematization

Mesh development for this study takes advantage of existing FEMA Northeast Florida–Georgia ADCIRC model Version 12b mesh. Using available shoreline and AIWW delineation data, this study re-generated the MIKE21 FM HD model mesh in the AIWW and in areas between the AIWW and the shoreline; and maintained the ADCIRC model mesh outside of these areas. Requirements for computational efficiency limited the MIKE21 FM HD mesh from Fort George Inlet to approximately 21.1 miles (mi) east (offshore boundary), 29.6 mi north (ocean north boundary), and 16.6 mi south (ocean south boundary); and more than 50 mi of Atlantic Intracoastal Waterway from south of Satilla River to the Atlantic Blvd. Bridge in Jacksonville, 14.5 mi of St. Marys River, 20.8 mi of Nassau River, 4.6 mi of Fort George River, and 10.6 mi of St. Johns River. At the area of interest in Sawpit Creek and the AIWW, small elements provided the means to delineate and evaluate in more detail the federal navigation channel’s hydraulic, wave, and sediment transport conditions.

To construct the existing condition model mesh, multiple sources provided the topographic and bathymetric data—(a) FEMA Northeast Florida–Georgia ADCIRC model Version 12b mesh; (b) the compiled and updated NOAA and USACE bathymetry data in AIWW between Nassau River and St. Johns River; (c) 2018 Nassau Sound and Nassau River bathymetric survey; and (d) 2019 USACE-SAJ AIWW bathymetric survey. Section 2.5 describes the application of these data sets to the model mesh. Figure 3.1 shows the existing condition model domain bed elevations referenced to North American Vertical Datum of 1988 (NAVD). The inset shows the bed elevations at portions of the AIWW, Sawpit Creek, Nassau River, Amelia River, and Nassau Sound. The mesh horizontal control references the Universal Transverse Mercator North American Datum of 1983 (NAD83) Zone 17.

The program MIKEZero (DHI, 2019) provided the user interface for model setup. The user constructs a mesh from several of the tools provided and then adds the appropriate resolution in the areas of interest. The program allows the user to input ASCII data files of digitized bathymetry and interpolate the bathymetry onto a mesh.

### Model Boundary Conditions

The final step in model setup involved specification of known boundary conditions at the external boundaries of the model mesh. MIKE21 FM HD model provides several options for external boundaries. For an unspecified mesh boundary, the program automatically assumes a land barrier with a “slip” boundary condition. In short, the flow at nodes on a slip boundary does not have velocity components perpendicular to the boundary. Specified boundary conditions include time-varying free surface elevation, flow, flux, and velocity. This study’s HD model applies time-varying elevation boundary conditions at the offshore, ocean north, ocean south, near Cumberland Wharf in Cumberland River, GA (AIWW north), Atlantic Blvd. Bridge (AIWW south), upstream of St. Marys River (near I-95), upstream of Nassau River (near Halfmoon Island, FL), and upstream of St. Johns River (at Dames Point Bridge) boundaries. If needed, the HD model can have time-varying flow sources/sinks to include inflows and outflows in waterways.

For calibration and verification model runs, differences between measured and predicted tides at Mayport Bar Pilot Dock allowed transformation of predicted tides at the offshore, ocean north, and ocean south boundaries to include meteorological influences. Also, for calibration and verification model runs, recorded water levels at tide gauges at St. Johns River at Dames Point (Station T1), AIWW at Atlantic Blvd. Bridge (Station T2), Nassau River near Halfmoon Island (Station T3), AIWW at Cumberland

Wharf in Cumberland River, GA (Station T7), and St. Marys River near I-95 (Station T8), provided water level forcing data. Table 2.2 provides the coordinates and period of records and Figure 2.2 shows the locations of the water level measurement stations.

For model application or production runs, temporally- and spatially-varying predicted tides (generated using the Canada Institute of Ocean Sciences or Admiralty method) at the offshore, ocean north, and ocean south boundaries; and temporally-varying NOAA-predicted tides at inshore water level boundaries provided the HD model water level forcing data.

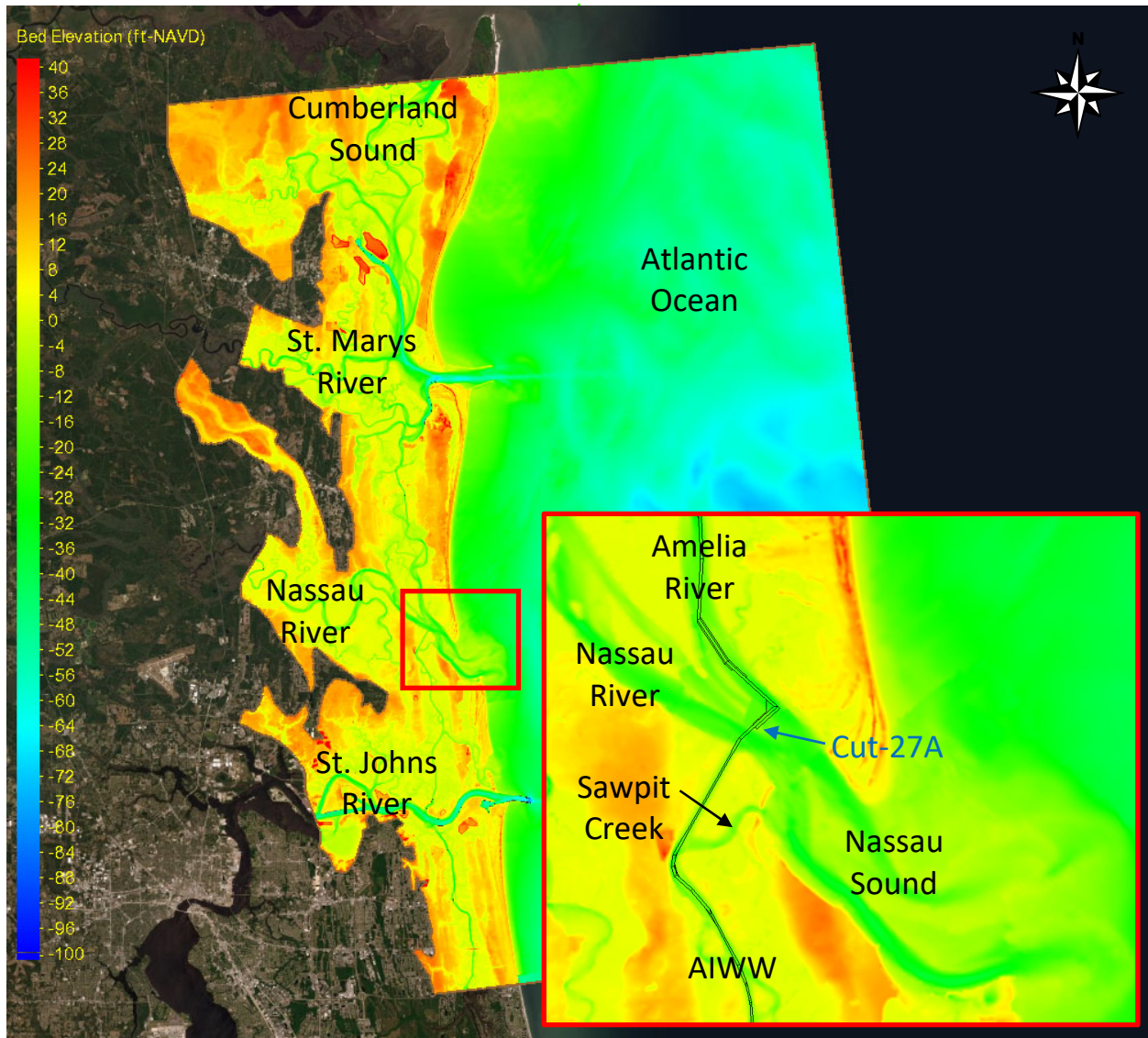


**Figure 3.1** Model Domain and Bed Elevations

### 3.1.2 Hydrodynamic Model Calibration

Calibration demonstrates a model’s capability to reproduce observed hydrodynamic and wave conditions in the study area. Calibration for this study consisted of iterative adjustments to model parameters until the model results agreed with the measured data. Measured water level at Stations T3

(Nassau Sound), T5 (Fort George River), T6 (near St. Mary's River entrance), and NOAA-measured water level at Mayport Bar Pilot Dock (NOAA 8720218); and measured flow velocities at Stations W1E, W1V, W2E, W2W, W3E, and W3W provided the HD model calibration data. Figure 2.2 shows the locations of these water level and velocity measurements stations.

This study used several statistical tools like the mean error (ME), root mean square error (RMSE), and correlation coefficient (CORREL) to quantify the goodness-of-fit of model results with measured data. The ME (see Equation 3.1) measures the average difference between the modeled and measured values; the RMSE (see Equation 3.2) measures the absolute differences between the modeled and measured values with large RMSE values indicating data outliers; and correlation coefficient (see Equation 3.3) quantifies the quality of fit of the model values to measured values (or the degree to which the variation of model values reflects the variation of the measured values):

$$ME(X_m, X_c) = \frac{1}{n} \sum_{i=1}^n (X_{m,i} - X_{c,i}) \quad \text{Equation 3.1}$$

$$RMSE(X_m, X_c) = \sqrt{\frac{1}{n} \sum_{i=1}^n (X_{m,i} - X_{c,i})^2} \quad \text{Equation 3.2}$$

$$CORREL(X_m, X_c) = \frac{\sum_{i=1}^n (X_{m,i} - \frac{1}{n} \sum_{i=1}^n X_{m,i}) (X_{c,i} - \frac{1}{n} \sum_{i=1}^n X_{c,i})}{\sqrt{\sum_{i=1}^n (X_{m,i} - \frac{1}{n} \sum_{i=1}^n X_{m,i})^2 \sum_{i=1}^n (X_{c,i} - \frac{1}{n} \sum_{i=1}^n X_{c,i})^2}} \quad \text{Equation 3.3}$$

where  $X_m$  are the measured values and  $X_c$  are the model calculated values. Correlation coefficients of -1 and 1 indicate a perfect negative and positive relationship between two data sets.

To incorporate wind effect on ocean predicted water levels in the model calibration and verification, this study added to the predicted tides along the model's ocean boundaries (offshore, ocean north, and ocean south boundaries) the time series difference between the measured water level and predicted astronomical tide level at Mayport Bar Pilot Dock (NOAA 8720218). This offsetting incorporated wind effects on the tide levels along the model's ocean boundaries. At inshore model boundaries, the measured water levels at Cumberland Wharf in Cumberland River, GA (NOAA 8678688), Atlantic Blvd. Bridge (NOAA 8720267), upstream of St. Marys River (NOAA 8720004), upstream of Nassau River (NOAA 8720093), and upstream of St. Johns River (NOAA 8720219) provided the model boundary conditions. Model calibration consisted of iterative adjustment of model bed resistance until model water levels at Stations T3, T5, T6, and Mayport Bar Pilot Dock became consistent with measured water level data. The HD model's consistency with water level measurements taken at Stations T3, T5, and T6 are most important because these are sediment transport pathways to Sawpit Creek, AIWW, and nearby waterways.

This study selected April 22 – May 10, 2019 as the calibration period and evaluated bed resistance Manning's  $n$  at 0.02 in most areas. Table 3.1 provides the mean error, RMSE, and correlation coefficient that relate modeled and measured water levels at Stations T3, T5, T6, and NOAA 8720218 for different Manning's  $n$  values. The table shows a Manning's  $n$  value of 0.020 provided the best mean error at Stations T5 and T6, RMSE at Station T5, and correlation coefficient statistics at Station T6; a Manning's  $n$  value of 0.017 provided best mean error at Station T3, RMSE at Station T6, and correlation coefficient statistics at Station T6; and a Manning's  $n$  value of 0.030 provided the best statistics mostly at NOAA 8720218. Given that a Manning's  $n$  value of 0.020 provided the best overall mean error and as the area of interest (Sawpit Creek and relevant AIWW cuts) lies closer to Stations T3, T5, and T6 than to

NOAA 8720218, this study selected a model calibration Manning’s n value of 0.020 for bed resistance calculation in the waterways.

**Table 3.1** Mean Error, RMSE, and Correlation Coefficients for Water Levels for Various Manning’s n Values at Select Stations during Hydrodynamic Model Calibration

Manning’s n	Location	Mean Error, ME (ft)	Root Mean Square Error, RMSE (ft)	Correlation Coefficient (CORREL)
0.017	Station T3	0.15*	0.35	0.983
0.017	Station T5	0.04	0.24	0.991
0.017	Station T6	-0.30	0.48*	0.983*
0.017	NOAA 8720218	0.17	0.30	0.991
0.020	Station T3	-0.18	0.34	0.985
0.020	Station T5	0.02*	0.23*	0.992
0.020	Station T6	-0.30*	0.50	0.981*
0.020	NOAA 8720218	0.16	0.29	0.991
0.030	Station T3	-0.21	0.31*	0.992*
0.030	Station T5	-0.02	0.25	0.993*
0.030	Station T6	-0.31	0.56	0.974
0.030	NOAA 8720218	0.12*	0.26*	0.992*

Note: \*Best statistical value

For a Manning’s n of 0.020, the comparison of the modeled and measured water levels in Table 3.1 shows mean error ME ranges -0.30 to +0.16 ft at Stations T3, T5, T6, and NOAA 8720218. Given a mean tidal range of approximately 5.16 ft (Station T3), 4.78 ft (Station T5), 5.95 ft (Station T6), and 4.52 ft (NOAA 8720218), the small ME values comprise only less than 0.4% – 5.0% of the mean tidal ranges at these stations. The model-calculated water level compares very well with recorded measurements—with a small RMSE range of 0.23 – 0.50 ft for the 19-day long calibration data set. The calibrated water level parameters—when compared to the measured water levels—resulted in correlation coefficients greater than 0.981. A positive correlation coefficient means modeled water levels increase with increasing measured water levels and vice-versa.

Figure 3.2 and Figure 3.3 show comparison of the calibration model-calculated and measured water level time series (hydrographs) at Stations T3, T5, T6, and NOAA 8720218 over the calibration period. Notably, Station T6 tide gauge was inadvertently installed lower than actual high tides and caused the deviations with high tides on May 4 – 10. In general, except for underestimations at low tides at Station T6 (likely due to unknown recent shoaling at the St. Marys River ocean inlet) and deviations due to local wind setups, Figure 3.2 and Figure 3.3 show very good agreement between data and model-calculated water elevations. Thus, given these very good visual comparisons and favorable statistics, this study considered the HD model’s water level calculation well calibrated.

As tidal flow velocity is the main driving force that will move sediment particles in the AIWW, the model must simulate well the tidal hydraulics to facilitate good estimates of sediment particle transport. As such, for flow velocity model calibration this study compared the May 10, 2019 modeled and measured depth-averaged velocity at Stations V1E, V2E, V2W, V3E, and V3W for various Manning’s

n values. Estimation of statistical tools was deemed unreliable for flow velocity model calibration because there were only 2 – 5 flow velocity measurements at each station on May 10. Therefore, this study relied on visual comparison to compare modeled and measured depth-averaged flow velocity  $V$  for various Manning's  $n$  values. The bed resistance parameter value used in the water level calibration proved adequate to provide best overall statistics with measured flow velocity.

For the calibrated Manning's  $n$  value of 0.020, Figure 3.4 to Figure 3.8 show comparisons of calibration model-calculated and measured depth-averaged flow speed (top plot) at the stations. Positive speed is northward and negative speed is southward. The middle and bottom plots in the figure show comparisons of modeled and measured depth-averaged flow velocity components along the  $x$ -direction (positive eastward) and  $y$ -direction (positive northward). The arrows drawn at the bottom portion of the top, middle, and bottom plots show the modeled and measured directions of the depth-averaged flow velocity. The arrows' directions are consistent with measurements except for very few times during tide slack and high wind events when local wind affects deflected or reversed measured flow direction. Expectedly, during flood and ebb flows, the flow velocity  $V_y$  component is the dominant flow velocity component. Thus, the top and bottom plots share very similar comparison trend between modeled and measured values.

The top, middle, and bottom plots in Figure 3.4 to Figure 3.8 show the calibrated model generally simulated very well the depth-averaged flow velocity magnitude (speed) and direction ( $V_x$  and  $V_y$  components) with the best comparison during times when local wind effects were minimal. High winds characterized the few times when modeled values deviated much from measurements. For example, the Fernandina Beach Municipal Airport and Mayport Pilot wind stations recorded 10 – 14 mph sustained southeasterly winds on May 10, 2019 (see Figure 2.3 and Figure 2.4) that reduced measured eastward-directed  $V_x$  and southward-directed  $V_y$ . In Figure 3.5, these strong and sustained southeasterly winds decreased measured southward velocity and caused the large deviation in modeled flow velocities from 11 a.m. to 2 p.m. Conversely, the southeasterly winds increased the measured northward flow velocities and caused the model underestimation between 2 p.m. to 4 p.m. In Figure 3.7 and Figure 3.8, southeasterly winds decreased the southward measured flow velocity and caused the model overestimations at between 12 p.m. and 2 p.m.

Based on favorable comparison statistics and very good visual comparisons of the model and measured flow velocity magnitude and directions (velocity components), the model is deemed well calibrated to transport sediment in the AIWW and nearby areas.

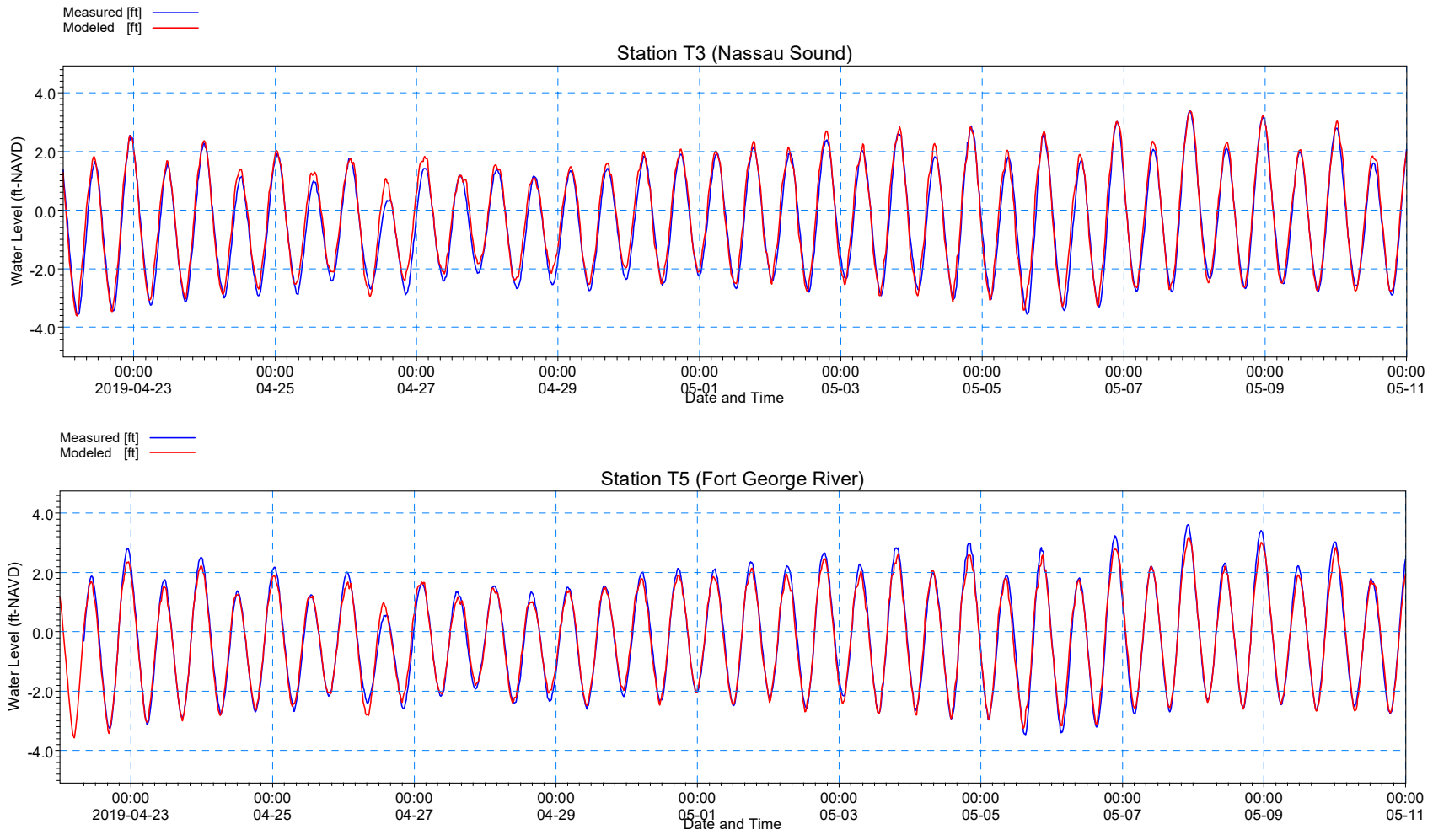


**Figure 3.2** Comparison of Modeled and Measured Water Levels at Stations T3 and T5 (Calibration Period)

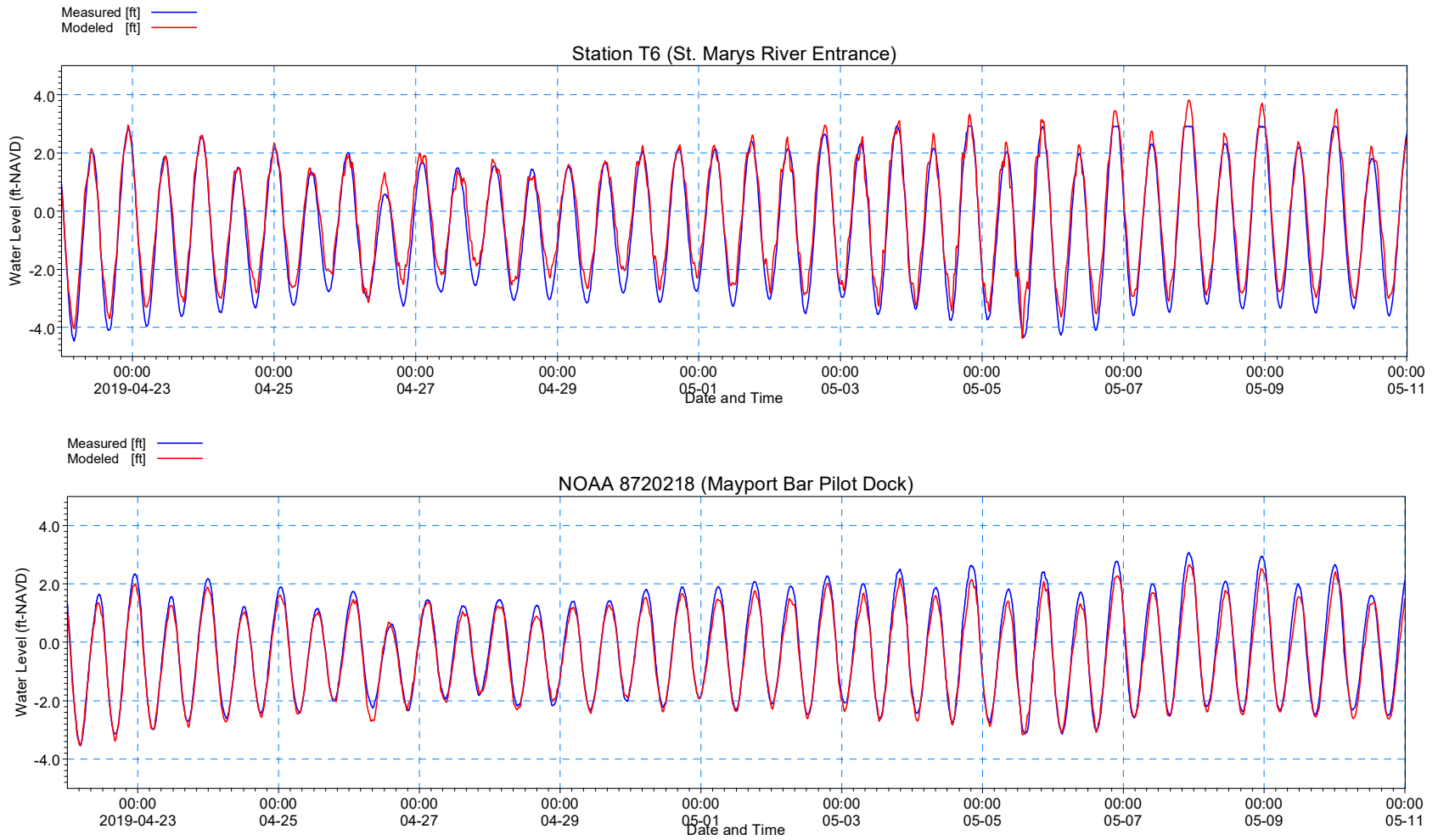


**Figure 3.3** Comparison of Modeled and Measured Water Levels at Stations T6 and NOAA 8720218 (Calibration Period)

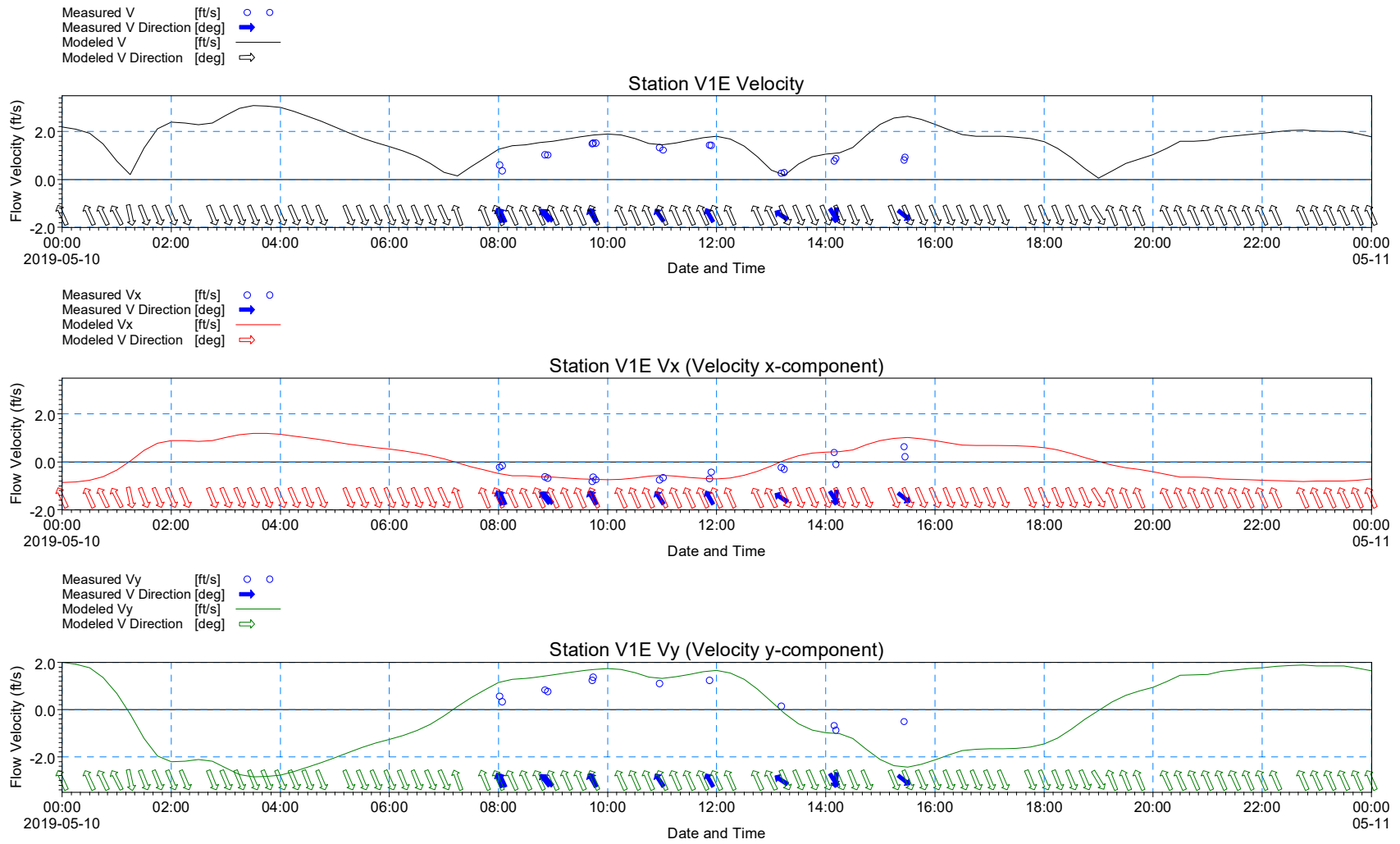


**Figure 3.4** Comparison of Modeled and Measured Velocity and Components at Station V1E (Calibration Period)

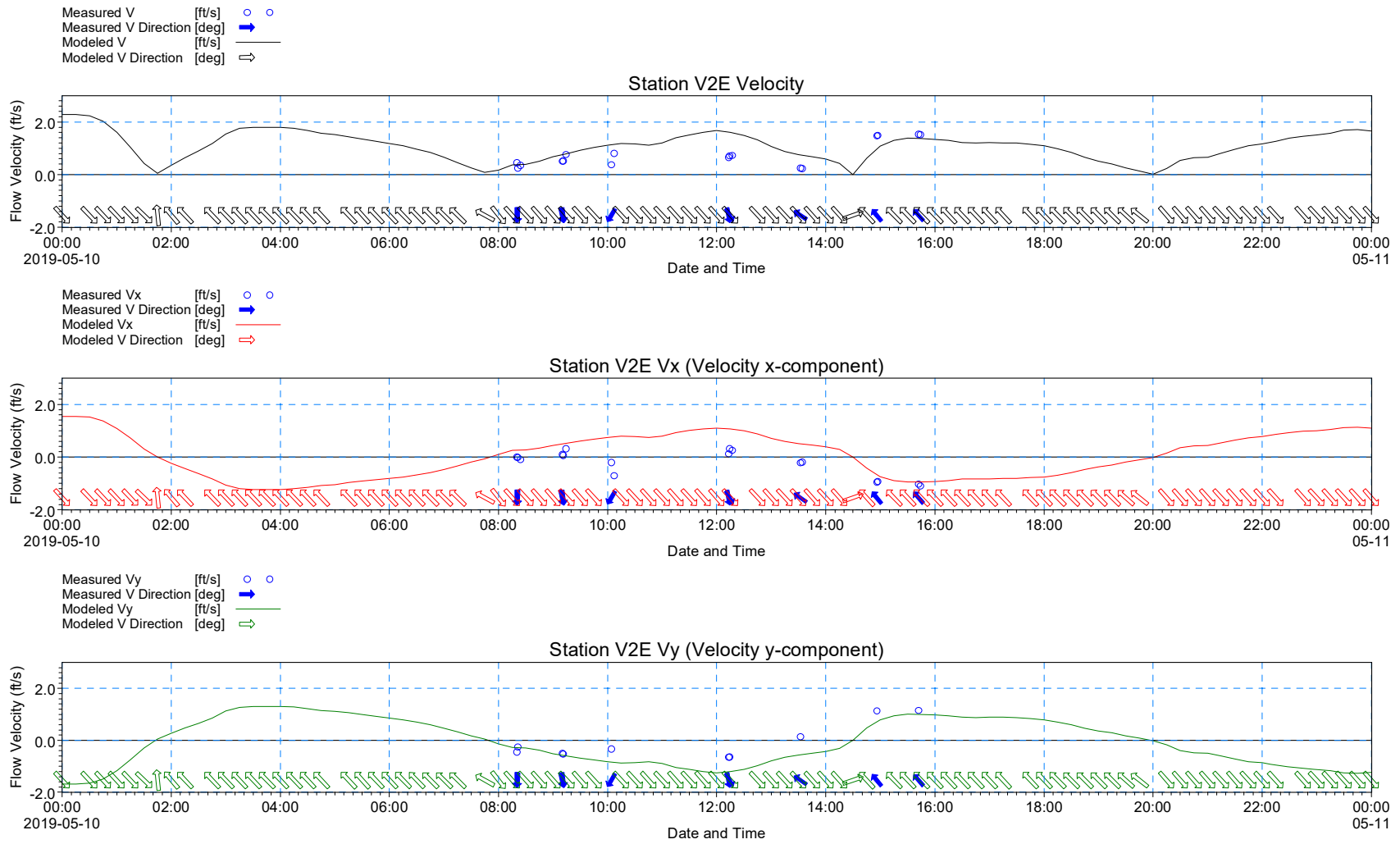


Figure 3.5 Comparison of Modeled and Measured Velocity and Components at Station V2E (Calibration Period)

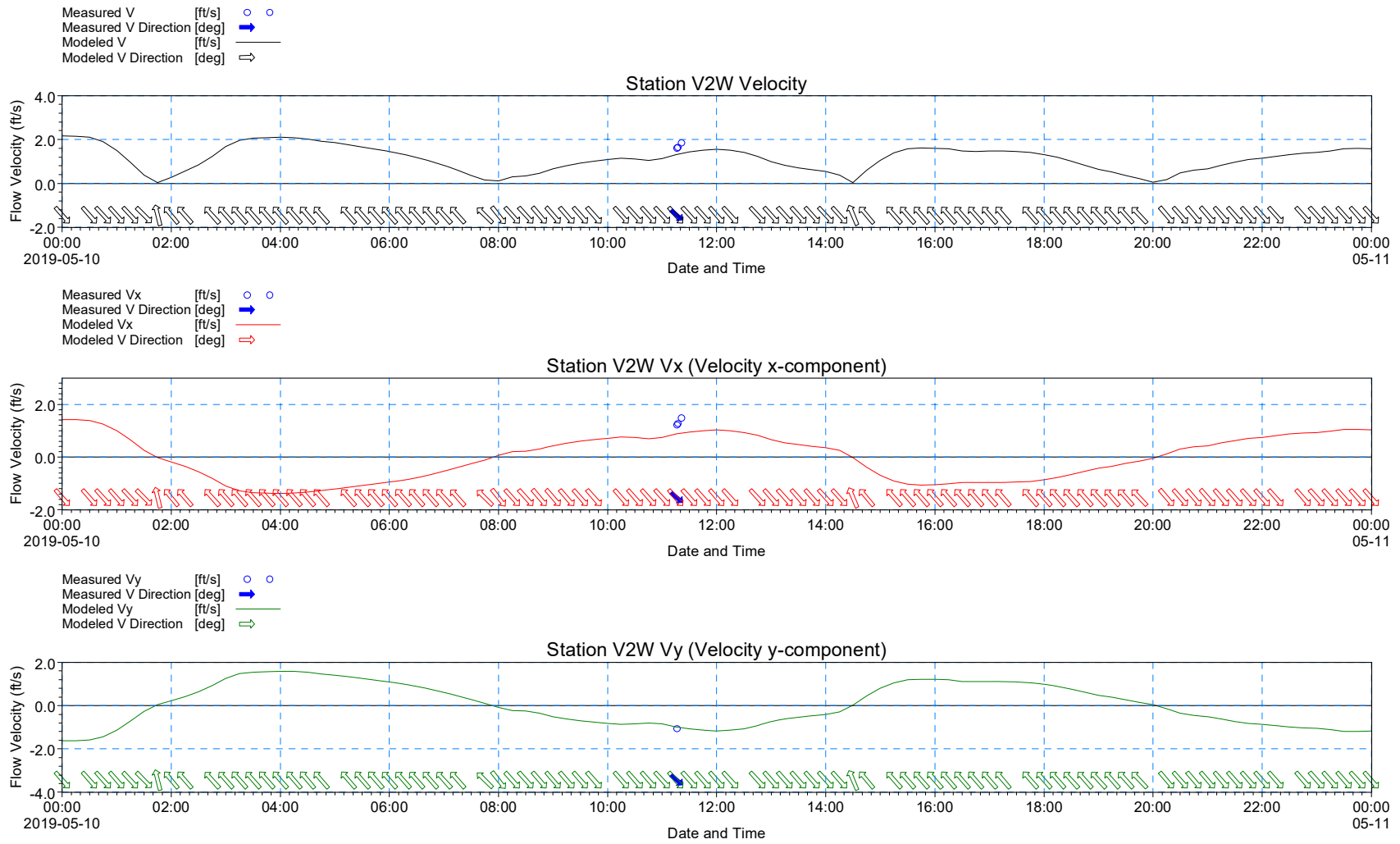


Figure 3.6 Comparison of Modeled and Measured Velocity and Components at Station V2W (Calibration Period)

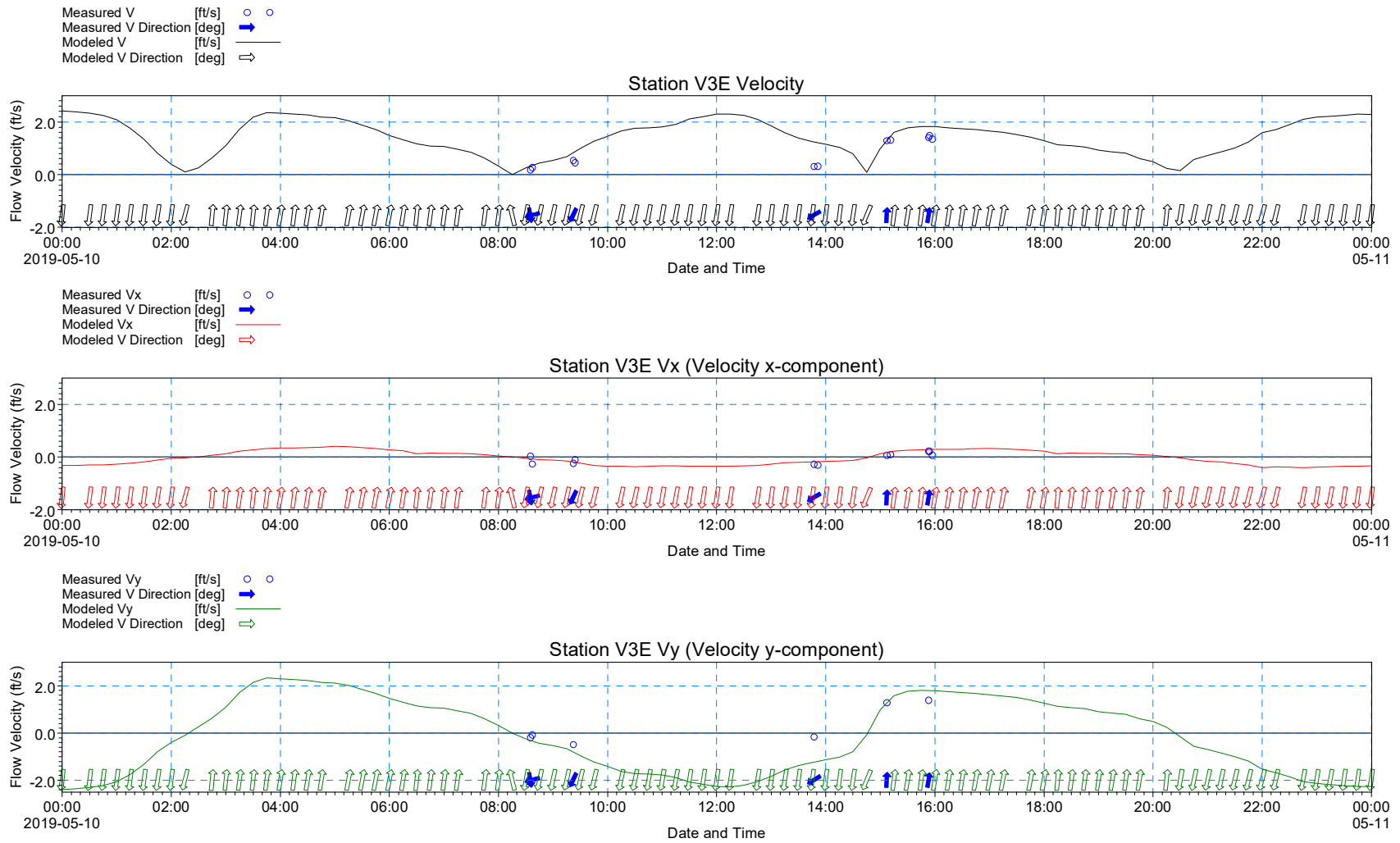
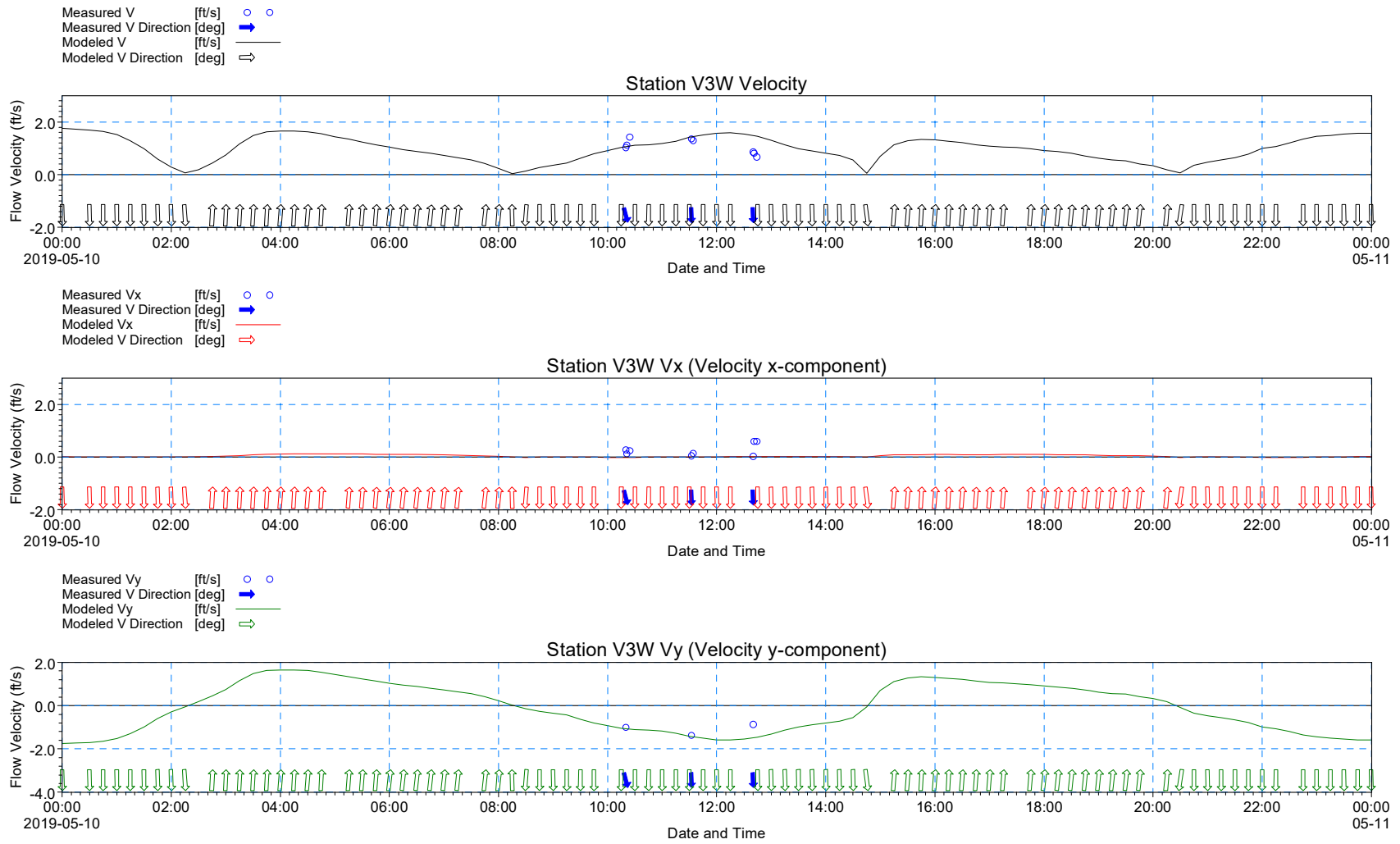


Figure 3.7 Comparison of Modeled and Measured Velocity and Components at Station V3E (Calibration Period)



**Figure 3.8** Comparison of Modeled and Measured Velocity and Components at Station V3W (Calibration Period)

### 3.1.1 Hydrodynamic Model Verification

Model verification ensures that the model parameters set to achieve good model performance during the calibration period also apply to simulations outside the calibration period. To verify the performance of the model with other data sets, this study selected the period May 11 – 22, 2019 as verification period. This study applied the model parameters as adjusted in model calibration to model verification so that the model verification simulation applied the same parameters as the calibration runs.

Comparison of model-calculated tide levels with the measured tide levels at Stations T3, T5, T6, and NOAA 8720218 verified the model performance. Table 3.2 provides the mean error, RMSE, and correlation coefficient that relate modeled and measured water levels at the station for various Manning's n values during model verification. In an indication of a well-calibrated model, the computed water surface elevations for Manning's n value of 0.020 in the waterways provides the best overall modeled and measured water level comparison statistics at Station T5 and a very close second best overall modeled and measured water level comparison statistics at Stations T3 and T6 (when compared to Manning's n value of 0.017). Manning's n value of 0.030 provided best statistics at NOAA 8720218. , This study selected a Manning's n value of 0.02 for the hydrodynamic model because (a) a Manning's n value of 0.02 provided best statistics (particularly ME) at model water level calibration and verification at Stations T3, T5, and T6; and it is nearer to Manning's n values applied in the FEMA Northeast Florida-Georgia Version 12b ADCIRC Model Mesh.

For a Manning's n value of 0.020, model results deviate from the 12-day long verification data set with a mean error range of -0.37 to 0.18 ft. The mean error is 1.3% to 6.2% of the mean tide range and the RMSE ranged only 0.25 – 0.57 ft at the select stations. The modeled water level—when compared to the measured data—resulted in correlation coefficient range of 0.983 – 0.993. The correlation range between measured and modeled water levels indicates very good agreement between modeled and measured water levels. Based on the very good statistics on comparison between the modeled and measured water levels, this study deems the HD model well verified to provide estimates of water levels in the project area.

Figure 3.9 and Figure 3.10 show comparison of the model-calculated and measured water level time series (hydrographs) at Stations T3, T5, T6, and NOAA 8720218 over the verification period. As in the model calibration, the plots show the applied model boundary conditions along the ocean's boundaries reproduce well the measured water levels at the select stations. Station T6 tide gauge was inadvertently installed lower than actual high tides and caused the May 14 – 21 high tide deviations. Except for deviations due to local wind setups, the figures show very good agreement between data and model-calculated water elevations.

Figure 3.11 to Figure 3.16 shows comparisons of modeled and measured depth-averaged flow speed (top plot) at select stations for the verification period. The middle and bottom plots in the figure show comparisons of modeled and measured depth-averaged flow velocity components along the x-direction (positive eastward) and y-direction (positive northward). Except near tide slacks, the arrows at the bottom in the top, middle, and bottom plots show the modeled depth-averaged flow velocity directions were consistent with the measured depth-averaged flow velocity directions. The top, middle, and bottom plots in Figure 3.11 to Figure 3.16 show the calibrated model generally simulated very well the depth-averaged flow velocity magnitude (speed) and direction ( $V_x$  and  $V_y$  components) with the best comparison during times when local wind effects were small. High winds characterized the few

times when modeled values deviated much from measurements. For example, the Fernandina Beach Municipal Airport and Mayport Pilot wind stations recorded 8 – 20 mph sustained southwesterly winds in the morning, northwesterly winds just before noon, and southeasterly winds in the afternoon on May 17, 2019 (see Figure 2.3 and Figure 2.4). In Figure 3.12, the morning southwesterly winds reduced measured southward-directed  $V_y$  and caused the model overestimation shown, the noon northwesterly winds increased measured eastward-directed  $V_x$  and southward-directed  $V_y$  that caused the model underestimation of  $V$  between 12 p.m. and 2 p.m. In Figure 3.13, the morning southwesterly winds increased the northward measured  $V$  and caused the model underestimations between 8 a.m. and 12 p.m.

Based on favorable comparison statistics and very good visual comparisons of the model and measured flow velocity magnitude and directions (velocity components) at select stations, the model is deemed well verified to transport sediment in the AIWW and nearby waterways.

**Table 3.2** Mean Error, RMSE, and Correlation Coefficients for Water Levels for Various Manning’s  $n$  Values at Select Stations during Hydrodynamic Model Verification

Manning’s $n$	Location	Mean Error, ME (ft)	Root Mean Square Error, RMSE (ft)	Correlation Coefficient (CORREL)
0.017	Station T3	-0.19	0.45	0.981
0.017	Station T5	-0.04*	0.27	0.992
0.017	Station T6	-0.37	0.55*	0.985*
0.017	NOAA 8720218	0.21	0.35	0.992
0.020	Station T3	-0.19*	0.42	0.984
0.020	Station T5	-0.06	0.25*	0.993*
0.020	Station T6	-0.37*	0.57	0.983
0.020	NOAA 8720218	0.18	0.32	0.992
0.030	Station T3	-0.24	0.36*	0.991*
0.030	Station T5	-0.13	0.31	0.993
0.030	Station T6	-0.38	0.64	0.976
0.030	NOAA 8720218	0.11*	0.28*	0.993*

Note: \*Best statistical value

### 3.1.1 Hydrodynamic Model Parameter Sensitivity Analysis

Performance of several HD model parameter sensitivity runs provided information on the influence of various model bed resistance values (e.g., Manning’s  $n$  values from 0.017 – 0.030) on flow velocity. Comparisons of the modeled and measured water level statistics and flow velocity data indicated the most appropriate values to apply for the study area. The sensitivity analysis shows model-calculated water level and flow velocity changed very little with bed resistance in the Manning’s  $n$  value range of 0.017 – 0.020 and provided slightly worse statistics on modeled and measured water level verification mean error comparisons with a Manning’s  $n$  value of 0.030 at Stations T3, T5, and T6. Thus, based on the model calibration and verification statistics, application of a bed resistance Manning’s  $n$  of 0.020 provides the best overall HD model validation.

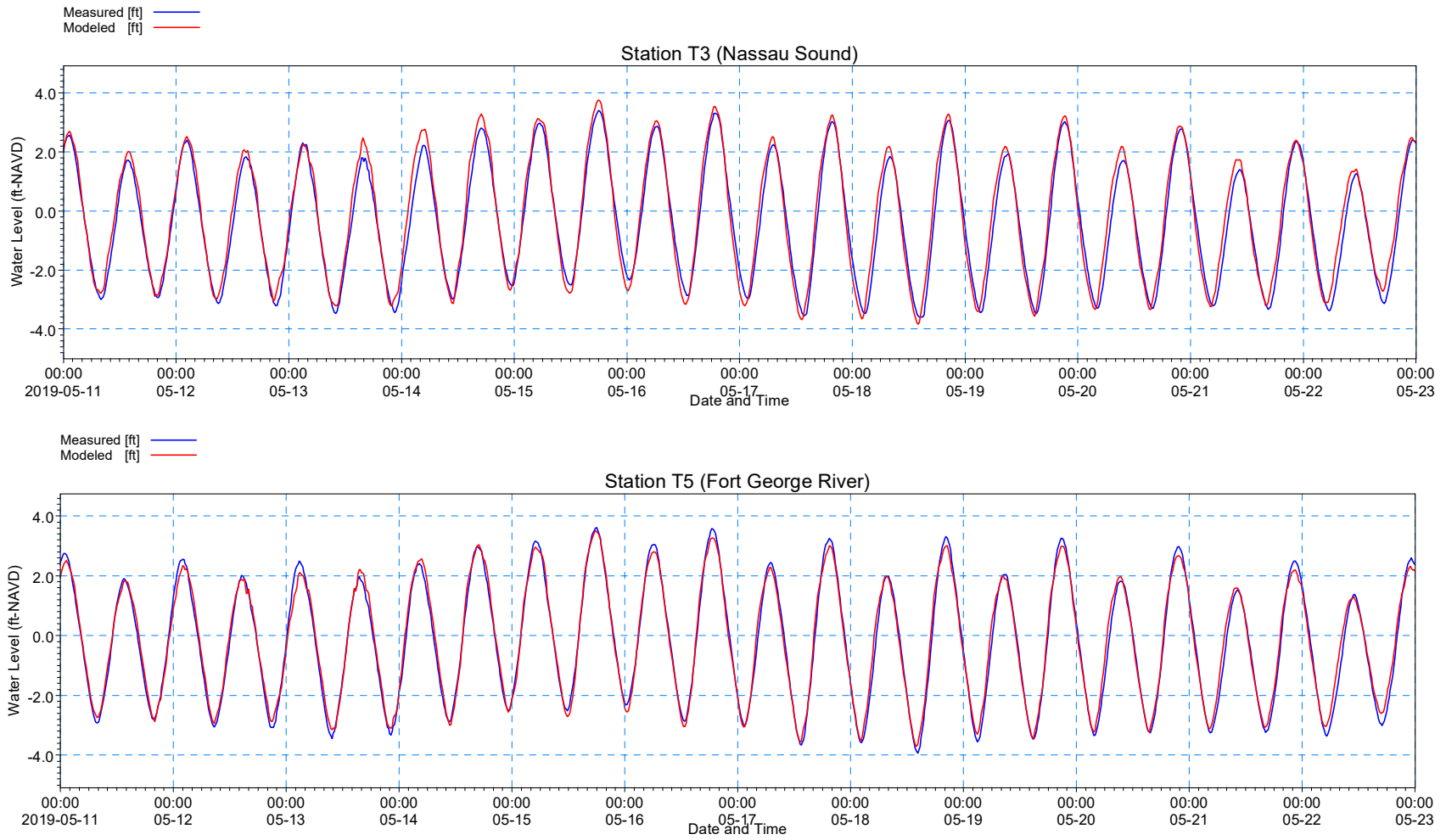


**Figure 3.9** Comparison of Modeled and Measured Water Levels at Stations T3 and T5 (Verification Period)

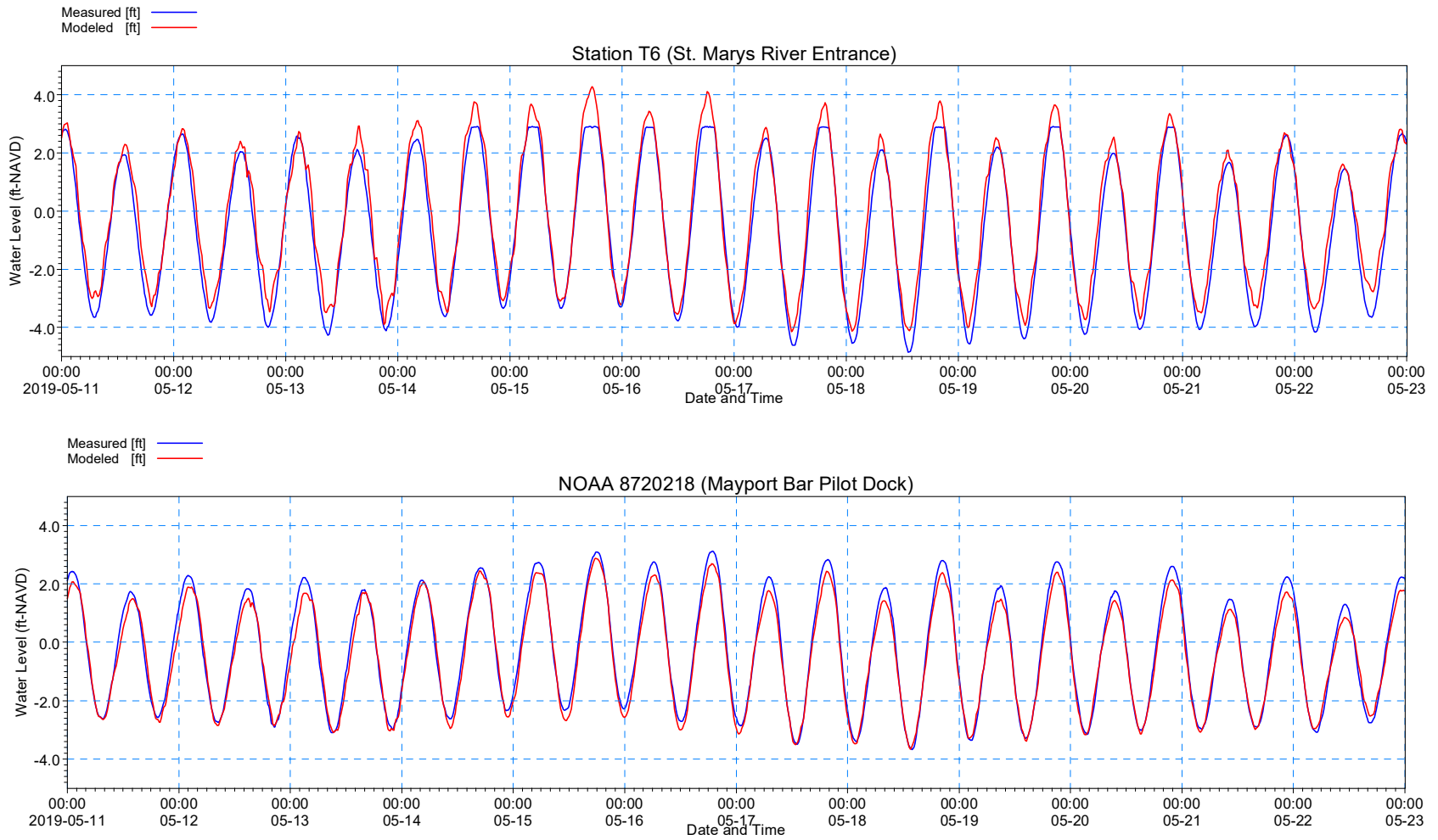


**Figure 3.10** Comparison of Modeled and Measured Water Levels at Stations T6 and NOAA 8720218 (Verification Period)

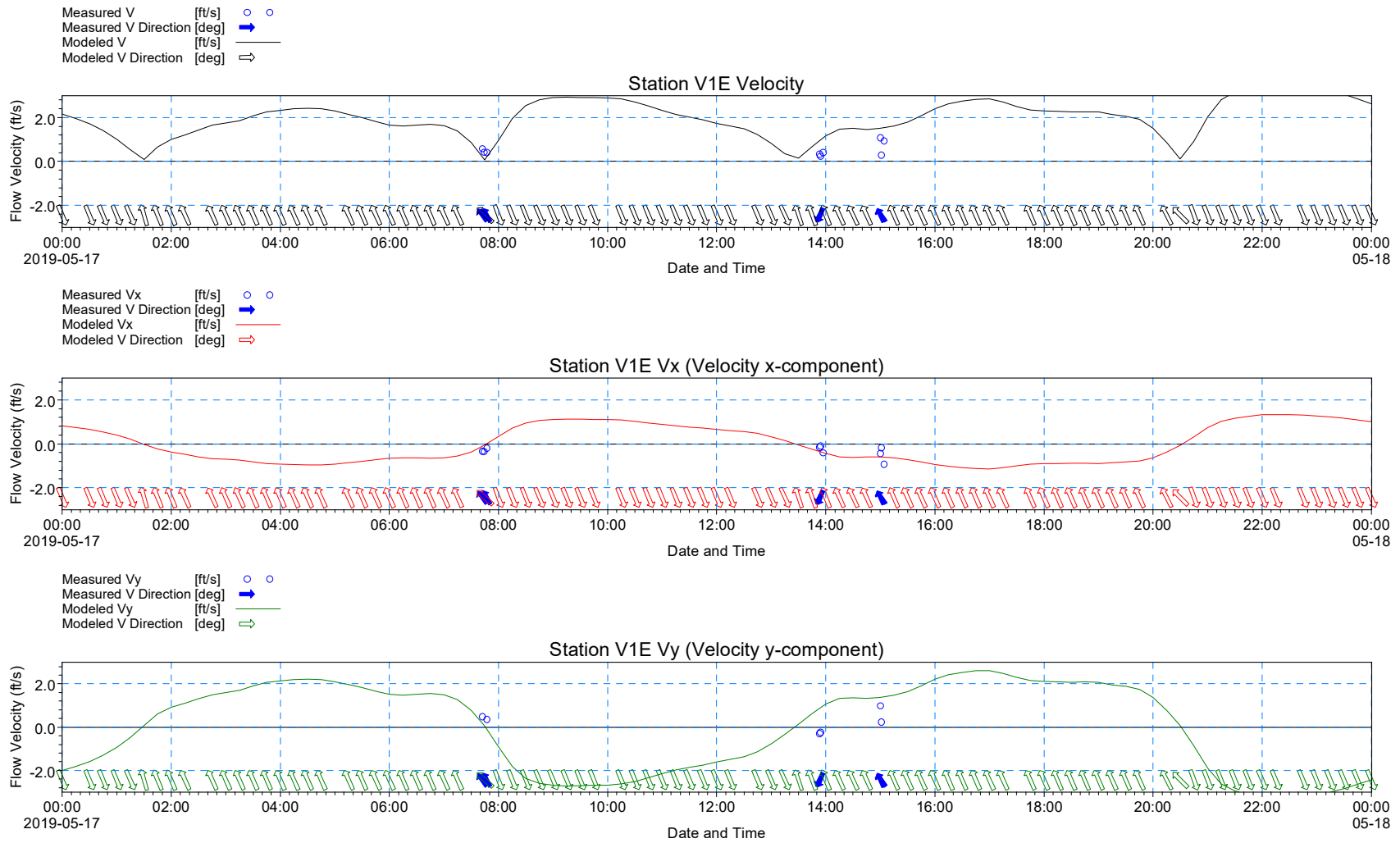
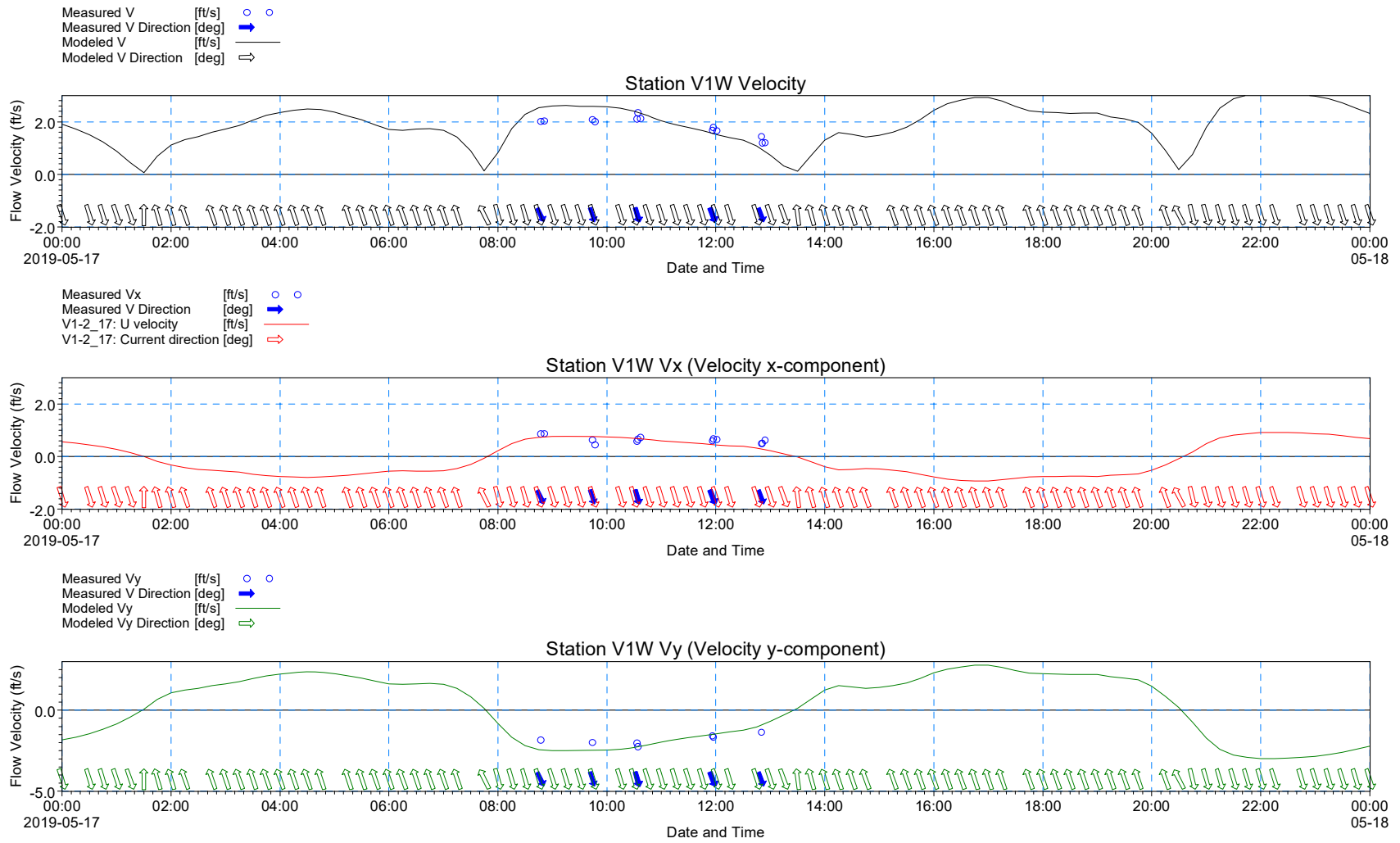


Figure 3.11 Comparison of Modeled and Measured Velocity and Components at Station V1E (Verification Period)



**Figure 3.12** Comparison of Modeled and Measured Velocity and Components at Station V1W (Verification Period)

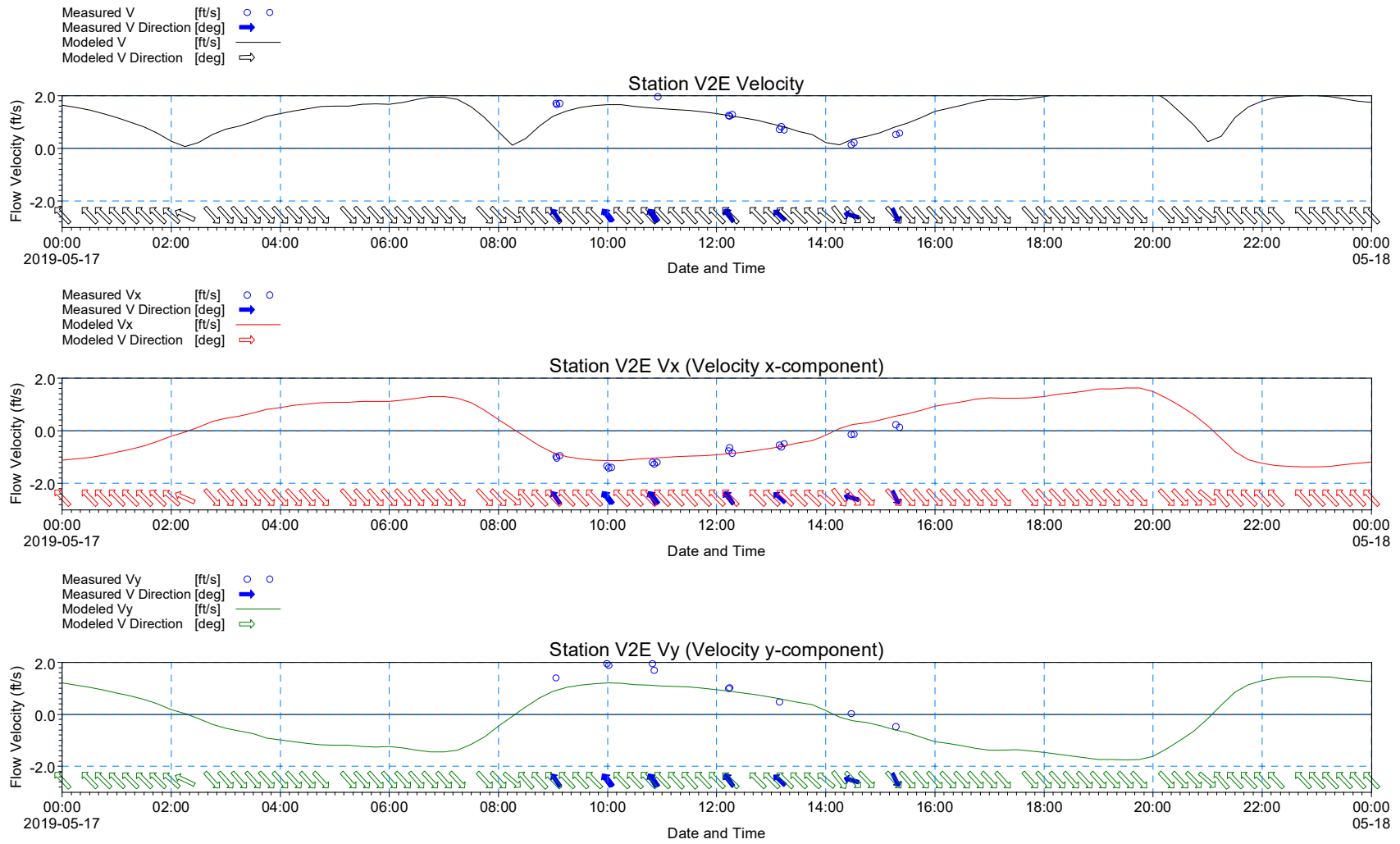


Figure 3.13 Comparison of Modeled and Measured Velocity and Components at Station V2E (Verification Period)

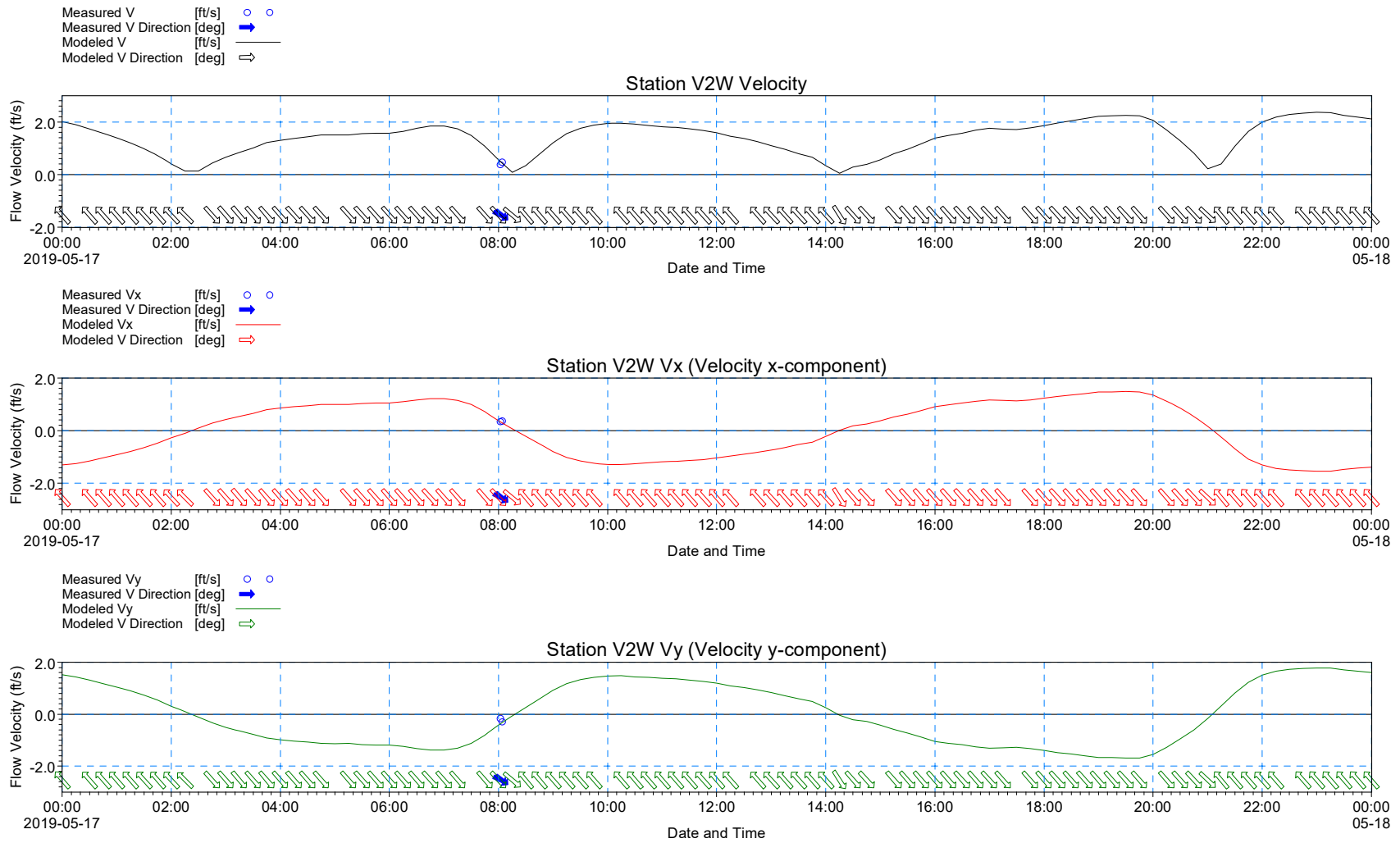


Figure 3.14 Comparison of Modeled and Measured Velocity and Components at Station V2W (Verification Period)

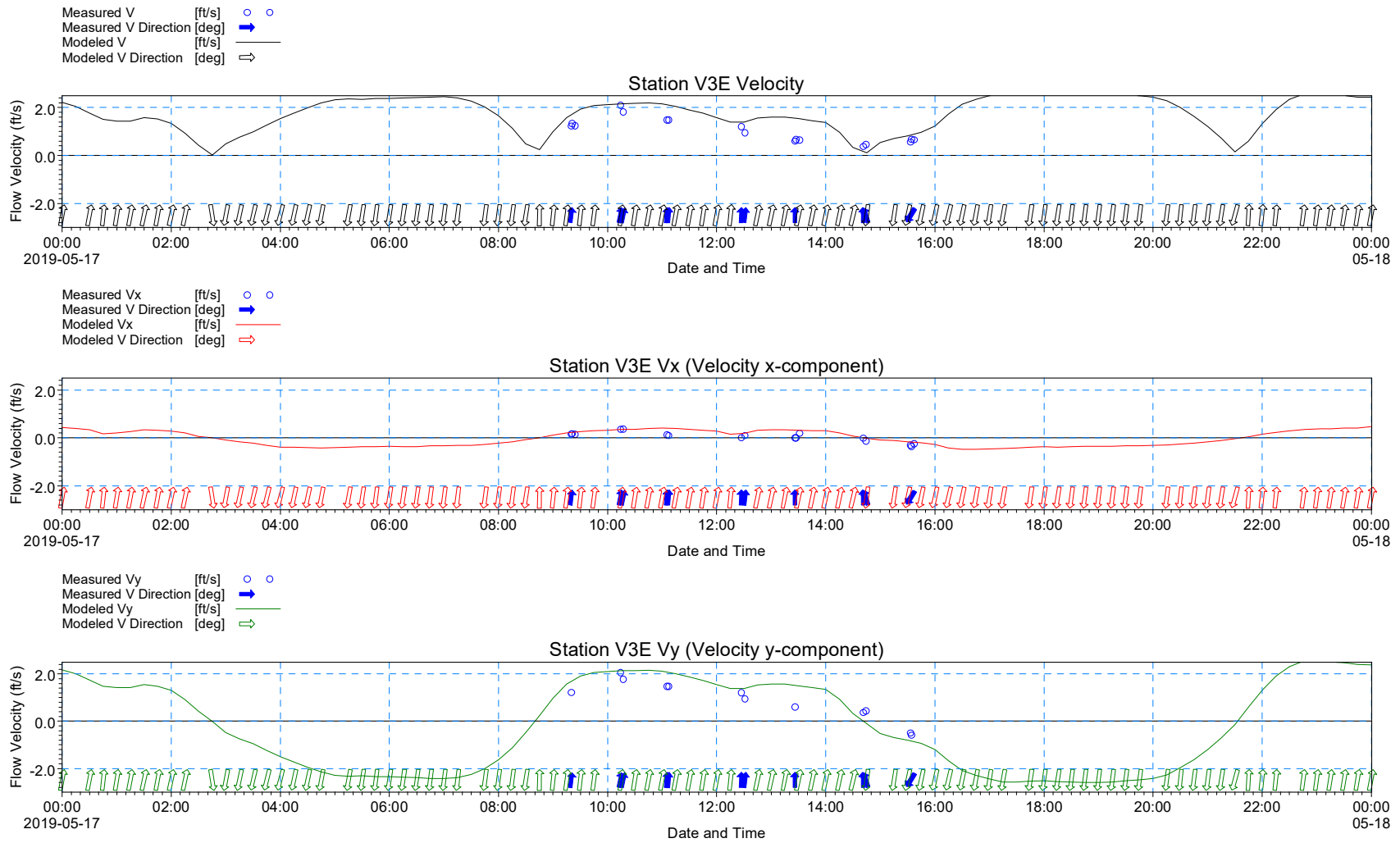


Figure 3.15 Comparison of Modeled and Measured Velocity and Components at Station V3E (Verification Period)

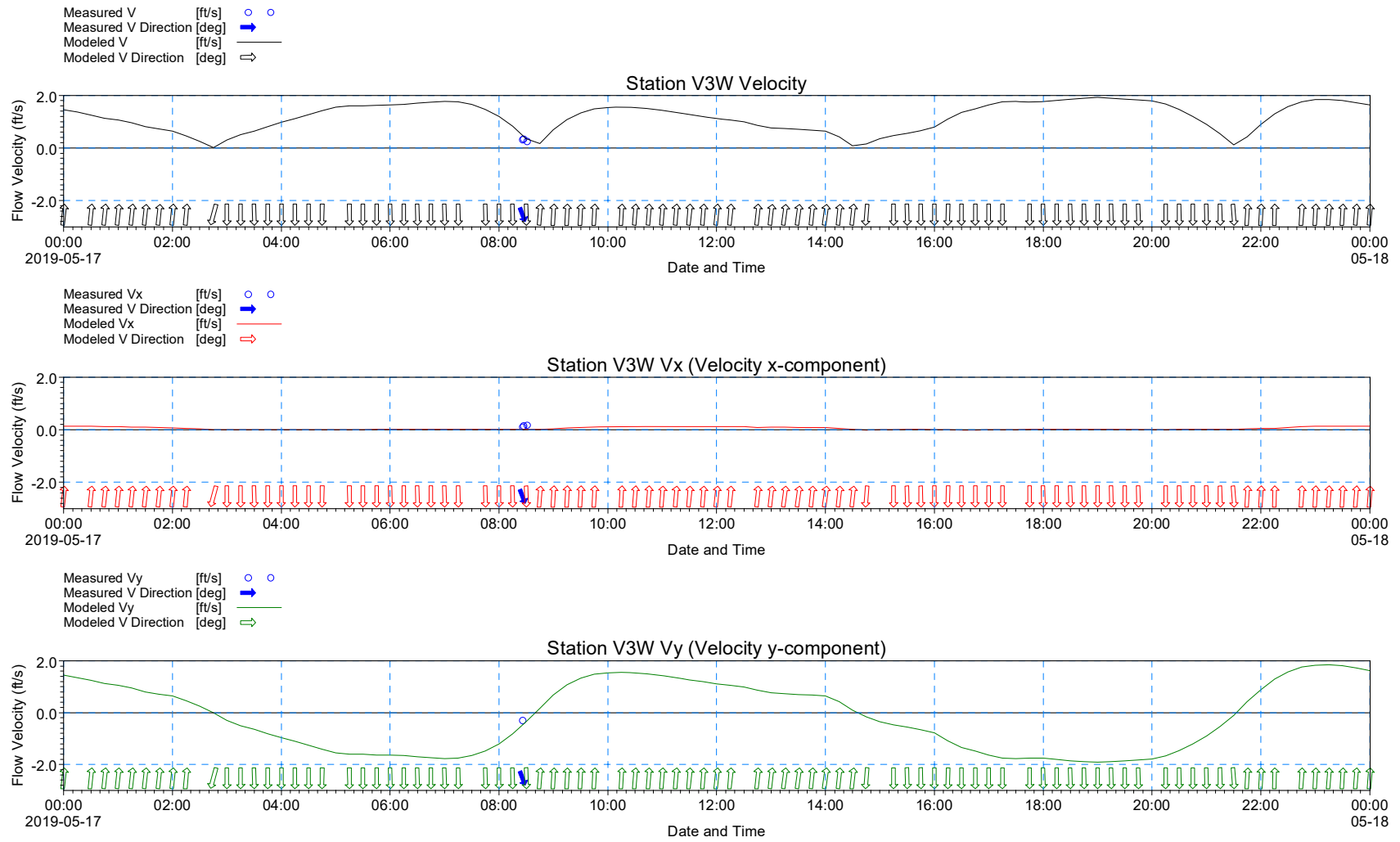


Figure 3.16 Comparison of Modeled and Measured Velocity and Components at Station V3W (Verification Period)

## **3.2 Wave Model (SW)**

The MIKE21 FM SW spectral wave model simulates growth, decay, and transformation of wind-generated waves and swell. The spectral wave model requires wave parameters or wind-sea and swell parameters at its boundaries. Given wave parameters at the boundaries, the SW model employs finite volume methods to solve the spectral wave action balance equation and produce representative discrete two-dimensional wave action density spectra. Model capabilities include refraction due to depth variations; wave-current interaction; diffraction by phase-decoupled refraction-diffraction approximation; non-linear wave-wave interaction; and dissipation due to wave breaking, bottom friction, and white-capping.

### *3.2.1 Wave Model Setup*

The wave model uses the same mesh constructed for the HD model. As such, the wave model and HD models share the same domain. The wave model applied a lateral boundary at the ocean north and ocean south boundaries. WIS Station 63402 hindcasted wave data that consists of significant wave height, peak wave period, and mean wave direction provided the offshore boundary data. The study applied no (zero) waves at the inshore model boundaries because wind-generated waves from these boundaries will not significantly affect AIWW and nearshore hydraulics.

### *3.2.2 Wave Model Parameters*

Parameters that can influence wave propagation in the SW model with directionally-decoupled parametric formulation include bottom friction and breaking parameters. Among the parameter options available for including wave breaking in the model, the specified default gamma option—equal to a constant 0.8—consistent with the breaking criterion associated with the ratio of wave height and water depth (0.78) at the wave breaking point was applied in the SW model. Note that for this study, the only reason to calibrate the wave breaking parameters was to establish the location of wave breaking and not to accurately simulate surf zone wave characteristics. Finally, based on DHI (2019) recommendations, this study applied Nikuradse roughness parameter of 0.003 – 0.131 ft (0.001 – 0.040 m) (i.e., 0.003 ft in shallow inshore areas and 0.131 ft in offshore areas).

## **3.3 Sediment Transport Model (ST)**

MIKE21 FM ST simulates non-cohesive (sand) sediment transport by using the flow velocity results from the HD model to calculate the movement of both bed load and suspended sediment. For purely tide-generated flows, the MIKE21 FM ST provides the Engelund and Hansen, van Rijn, and Engelund and Fredsøe formulas for bed load and suspended sediment. For combined tide-generated and wave-generated flows, the model provides a look-up table of sediment transport for MIKE21 ST calculations. The MIKE21 ST morphology calculation provides the change in bed elevation from model-calculated sediment erosion and deposition.

The sediment transport model uses the same mesh constructed for the HD model. As such, all three models (hydrodynamic, wave, and sediment transport) share the same domain. The study applied zero sediment flux gradient at the boundaries of the sediment transport model. Given the considerable distances between model boundaries, this assumption will not significantly affect sediment transport at AIWW and nearby nearshore areas.

Surface grab samples in Sawpit Creek and nearby waterways (see Figure 2.14) provided the sediment characteristics applied in the model. Table 2.4 provides the sediment grab samples gradation data. Using the data from this table, this study developed an average median grain size diameter  $D_{50}$  of 0.16 mm and average grading coefficient of 2.5 to define the median grain size and gradation input in the ST model.

The ST model calculates the resulting transport of non-cohesive materials based on flow conditions from the HD model and wave radiation conditions from the SW model. As the HD and SW model results were applied as input to the ST model, this study applied combined currents from tides and waves as the driving mechanism for sediment transport. For combined current and waves, the sediment transport rates are found by interpolation from a sediment transport table. The Generation of Q3D Sediment Transport Tables tool in MIKEZero created the sediment transport table.

### 3.4 Sediment Particle Tracking Model (PT)

The sediment particle tracking (PT) model uses the flow velocity field calculated by the HD model to compute the movement of deposited, eroded, and suspended sediment particles. The PT model can (a) use the same model mesh as the HD model; (b) simulate the fate of the dredged material sediment plume; and (c) simulate the transport, erosion, and deposition of multi-class sediments from stationary or moving sources and sinks to identify potential sources of sediment erosion and locations of deposition.

The PT model requires as model input sediment properties that can include sediment settling rate, critical shear stress for erosion, and mass rate of dredged material release into the water column (for analysis of fate of dredged material plume). The PT model can simultaneously simulate multi-class sediments (i.e., sediments with various sizes and characteristics) that flow in (sediment mass source rate) or out (sediment mass sink rate) at different time-varying (or time constant) horizontal locations. Model capabilities include application of dispersion by scaled eddy viscosity; and simulation of spatially- and temporally-varying suspended and deposited dredged material transport, sediment erosion and resuspension, and sediment deposition.

PT model validation requires field measured data of the sediment settling rate, critical shear stress for erosion, and mass rate of dredged material release into the water column (for analysis of fate of dredged material plume). Unfortunately, this data from past dredging events at the Sawpit Creek area is not presently available. In lieu of PT model validation, this study used established data and equations in literature to estimate the required PT model input data.

#### 3.4.1 Empirical Estimation of Sediment Settling Velocity

Suspended sediments settle due to gravitational forces. Settling time and velocity depend on the size and specific gravity of the suspended particle and water temperature. As direct measurements of settling velocity from sediment samples are unavailable, this study presents three methods to estimate settling velocity based on Reynold's Number,  $Re = (v_s D_{50} / \nu)$ :

1. If  $Re < 1$ , Stoke's law suggests that

$$v_s = \frac{(SG_{\text{sediment}} - 1)D_{50}^2 g}{18\nu} \quad \text{Equation 3.4}$$

where  $v_s$  is settling velocity in ft/s,  $SG_{\text{sediment}}$  is specific gravity of sediment (2.65),  $D_{50}$  is median grain size of sediment in ft,  $g$  is gravitational acceleration and  $\nu$  is kinematic viscosity of water in  $\text{ft}^2/\text{s}$  ( $1.134215 \cdot 10^{-5} \text{ft}^2/\text{s}$ ). Calculation of settling velocity is an iterative procedure as Reynold's number depends on settling velocity.

2. If  $1 < Re < 2000$ , Figure 3.17 provides settling velocity estimates for spherical particles. Figure 3.17 can overestimate settling velocities because it does not consider irregularly shaped particles.
3. If  $Re > 2000$ , Newton's first law of motion provides

$$v_s = \sqrt{\frac{4gD_{50}(SG_{\text{sediment}}-1)}{3C_D}} \quad \text{Equation 3.5}$$

where  $C_D$  is the drag coefficient ( $C_D = \frac{24}{Re}$ ).

Empirical estimation of sedimentation rates employs the following assumptions for settling velocity calculations:

- The sediment particles settle continuously until the particles deposit at the bottom of the channel.
- Particle interactions, cross currents, and water temperature do not significantly affect settling velocities.

Using any of the above methods, this study applied a sand settling velocity of 0.08 ft/s in the PT model.

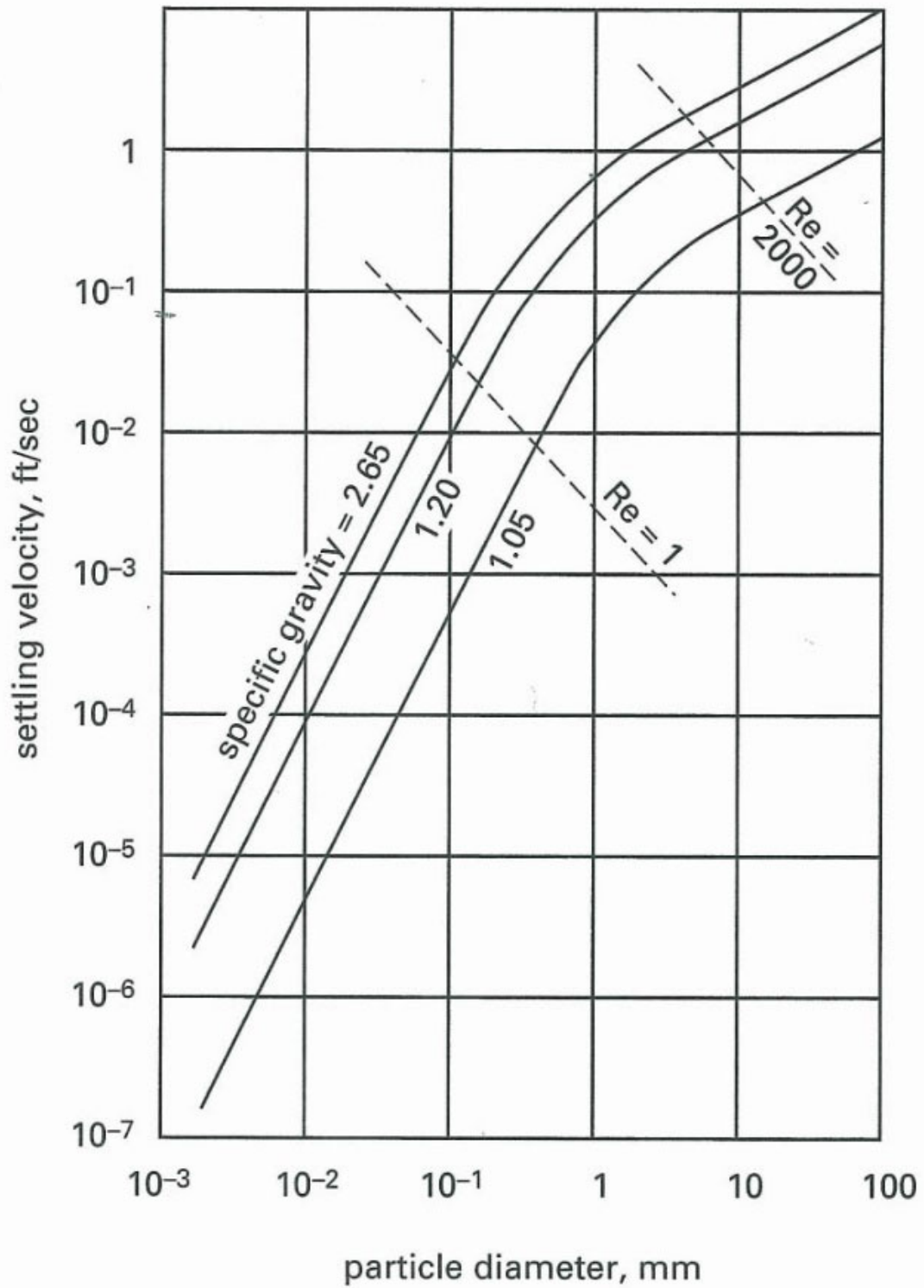


**Figure 3.17** Settling Velocity Diagram for  $1 < Re < 2000$

### 3.4.2 Estimation of Critical Velocity for Sediment Erosion and Re-suspension

Critical shear stress  $\tau_c$  is the shear stress from water flow that initiates sediment erosion. Given the water temperature, the solid black line in Shield's Diagram (Figure 3.18) provides the means to estimate the critical shear stress  $\tau_c$  for a given sediment median diameter  $D_{50}$ . Notably, the diagram provides (a) six lines for water temperatures 32°, 40°, 50°, 60°, 70°, and 80° Fahrenheit when  $D_{50} < 0.8$  mm; (b) two lines (for water temperature 32° and 80° Fahrenheit) when  $0.8 \text{ mm} < D_{50} < 6.0 \text{ mm}$ ; and (c) one line when  $D_{50} > 6.0 \text{ mm}$ .

Equation 3.6 provides the relationship between critical depth-averaged velocity  $V_c$ , water mass density  $\rho$ , water depth  $h$ , and critical shear stress  $\tau_c$ . Sediment transport (i.e., erosion) occurs when the flow velocity exceeds the critical velocity  $V_c$ .

$$V_c = 2.5 \ln \left( \frac{11h}{k_s} \right) \sqrt{\frac{g \tau_c}{\rho}} \quad \text{Equation 3.6}$$

where  $k_s$  is roughness length approximated at  $k_s = 20 * D_{50}$  and  $g$  is the acceleration due to gravity.

Alternatively, for initiation of erosion/resuspension, Table 7 in Berenbrock and Tranmer (2008) (<https://pubs.usgs.gov/sir/2008/5093/table7.html>) provides a table for various sediment size ranges. The table provides critical shear stresses of 0.110 – 0.194 newtons per square meter ( $\text{N/m}^2$ ) for sand with median grain size of 0.09 – 0.21 mm.

Consistent with the abovementioned table, Figure 3.18 and Equation 3.6 provide as input to the PT model a critical shear stresses of approximately 0.17  $\text{N/m}^2$  for a sediment median grain size  $D_{50} = 0.16 \text{ mm}$ .

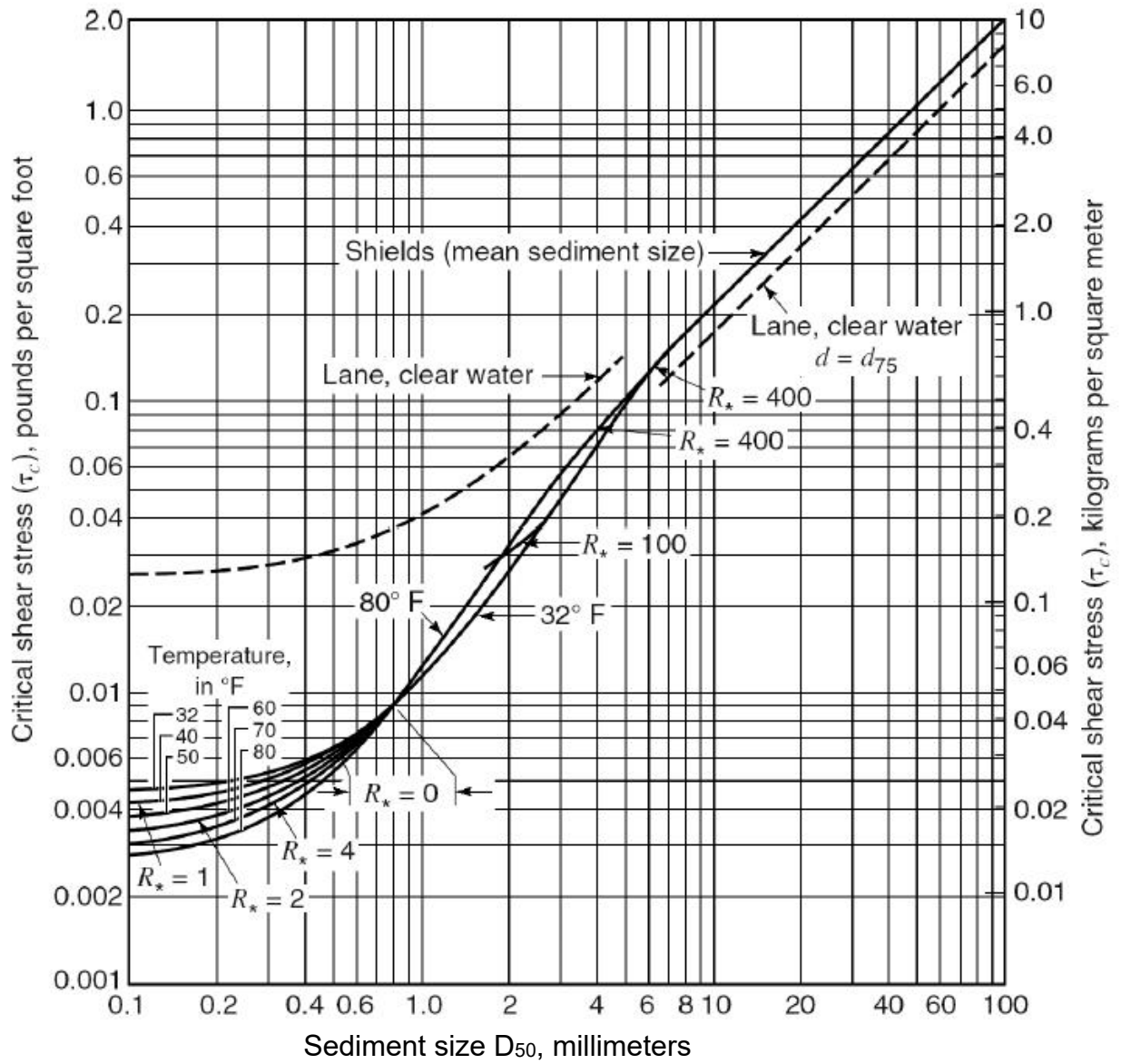


Figure 3.18 Shield's Diagram

#### **4.0 EVALUATION OF PERFORMANCE OF SHOALING-REDUCTION DESIGNS**

Selection of the locations of sediment basins requires understanding of the sources and pathways of sediment transport. The sediments in the AIWW, from Cut-1 in Duval County to Cut-N-FHP-10 in Nassau County, come from nearshore and upland areas. However, for most of this study's area of interest from Cuts 23 – 27N, sediments come mainly from Atlantic Ocean nearshore erosion that enters any of the four nearby inlets—St. Marys River mouth, Nassau Sound, Fort George River mouth, and St. Johns River mouth. In the nearshore areas, wave breaking primarily causes sediment to erode, suspend, and move in the alongshore direction of wave propagation. The tide- and wave-induced currents move the sediments from the nearshore area, through inlets, and through the AIWW until currents weaken and deposit the sediment on the channel bed. As currents become stronger, currents can erode the deposited sediment, bring the sediment to suspension, and move the sediment farther in the direction of flow.

The AIWW and nearby waterways experience bi-directional flow—inshore at flood and offshore at ebb. Thus, the sediments can move northward and southward in the AIWW until they finally deposit at locations where prevailing currents can no longer erode them. Locations where most of the transported sediments finally deposit experience large shoaling rates. Since 2006, these locations include Cuts 24, 25, 26, 26A, and 27 in Duval County and Cut-27A, Cut-27C, and Cuts 27G – 27M in Nassau County. Historical dredging records show the largest shoaling volumes occur in Cut-27A and Cut-27C. Cuts 27G – 27M lie in an area where Amelia River widens northward then meanders eastward. This river widening and meandering slow down both flood and ebb flows, induce sediment deposition, and likely is the main reason for shoaling at Cuts 27G – 27M.

This chapter aims to determine sediment sources and pathways that lead to high shoaling rates at Cut-23 – Cut-27N and find suitable locations of sediment deposition basin and/or structures to reduce shoaling. The paragraphs below describe the (1) analysis to identify sources of sediments; (2) delineation of sediment transport pathways and alternative designs to reduce shoaling at select locations; and (3) evaluation of the performance of sediment basins and/or structures to reduce shoaling at select locations.

##### **4.1 Representative Hydraulic Condition**

Littoral transport, the longshore movement of sediment along the coast is dominated by wave and tidal processes in inlets. Longshore currents generated by waves breaking obliquely to the coast drive littoral transport. In turn, the direction of wave approach and the angle of the wave crest to the shore influence the direction of littoral transport. Thus, inclusion of littoral transports through inlets is important for a good estimation of shoaling rates at sediment basins in estuaries. As such, it is important that an appropriate representative hydraulic condition characterized by normal tides and waves that produce the average gross littoral transport at select nearshore locations is selected.

Littoral transport magnitude and direction can vary from season, day, or hour because waves can vary with the same time scale. Thus, the estimation of the shoaling rate in a sediment basin and morphological change (i.e., change in bed elevation) requires simulation of sediment transport over, at least, a full year. However, such long-term simulations require lengthy computational time that goes beyond the schedule of this study. Alternatively, this study simulated one-month-long representative period from a representative year to estimate basin shoaling rates and then prorated the computed basin shoaling rates for an average year (i.e., a year with average gross littoral transport). Notably, the

model calculated shoaling rates associated with the representative month will likely not reflect the long-term basin shoaling rate—an acceptable approximation given that future hydraulic conditions (tides and waves) are unknown. Further, the basin trapping efficiency diminishes as sediment deposits in the basin. However, the prorated shoaling rate offers a good approximation of the shoaling rate of an alternative to reduce in-channel shoaling relative to the shoaling rate for baseline conditions (no basins and/or structures). Moreover, the prorated shoaling rate provides an effective way of determining which alternative performs best to reduce in-channel shoaling. Comparison of the shoaling rates for baseline and alternatives provides the means to estimate shoaling rates at select AIWW cuts when sediment basins and/or structures are constructed.

To find the representative month in an average year, this study reviewed the Wave information Study (WIS) Station 63402 hindcasted hourly wave records for the period 1980 – 2017. This WIS station, as well as predicted tides at Jacksonville Beach (NOAA 8720291), provided the offshore boundary conditions for the MIKE Littoral Process (LP) model simulation for the period 1980 – 2017. Littoral process model calibration was unnecessary because this study only needed to determine the representative month in an average year—that is, an accurate estimation of the gross transport is not essential as all gross littoral transport estimates applied the same model parameters and were compared relative to each other.

Using the results from the LP model, this study (a) estimated the annual gross littoral transport for each year in 1980 – 2017; (b) calculated the average annual gross littoral transport for the period 1980 – 2017 at three profiles (see Figure 4.1); and (c) selected 2000 as the year that provides an annual gross transport nearest to the calculated annual average at the three profiles. Then, this study used the LP model to calculate the monthly gross littoral transport for January – December 2000. Figure 4.2 shows January and March provide the monthly gross littoral transport that are nearest to the calculated average monthly gross littoral transport in 2000 at Profile 2—the profile nearest to the area of interest (Nassau Sound and AIWW Cuts 23 – 27N). In the figure, green, blue, red, and black bars represent low, medium, high, and average gross transport months. Between January and March, March provides a net littoral transport nearer to the annual average net transport. Thus, the predicted tides and hindcasted waves in March 2000 were applied as offshore boundary conditions for model calculation of baseline and design alternatives tides, waves, sediment transport, and shoaling rates for the representative month.

## **4.2 Sediment Sources, Transport Pathways, and Proposed Basins**

This study applied the PT model to identify the inlets that serve as the main pathway for sediments that deposit in Cuts 23 – 27N. The PT model applied uniquely-colored sediment tracers at each offshore sediment source—offshore of St. Mary’s River, offshore of Nassau Sound, offshore of Fort George River, and offshore of St. Johns River—to distinguish the sediment transport tracks and final place of deposition for each sediment tracer. All the sediment tracers have the same settling velocity and critical shear stress for erosion as described in Section 3.4 but have different colors—green sediments from offshore of St. Marys River, red sediments from offshore of Nassau Sound, pink sediments from offshore of Fort George River, and blue sediments from offshore of St. Johns River. Figure 4.3 and Figure 4.4 shows sediment deposition locations and transport pathways at the end of the representative month.

Figure 4.3 shows particle tracks characterize ebb shoal formation just east of the mouth of St. Marys River; 'green' sediments from offshore of St. Marys River moved 3 miles southward through the AIWW to Cut-C with most of the sediments deposited westward along St. Marys River; and 'green' sediments from the north did not reach south of Cut-27M and likely did not cause the shoaling south of Cut-27M. Given these modeled transport pattern, no sediment basin is proposed north of Cut-27M as this area is not in the pathway of sediments that deposit in Cuts 23 – 27M.

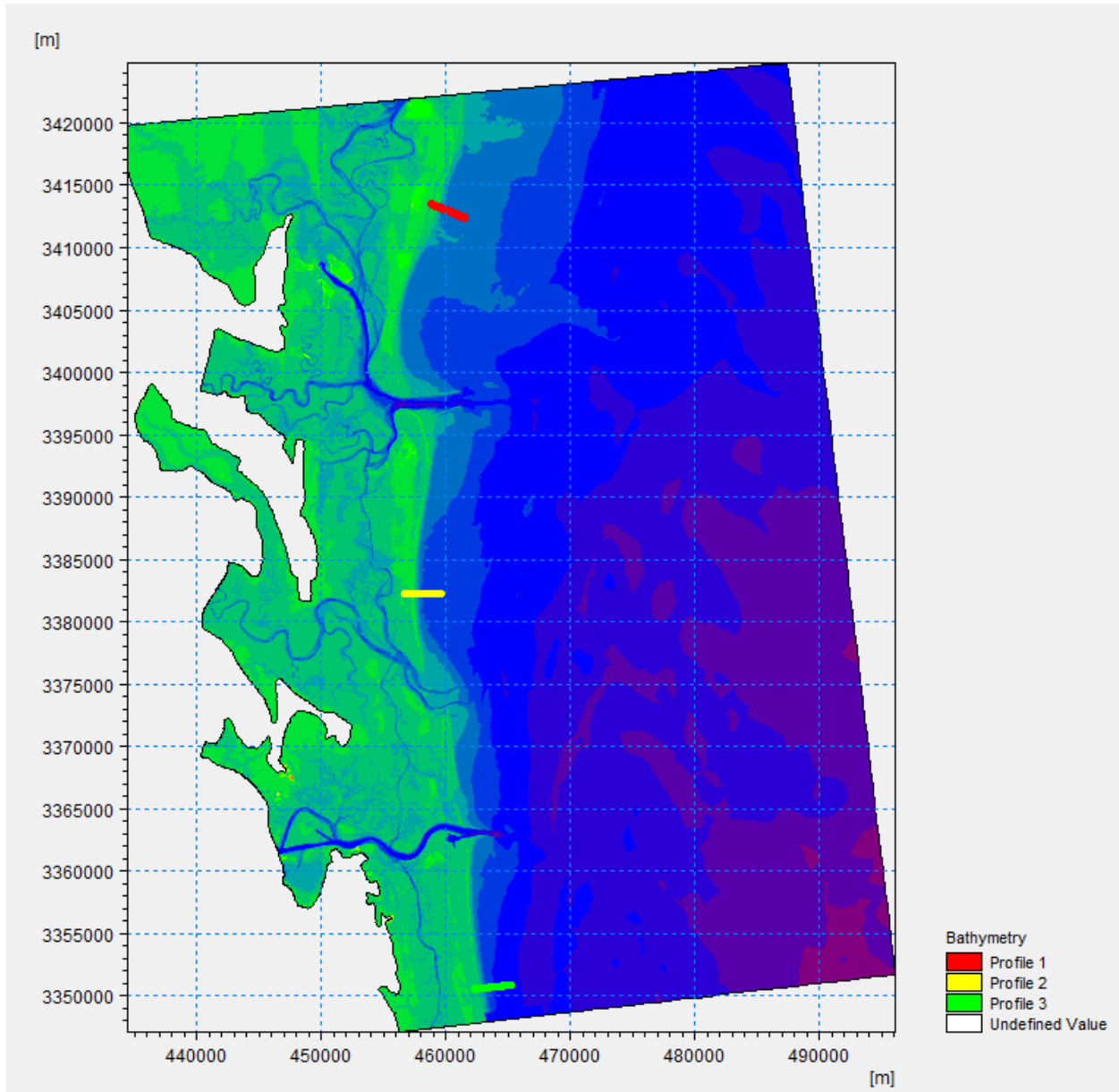


**Figure 4.1** Locations of Profiles for Littoral Gross Transport Calculation

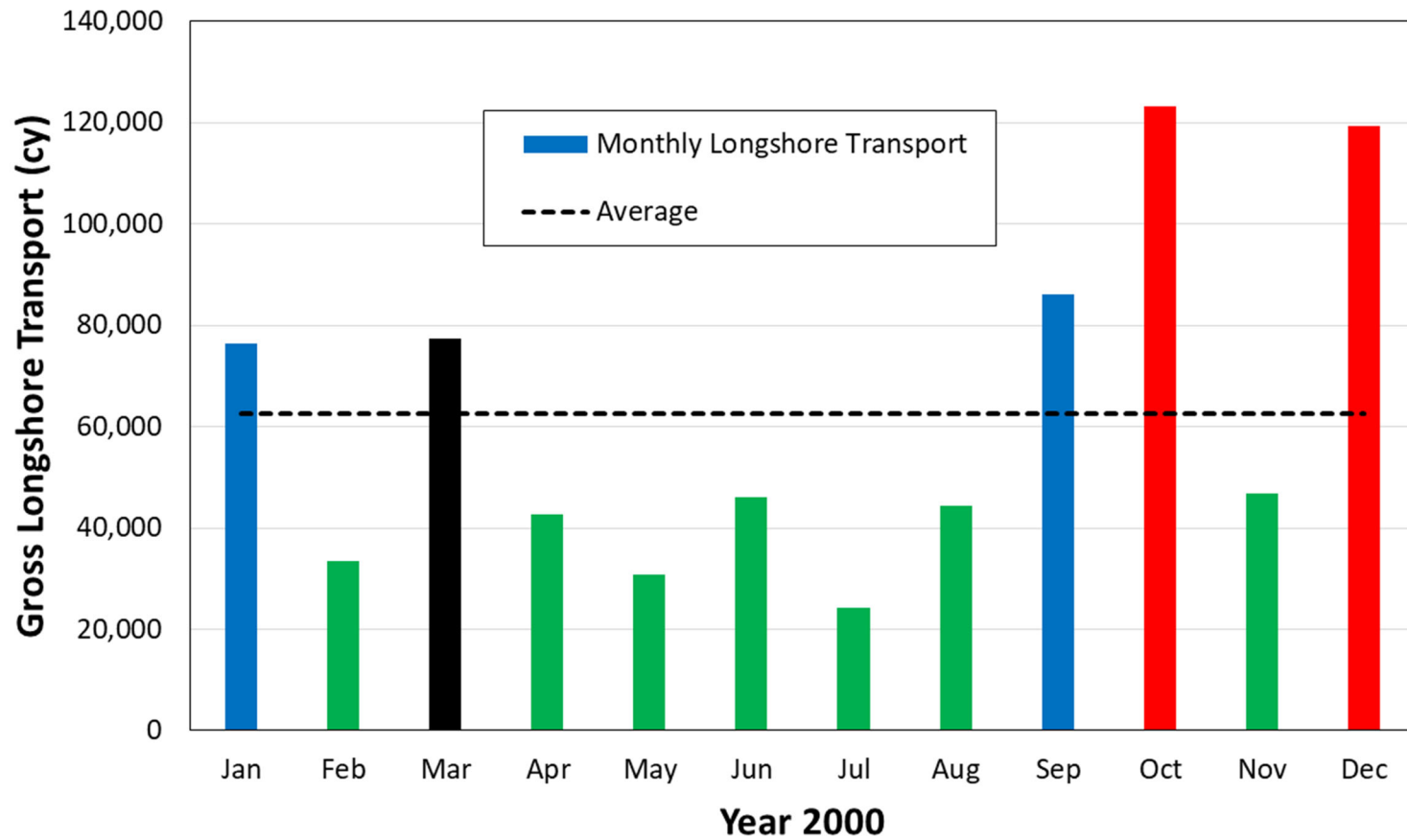


Figure 4.2 Monthly Gross Longshore Transport for the Year with Average Annual Gross Transport

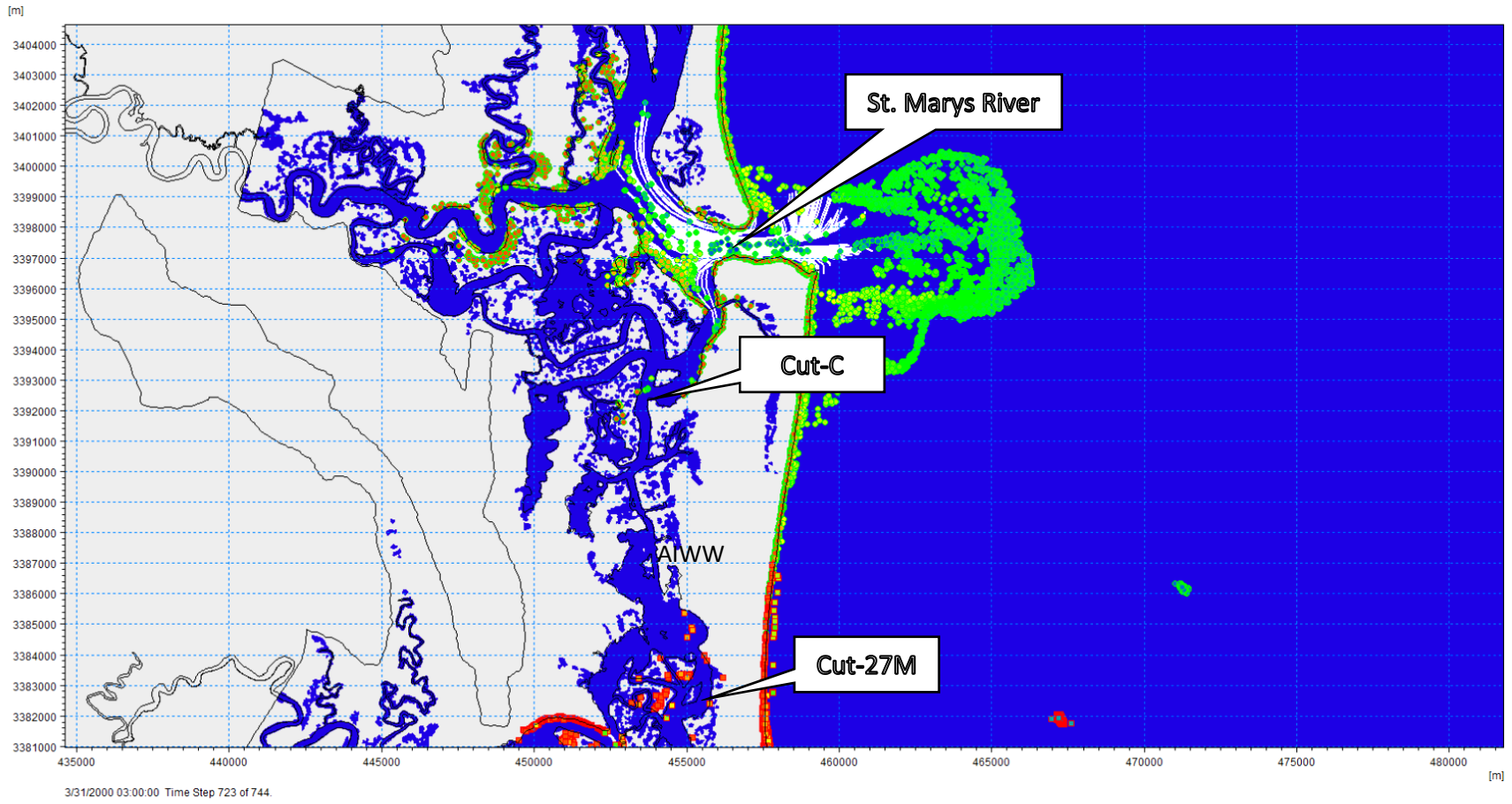
#### 4.2.1 Discarded Sediment Basin/Structures Alternatives

Figure 4.3 and Figure 4.4 show sediment shoaling in Cut-27G to Cut-27M is likely caused by ‘red’ sediments from Nassau Sound. The figures show no substantial shoaling north of Cut-27M—a pattern consistent with historical observation that large shoaling occurs south of Cut-27M. Model results show Nassau Sound flood current loses strength around Cut-27M thus limiting heavy shoaling southward of Cut-27M. As Amelia River widens northward and meanders eastward, its flow velocity reduces which makes the area east of Cut-27F to Cut-27J (Figure 4.5) ideal to trap sediments and reduce shoaling in Cut-27G to Cut-27M. However, initial model results show this basin’s impact is limited only to nearby cuts, do not extend to Cut-27A to Cut-27C, and is deemed uneconomical because it requires a large dredge volume.

Figure 4.4 shows shoaling in Cut-24 to Cut-27F is likely caused by ‘red’ sediments from Nassau Sound. PT model results show sediments that went to these cuts either entered through the north end of Cut-27; first deposited on the island immediately east of Cut-27 at low tide and re-suspended and moved to Cuts-24 to Cut-27 on the next high tide; or entered Sawpit Creek and moved south to Cut-26A to Cut-24. Model results do not show much shoaling south of Cut-23—a pattern consistent with historical observation that large shoaling occurs northward of Cut-23. Given these sediment transport pathways, Figure 4.6 shows an initially-considered sediment basin east of Sawpit Creek along the south tidal channel of Nassau Sound that can reduce sediment transport along the south tidal channel. Two sets of groynes—Groyne 2W and 2E along the south bank of the south tidal channel aim to deflect sediments away from Sawpit Creek and Groyne 1W and 1E on each side of the north end of Cut-27 aim to force sediments moving along Nassau River to bypass Cut-27; and an impermeable reef along the east side of the island between Cut-27 and Sawpit Creek—were also initially-considered to direct sediments away from Sawpit Creek and Cuts 24 – 27. However, initial modeling with the four groynes and reef and sediment basin showed that shoaling at Cut-27 will likely increase with the construction of these structures and the basin in the south tidal channel. Subsequent model simulations show basin construction in the south tidal channel can redistribute Nassau Sound flood flow to increase flow through the south tidal channel and thereby allow more sediments to pass through Cut-27. As the structures did not effectively deflect sediment away from Cut-27 and given the increased cost associated with construction of these structures, the groynes and reef were no longer considered as part of any shoaling reduction alternative.

Figure 4.4 shows large deposition (‘pink’ sediments) along Fort George River—a pattern consistent with historically large shoaling in this river. The large shoaling extends to Cut-11 and the few sediments that got into the AIWW and Sisters Creek were transported southward to Cut-3 which resulted in slight shoaling from Cut-11 to Cut-3. Initial model results show a sediment basin in Fort George River located east of Cut-11 (see Figure 4.7) cannot sufficiently capture sediments before they enter Cut-11 and thus cannot reduce in-channel shoaling in this part of the AIWW. Based on this model results, this study did not further evaluate any other basin alternatives in Fort George River as these basins rapidly fill up and therefore will not substantially reduce shoaling in the AIWW.

Given the above findings, this study does not recommend basin construction near Cut-27G and Cut-11. As historical dredging records show the largest shoaling volumes occur in Cut-27A and Cut-27C, this study prioritized finding shoaling reduction alternatives for these cuts.



**Figure 4.3** Particle Track and Deposition from Various Sediment Sources in Nassau County, FL and Camden County, GA

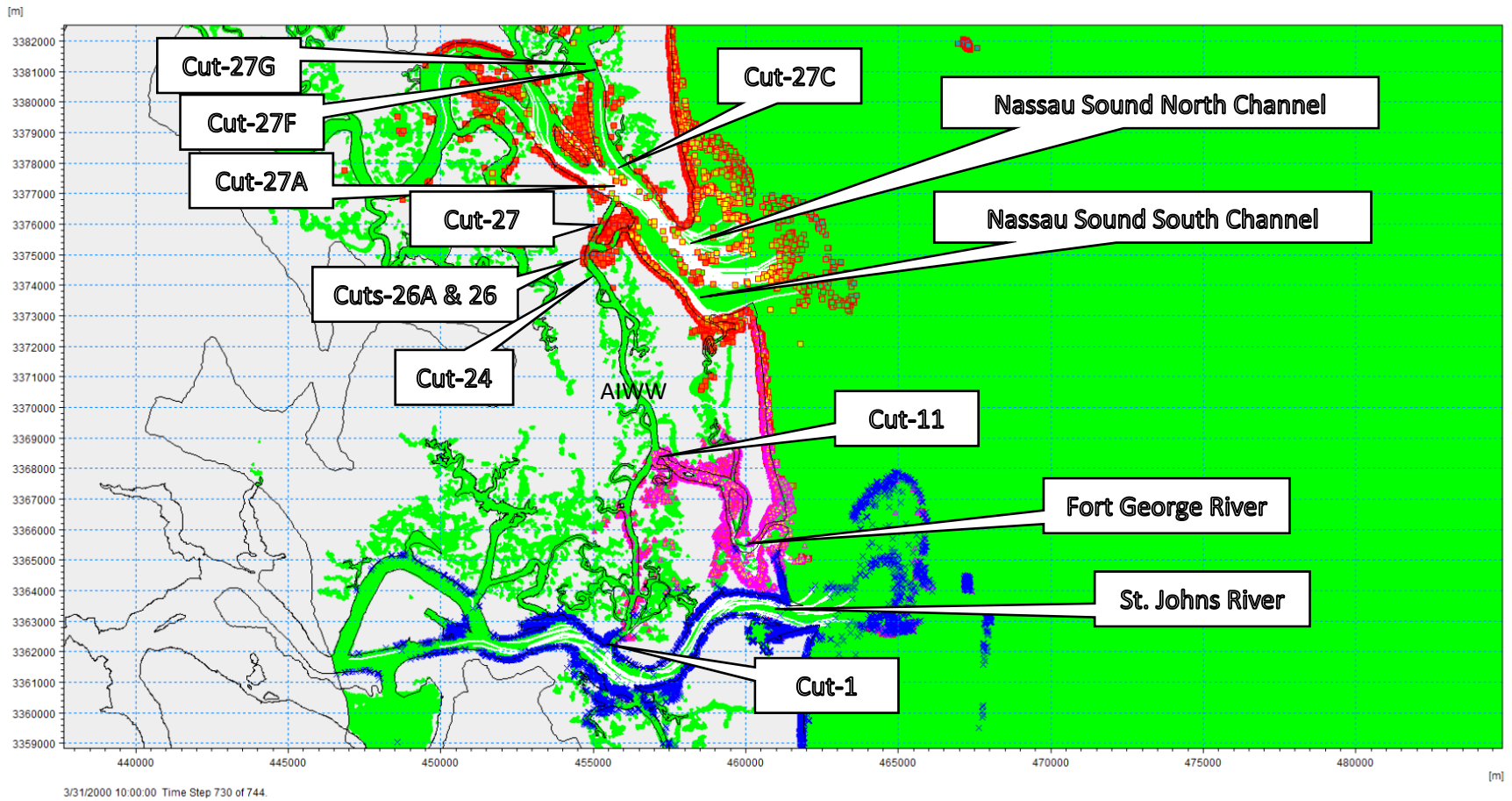


Figure 4.4 Particle Track and Deposition from Various Sediment Sources in Nassau and Duval Counties, FL

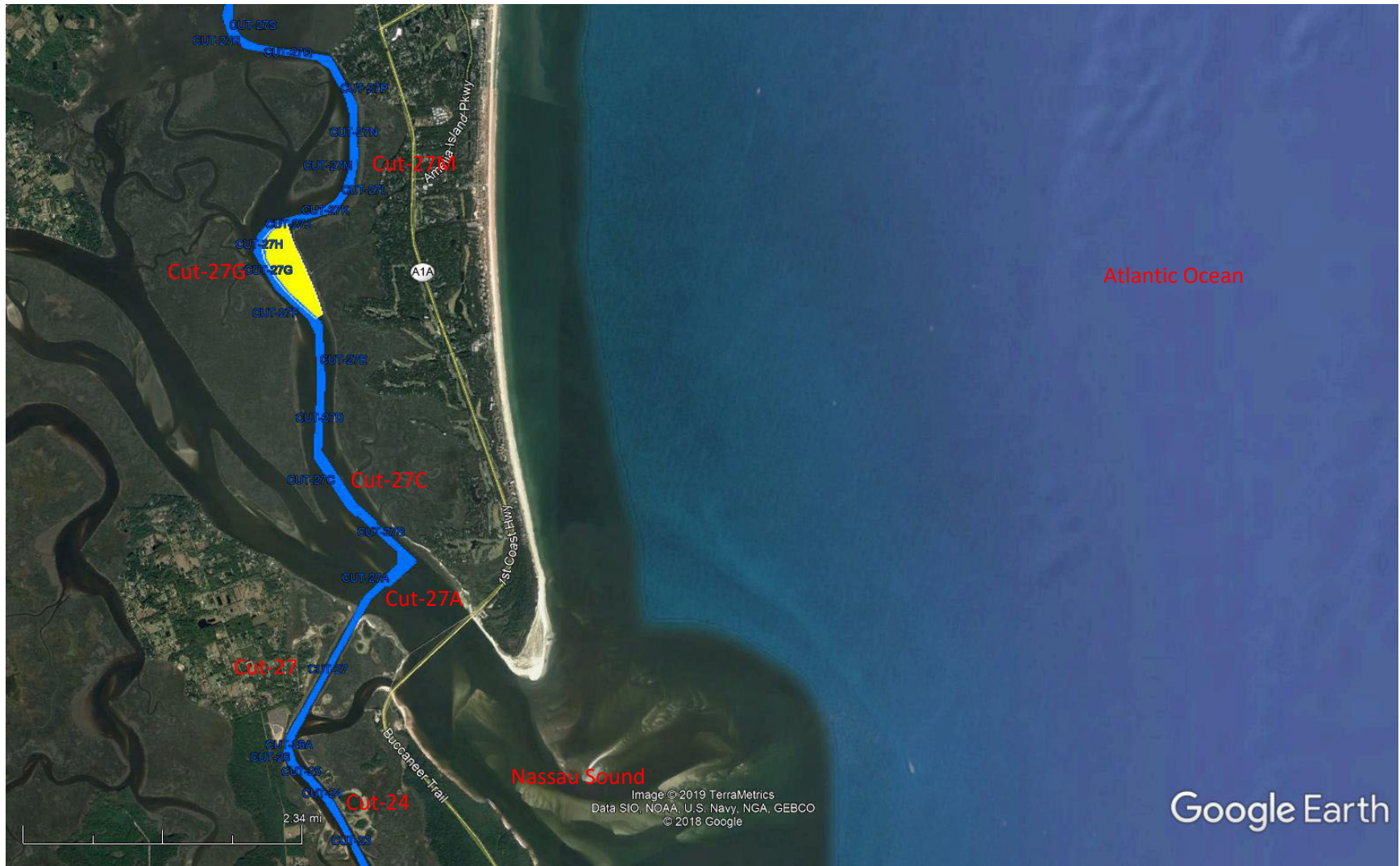


Figure 4.5 Sediment Basin near Cut-27F to Cut-27J (not recommended due to locally-limited effect)



**Figure 4.6** Locations of Sediment Basin, Groynes, and Reef near Sawpit Creek (Structures not recommended due to substantially increased shoaling in Cut-27)



**Figure 4.7** Location of Sediment Basin near Cut-11 (not recommended due to rapid basin shoaling and poor in-channel reduction performance)

#### 4.2.2 Proposed Basin Alternatives for In-Channel Shoaling Reduction

Model results shows sediment basins at several locations in Nassau River (adjacent to Cut-27A) and the southern stretch of Amelia River (adjacent to Cut-27B and Cut-27C) provide substantial in-channel shoaling reduction performance. In addition to the AIWW and wideners (white), Figure 4.8 shows these basins as Basin 1 (brown), Basin 2 (green), Basin 3 (yellow), Basin 4 (red), Basin 5 (light blue), Basin 5 (purple), and Basin 7 (orange). Table 4.1 provides the basins characteristics; and Table B.1 in Appendix C provides each basin's bottom corners coordinates. Notably, most of the bed elevation in Basin 5 is already below -14 ft-MLLW (i.e., -12 ft-MLLW plus 2 ft over dredge) so the amount of dredge volume shown for Basin 5 is very small.

Model results indicate that an erosion-prone area near the south bank of Nassau River and near the confluence with Sawpit Creek is a source of sediments that deposits into Cut-27A. Therefore, dredging one to three basins (Basins 1, 2, and 3 as shown in Figure 4.8) can remove a substantial amount of erodible material that shoals into Cut-27A. Non-construction of Basin 2 makes Basins 1 and 3 non-contiguous and avoids disturbance of the riverbed underneath the SR-A1A Bridge and old Crady Bridge. Model results also indicate sediment transport pathways across the northern two-thirds of Cut-27A and deposition along an approximate 3,000-ft distance northwest from Cut-27A. Thus, construction of sediment Basins 4 and 5 can likely reduce Cut-27A in-channel shoaling. Finally, located along the west and east sides of Cut-27B and Cut-27C, Basins 6 and 7 could provide buffer storage for sediment that shoals in the channel.

To evaluate the performance of various combinations of basins in trapping sediments and reducing in-channel shoaling, this study evaluated and compared the shoaling volumes calculated for basin Alternatives A – F using the hydraulic conditions of the representative month. Table 4.2 lists the basins included in each alternative. At the basin locations, this study lowered bed elevations to the design basin bed elevation to include the basins in the Baseline model mesh. In the basin area, if a Baseline mesh node bed elevation is lower than the design bed elevation, the Baseline mesh node elevation is retained. The model simulations applied the same boundary conditions and model parameters determined at model calibration.

Comparisons of navigation channel and basin shoaling for Baseline (no basin) and Alternatives A – F provided the means to evaluate an alternative's performance to reduce shoaling in the navigation channel and to trap sediments in the basins. Multiplication of the bed level change at mesh elements by the mesh elements' areas in the navigation channel and basins provided 1/12 of the estimated annual in-channel and in-basin shoaling volume. To determine hydraulic effects of basins, this study evaluated differences in flow velocity from baseline conditions but did not further evaluate differences in wave properties because offshore wave energy mostly dissipates if ever offshore waves reach the AIWW—i.e., offshore wave heights are very small at AIWW and thus any change in wave heights caused by the basins will not substantially change currents and sediment transport.



**Figure 4.8** Locations of Proposed Sediment Basins to Reduce In-Channel Shoaling

**Table 4.1** Proposed Basins Characteristics

Parameter	Proposed Basins						
	1	2	3	4	5	6	7
Longest Length, L (ft)	800	2,690	960	1,960	1,740	3,020	6,440
Widest Width, W (ft)	740	800	930	1,110	500	190	290
Bed Elevation (ft-NAVD)	17.2	17.2	17.2	17.2	17.2	17.2	17.2
Area (acres)	8	32	20	48	16	22	24
Dredging Volume (cy)	62,270	214,290	31,250	49,880	680	29,140	51,070

**Table 4.2** Basins in Proposed Alternatives

Alternatives	Included Basin						
	1	2	3	4	5	6	7
Baseline (no basins)							
Alternative A				X	X		
Alternative B	X	X	X	X	X		
Alternative C	X		X	X	X		
Alternative D	X		X	X	X	X	X
Alternative E	X	X	X	X	X	X	X
Alternative F				X	X	X	

### 4.3 Shoaling Rates in Navigation Channel

This study estimated the pro-rated annual shoaling rate for Cuts 23 – 27N by multiplying the representative month's shoaled volume in these cuts by a factor of 12. Comparisons of each basin alternative with Baseline shoaling rates provided the percent change to in-channel shoaling for each basin alternative. Table 4.3 shows a basin alternative's modeled in-channel shoaling rates as percentages of Baseline conditions in-channel shoaling rates. A percentage near 100% indicates no substantial change in shoaling for a given cut. Table 4.3 shows Alternative A substantially reduces Cut-27A shoaling to 63%. Alternative B substantially reduces Cut-27A shoaling to 51% but slightly increases Cut-27 shoaling to 114%. Alternative C substantially reduces Cut-27A shoaling to 61%. Alternative D substantially reduces Cut-27A shoaling to 60% and substantially reduces Cut-27C shoaling to -6% (i.e., turns Cut-27C from depositional to erosional). Similarly, Alternative E substantially reduces Cut-27A shoaling to 50% and substantially reduces Cut-27C shoaling to -8% but increases Cut-27 shoaling to 113%. Alternative F substantially reduces Cut-27A shoaling to 64% and substantially reduces Cut-27C shoaling to 61%. Interestingly, at Cut-26 and Cut-27G, model results show small Baseline erosions and alternatives model results show slightly more erosion (i.e., less shoaling).

Table 4.3 shows the effect of Basins 1 – 7 is mostly limited to Cuts 27, 27A, and 27C as modeled shoaling changed very little in the other cuts. Basins 6 and 7 have no substantial effect on Cut-27B shoaling because these basins' bed elevations adjacent to Cut-27B did not differ from Baseline bed elevations as Baseline bed elevations were already below -14 ft-MLLW in the Basins 6 and 7 locations. Thus, model results do not show substantial changes in Cut-27B shoaling for Alternatives D and E.

Model results show Basins 3 and 7 will likely fill in the first year and Basin 1 will likely fill in the first two years after basin construction. Thus, the in-channel shoaling reduction benefits from these basins will be short-lived. Given the short-duration effects of Basins 1, 3, and 7, this study estimates that Cut-27A dredging intervals are 9 years for Alternative A; 11 years for Alternative B; 9 years for Alternative C; 10 years for Alternatives D and E; and 9 years for Alternative F. Notably, when Basin 7 fills up, Alternatives D and E will likely perform similar to Alternative F from the second year after dredging.

This study applied an average representative one-month period to estimate the shoaling rates and dredging intervals because long-term model simulations (i.e., simulation periods of several months or years) require very long computational times that go beyond the project schedule. Given that channels and basins sediment trapping efficiency decrease as sediments fill in, the average long-term shoaling rates can be different than those presented in this study. Moreover, future hydraulic conditions (tides and waves) could be different from those characterized for the selected representative month and extreme episodic events (storm surge and high wave events) can also cause additional deposition and erosion. For example, extreme storms can erode large amounts of sediments from the Nassau Sound ebb shoal and transport these sediments to shoal in large volumes in the AIWW. Long-term model simulation incorporates more variations in channel and basin sediment trapping efficiency and incorporates more temporal variation of hydraulic conditions. Thus, long-term model simulations can provide a better estimate of the effect of basins to in-channel shoaling.

### 4.4 Sediment Transport Model Parameter Sensitivity Analysis

This study evaluated the sensitivity of calculated shoaling rates with changes in sediment median grain size and grading coefficient. As this study focuses on reducing shoaling at or near Cut-27A, this study selected a sediment median grain size of 0.20 mm and grading coefficient of 1.5 which are more representative of the sediment samples from Cut-27A (see Table 2.4). Using these sediment grain

size and grading coefficient values, Table 4.4 shows the alternatives modeled in-channel shoaling rates as percentages of Baseline conditions in-channel shoaling rates. Comparison of shoaling percent values in Table 4.3 and Table 4.4 shows the calculated shoaling at Cut-27A mostly decreases by about 2 – 5% of the when sediment median diameter was changed from 0.16 to 0.20 mm and grading coefficient was changed from 2.5 to 1.5. This means that the basin alternatives will likely perform better in reducing in-channel shoaling; their dredging intervals could become slightly longer; and annual savings could increase when coarser sediment and sediment size more similar to Cut-27A sampled sediments is used in the model simulations.

**Table 4.3** Modeled Shoaling Rates as a Percentage of Baseline Shoaling Rates  
(D<sub>50</sub> = 0.16 mm, Grading Coefficient = 2.5)

Cut	Basin Alternatives					
	Alt. A	Alt. B	Alt. C	Alt. D	Alt. E	Alt. F
23	100%	102%	101%	101%	101%	100%
24	100%	102%	101%	101%	102%	100%
25	100%	103%	101%	101%	102%	100%
26	105%	99%	103%	101%	99%	103%
26A	100%	101%	101%	101%	101%	100%
27	101%	114%	101%	100%	113%	100%
27A	63%	51%	61%	60%	50%	64%
27B	99%	98%	99%	94%	92%	96%
27C	100%	98%	99%	-6%	-8%	61%
27D	100%	101%	100%	99%	99%	99%
27E	100%	99%	100%	99%	98%	99%
27F	101%	103%	101%	103%	106%	101%
27G	105%	111%	106%	118%	132%	112%
27H	100%	101%	100%	102%	103%	101%
27J	100%	101%	100%	102%	103%	100%
27K	100%	103%	101%	103%	105%	101%
27L	100%	103%	101%	103%	106%	101%
27M	100%	102%	101%	102%	104%	101%
27N	100%	102%	101%	103%	105%	101%
<b>Dredging Interval* (years)</b>	<b>9</b>	<b>11</b>	<b>9</b>	<b>10</b>	<b>10</b>	<b>9</b>

Notes: \* Dredging interval determined from Cut-27A dredging interval. Baseline historical dredging interval averages six years.

**Table 4.4** Modeled Shoaling Rates as a Percentage of Baseline Shoaling Rates  
(D<sub>50</sub> = 0.20 mm, Grading Coefficient = 1.5)

Cut	Basin Alternatives					
	Alt. A	Alt. B	Alt. C	Alt. D	Alt. E	Alt. F
23	100%	102%	101%	101%	102%	100%
24	100%	102%	101%	101%	102%	100%
25	100%	102%	101%	101%	102%	100%
26	98%	96%	96%	96%	96%	95%
26A	100%	102%	101%	101%	102%	100%
27	99%	114%	98%	98%	113%	99%
27A	58%	49%	56%	55%	48%	58%
27B	99%	98%	99%	96%	95%	97%
27C	100%	100%	100%	-7%	-8%	57%
27D	100%	102%	101%	99%	100%	101%
27E	100%	101%	101%	102%	103%	101%
27F	101%	101%	101%	101%	103%	100%
27G	101%	103%	100%	104%	104%	103%
27H	100%	102%	100%	102%	103%	101%
27J	100%	102%	101%	102%	103%	101%
27K	100%	103%	101%	103%	106%	101%
27L	100%	103%	101%	104%	106%	101%
27M	100%	103%	101%	103%	105%	101%
27N	100%	103%	101%	104%	107%	101%
<b>Dredging Interval* (years)</b>	<b>10</b>	<b>11</b>	<b>10</b>	<b>10</b>	<b>10</b>	<b>10</b>

Notes: \* Dredging interval determined from Cut-27A dredging interval. Baseline historical dredging interval averages six years.

#### 4.5 Cost Comparison of Basin Alternatives

Comparisons of Baseline (no basins) and Alternatives A – F costs require evaluation of three factors—dredging frequency, dredging cost, and other related costs (e.g., engineering, permitting, bid administration, construction observation, etc.). Results of the model simulations for the Baseline and Alternatives A – F provide the dredging frequency (see Table 4.3). Review of historical USACE dredging data (Table 4.5) and submitted offers for the most recent USACE Sawpit Creek area dredging in 2018 (Table 4.6) provided the basis for estimating dredging cost, including mobilization/demobilization cost and unit costs (cost per cubic yard). Notably, the costs of three previous dredging events (i.e., 2006, 2013, and 2018) varied from \$4.058 to \$5.329 million (Table 4.5) and offerors’ mobilization/demobilization costs for the most recent dredging event in 2018 ranged \$788,250 – \$3,500,000. To estimate the dredging cost starting at the next Sawpit Creek area dredging in 2024, this study adopted the government estimate of the mobilization and demobilization in 2018 of \$1,727,000 (Table 4.6) and

the unit dredging cost of \$8.89/cy in 2018 (Table 4.5) and applied the new federal annual interest rate for 2020 of 2.750% to estimate a mobilization/demobilization cost of \$2,032,279 and yardage unit cost of \$10.46/cy for the 2024 maintenance dredging and subsequent dredging.

**Table 4.5** Summary of Historical Maintenance Dredging in Sawpit Creek Area (2006 – 2018)

Source: USACE-SAJ

Year	Total Dredge Volume (cy)	Unit Cost (\$/cy)	Total Cost
2006	429,163	\$9.46	\$4,058,191
2013	519,556	\$7.69	\$3,992,972
2018	599,785	\$8.89	\$5,329,635

**Table 4.6** Summary of Offers for 2018 Dredging of Sawpit Creek Area

Source: USACE-SAJ

Cost	Government Original Estimate	Offer No. 1	Offer No. 2	Offer No. 3
Mobilization and Demobilization	\$1,727,000	\$3,500,000	\$788,250	\$3,372,000
Base Excavation and Beach Placement (unit cost)	\$2,952,000 (\$9.00/cy)	\$2,542,000 (\$7.75/cy)	\$2,578,080 (\$7.86/cy)	\$3,444,000 (\$10.50/cy)
Base Excavation and Upland Placement (unit cost)	\$196,500 (\$6.55/cy)	\$255,000 (\$8.50/cy)	\$202,200 (\$6.74/cy)	\$450,000 (\$15.00/cy)
Other Costs including Beach Tilling, Turbidity Monitoring, Environmental Species Monitoring, Standby Time, Liability Insurance, and Additional Dredging Options A – D	\$2,150,000	\$2,700,000	\$1,839,580	\$1,983,900
<b>TOTAL COST</b>	<b>\$7,316,000</b>	<b>\$9,210,000</b>	<b>\$5,464,479</b>	<b>\$9,499,472</b>

In comparing the cost of each functionally feasible alternative, the cost analysis also considered other costs, including costs associated with permitting, environmental study, engineering and design, and construction administration for each dredging event (Table 4.7).

**Table 4.7** Other Costs Associated with Dredging Projects

Item	Initial Amount	Remarks
Permitting	\$50,000	Additional recurring cost of \$15,000 for each dredging event
Environmental	\$20,000	Additional recurring cost of \$5,000 per acre for each dredging event
Engineering and Design	\$110,000	Additional recurring cost of 5% of the dredging cost for each dredging event
Construction Administration	\$0	Recurring cost of 10% of the dredging cost for each dredging event

Table 4.8 provides the costs breakdown for the total dredging, environmental and permitting, engineering and design, and construction administration. Using an annual interest rate of 2.750%, Table 4.8 provides estimates of the equivalent uniform annual cost for the Baseline and Alternatives A – F for project design life that range 45 – 55 years depending on the Baseline and alternative dredging interval.

This study estimated the Baseline maintenance dredging equivalent uniform annual cost at \$2,583,000 at a project design life of 48 years. This cost involves dredging the Sawpit Creek area at historical dredging volumes and without any of the proposed basins. The following paragraphs summarize the results of the cost analyses.

Alternative A includes Baseline and Basins 4 and 5 dredging and would likely change the frequency of dredging operation to once every nine years. Each dredging operation would remove approximately 566,728 cy at an equivalent uniform annual cost of \$1,795,000. Compared to the baseline equivalent uniform annual cost, the estimated annual savings of \$788,000 is substantial and the largest among the analyzed alternatives.

Alternative B includes Baseline and Basins 1, 2, 3, 4, and 5 dredging. Model results show Basin 3 could fill in the first year and Basin 1 could fill in the second year after dredging. Thus, this study estimates Alternative B would likely change the frequency of dredging operation to once every 11 years. Each dredging operation would remove approximately 874,536 cy at an equivalent uniform annual cost of \$2,289,000. Compared to the baseline equivalent uniform annual cost, the estimated annual savings of \$294,000 is substantial and the fifth largest among the analyzed alternatives.

Alternative C includes Baseline and Basins 1, 3, 4, and 5 dredging. Model results show Basin 3 could fill in the first year and Basin 1 could fill in the second year after dredging. Thus, this study estimates Alternative C would likely change the frequency of dredging operation to once every nine years. Each dredging operation would remove approximately 660,248 cy at an equivalent uniform annual cost of \$2,014,000. Compared to the baseline equivalent uniform annual cost, the estimated annual savings of \$569,000 is substantial and the second largest among the analyzed alternatives.

Alternative D includes Baseline and Basins 1, 3, 4, 5, 6, and 7 dredging. Model results show Basins 3 and 7 could fill in the first year and Basin 1 could fill in the second year after dredging. Thus, this study estimates Alternative D would likely change the frequency of dredging operation to once every 10 years. Each dredging operation would remove approximately 740,463 cy at an equivalent uniform annual cost of \$2,092,000. Compared to the baseline equivalent uniform annual cost, the estimated annual savings of \$491,000 is substantial and the third largest among the analyzed alternatives.

Alternative E includes Baseline and Basins 1, 2, 3, 4, 5, 6, and 7 dredging. Model results show Basins 3 and 7 could fill in the first year and Basin 1 could fill in the second year after dredging. Thus, this study estimates Alternative E would likely change the frequency of dredging operation to once every 10 years. Each dredging operation would remove approximately 954,751 cy at an equivalent uniform annual cost of \$2,569,000. Compared to the baseline equivalent uniform annual cost, the estimated annual savings of \$14,000 is very small, sensitive to fluctuation in the interest rate, and the least among the analyzed alternatives.

Alternative F includes Baseline and Basins 4, 5, and 6 dredging. This study estimates Alternative F would likely change the frequency of Cut-27A dredging operation to once every nine years. Moreover, model results show this alternative can also substantially decrease Cut-27C shoaling to 61%. Each

dredging operation would remove approximately 595,868 cy at an equivalent uniform annual cost of \$1,863,000. Compared to the baseline equivalent uniform annual cost, the estimated annual savings of \$720,000 is substantial and the second largest among the analyzed alternatives. Alternative F is the best performing alternative for in-channel shoaling reduction because it substantially decreases in-channel shoaling at both Cut-27A and Cut-27C.

Based on the in-channel shoaling reduction performance of Alternatives A, B, C, D, E, and F; and their cost evaluations, this study ranks these alternatives as Alternative F (first), Alternative A (second), Alternative C (third), Alternative D (fourth), Alternative B (fifth), and Alternative E (sixth). This study does not recommend Alternative E for further consideration because it provides only a small estimated annual savings which is well within uncertainties in dredge volume calculations and dredge maintenance cost estimation. The next section shows the impact of the alternatives to the flow velocity.

**Table 4.8** Details of Equivalent Uniform Annual Cost Estimates

	Parameter	Baseline	Alt. A	Alt. B	Alt. C	Alt. D	Alt. E	Alt. F
<b>A.</b>	Dredging Frequency (years)	6	9	11	9	10	10	9
<b>B.</b>	Project Life (years)	48	45	55	45	50	50	45
<b>C.</b>	Number of Dredging Events	8	5	5	5	5	5	5
<b>D.</b>	Quantity (cubic yards per event)	516,168	566,728	874,536	660,248	740,463	954,751	595,868
<b>E.</b>	Total Yardage (cubic yards)	4,129,344	2,833,640	4,372,680	3,301,240	3,702,315	4,773,755	3,575,208
<b>F.</b>	Yardage Cost (Per Dredging Event)	\$5,399,876	\$5,928,808	\$9,148,933	\$6,907,165	\$7,746,332	\$9,988,100	\$6,233,656
<b>G.</b>	Mobilization/Demobilization Cost	\$2,032,279	\$2,032,279	\$2,032,279	\$2,032,279	\$2,032,279	\$2,032,279	\$2,032,279
<b>H.</b>	Total Dredging Cost (F+G)	\$7,432,155	\$7,961,087	\$11,181,212	\$8,939,444	\$9,778,611	\$12,020,379	\$8,265,935
<b>I.</b>	Permitting Cost (initial \$50,000 and \$15,000 at every dredging event)	n/a	\$15,000	\$15,000	\$15,000	\$15,000	\$15,000	\$15,000
<b>J.</b>	Environmental Study Cost (initial \$20,000 and \$5,000 per acre at every dredging event)	\$0	\$0	\$0	\$0	\$0	\$0	\$0
<b>K.</b>	E&D Cost (initial \$110,000 and 5% of Total Dredging Cost at every dredging event)	\$371,608	\$398,054	\$559,061	\$446,972	\$488,931	\$601,019	\$413,297
<b>L.</b>	Construction Administration Cost (10% of Total Dredging Cost)	\$743,216	\$796,109	\$1,118,121	\$893,944	\$977,861	\$1,202,038	\$826,593
<b>M.</b>	Total Cost (H + I + J + K + L)	\$8,546,979	\$9,170,250	\$12,873,393	\$10,295,361	\$11,260,403	\$13,838,435	\$9,520,825
<b>N.</b>	Total Cost (Rounded to Nearest Thousand)	\$8,547,000	\$9,170,000	\$12,873,000	\$10,295,000	\$11,260,000	\$13,838,000	\$9,521,000
<b>O.</b>	Equivalent Uniform Annual Cost	\$2,583,000	\$1,795,000	\$2,289,000	\$2,014,000	\$2,092,000	\$2,569,000	\$1,863,000
<b>P.</b>	<b>Annual Savings</b>	<b>n/a</b>	<b>\$788,000</b>	<b>\$294,000</b>	<b>\$569,000</b>	<b>\$491,000</b>	<b>\$14,000</b>	<b>\$720,000</b>

Notes:

- The estimated materials and unit costs represent Taylor Engineering's best judgment as a professional design firm familiar with the

type of construction proposed. Taylor Engineering has no control over the availability or cost of labor, equipment or materials, market conditions, or the contractor's methods of pricing. Accordingly, Taylor Engineering makes no warranty, express or implied, that the actual bids or negotiated prices will not vary from the cost shown in the table.

9. All quantities estimated as in-place approximate quantities.
10. Construction cost may change due to fluctuations in the prices of materials and petroleum.
11. This project does not anticipate encountering hazardous materials nor require special handling.
12. Equivalent uniform annual cost represents total of initial and annual maintenance costs and associated dredging costs. Cost estimation assumes a 45- to 55-year project life and an interest rate of 2.750%.
13. Total dredging cost includes typical Sawpit Creek area and proposed basin shoal dredging maintenance costs.
14. Maintenance dredging occurs when Cut-27A shoals to bed elevations at or shallower than authorized project depth.

## 4.6 Hydraulic Impacts of Basin Alternatives

### 4.6.1 Peak Flow Velocities

To evaluate the effect on the flow velocity field of each basin alternative relative to Baseline conditions, this study compared the modeled peak flood and ebb flow velocities of each alternative with Baseline peak flood and ebb flow velocities. Flood and ebb through Nassau Sound mainly pass through the north tidal channel on the ebb shoal (which conveys flows through Amelia River and across the northern portion of Cut-27A) and the south tidal channel (which conveys flows to Sawpit Creek, Cut-27, and across the southern portion of Cut-27A). Figure 4.9 shows Baseline peak flood velocity increases to approximately 4.0 fps as it passes the southern tip of Amelia Island and decreases to around 2.7 fps on its way northwestward to Amelia River and 2.5 fps westward to Cut-27A and Nassau River. The increasing velocity gradient in the flow direction at the southern tip of Amelia Island erodes the ebb shoal, carries sediment northwestward, and deposits sediments along a flow path southeast to northwest of Cut-27A. This flow pattern explains the observed shoal formation within 2,300 ft southeast to 1,000 ft northwest of Cut-27A. Construction of Basins 4 and 5 brings down this shoal's bed elevation to below -14 ft-MLLW and removes a source of sediments that shoal into Cut-27A. Figure 4.9 also shows peak flood flow velocity increases to 4.0 fps at the south ends of the SR-A1A Bridge and Old Crady Bridge and then decreases on its way to cross the southern portion of Cut-27A. This flow pattern is consistent with the observed erosion underneath the two bridges and deposition in the southern portion of Cut-27A. Construction of Basins 1 and 2 removes some of the sources of eroding sediments southeast and underneath the bridges and Basin 3 construction provides a sediment trap for sediments before they reach Cut-27A. Figure 4.9 also shows peak flood flow enters Sawpit Creek at almost twice the speed as the peak flood flow through Cut-27. Sawpit Creek flood flow velocity slows down as it reaches Cut-27 and explains shoaling at this location.

Figure 4.10 shows Baseline peak ebb velocity increases from 1.5 fps to 2.5 fps as it passes through mid-length of Cut-27A. This increasing flow velocity gradient in the flow direction causes erosion and decreases Cut-27A shoaling. However, Cut-27A experiences net shoaling because flood deposition is larger than ebb erosion. Construction of Basin 5 help maintain the increasing ebb flow velocity through Cut-27A.

Figure 4.11 shows the difference when Baseline peak flood flow velocity is subtracted from the Alternative A peak flood flow velocity. A red contour indicates increase and blue contour indicates decrease in flow velocity compared to Baseline conditions. The figure shows peak flood flow velocity can decrease by about 0.3 fps at Basin 4 as the Basin 4 location is deeper in Alternative A than at Baseline conditions. Figure 4.12 shows the difference when Baseline peak ebb flow velocity is subtracted from the Alternative A peak ebb flow velocity. The figure shows peak ebb flow can decrease by 0.3 fps at Basin 4. Other velocity reductions (blue) or velocity increase (red) at the shoreline are attributed to wetting and drying and not due to any basin.

Figure 4.13 shows the difference when Baseline peak flood flow velocity is subtracted from the Alternative B peak flood flow velocity. The figure shows Basins 1, 2, and 3 construction can divert more flow from the north tidal channel to the south tidal channel. This increases flow through the south tidal channel and through Basins 1, 2, and 3. Model results show peak flood flow velocity can increase by 0.2 fps at Basin 1; decrease by 0.5 fps at Basin 2 (just south of SR-A1A Bridge); decrease by 0.2 fps at mid-length of SR-A1A Bridge and Old Crady Bridge; increase by 0.5 fps northwest of Old Crady Bridge; and

increase by 0.2 fps along Nassau River south shoreline between Cut-27 and Old Crady Bridge. Model results also show the flow diversion to the south tidal channel can reduce peak flood flow velocity by 0.1 fps at the north ends of SR-A1A Bridge and Old Crady Bridge and by 0.4 fps at Basin 4. Figure 4.14 shows the effect of Basins 1, 2, and 3 is limited to the basin areas and minimally to locations along the bridges. The figure shows peak ebb flow velocity can decrease by 0.3 fps at Basin 4 and Basin 2, by 0.2 fps at Basin 3, and by 0.1 fps at select locations along the bridges; and increase by 0.2 – 0.3 fps at Basin 2 (north of SR-A1A Bridge) and Basin 1 and at the southern portion of Cut-27A. Other velocity reductions (blue) or velocity increase (red) at the shoreline are attributed to wetting and drying and not due to any basin.

Figure 4.15 shows the difference when Baseline peak flood flow velocity is subtracted from the Alternative C peak flood flow velocity. The figure shows peak flood velocity can decrease by 0.5 fps at Basins 1 and 2 and adjacent shoreline; decrease by 0.3 fps at Basins 3 and 4; and increase by 0.1 fps at a few locations along the southern half of SR-A1A Bridge and Old Crady Bridge. Figure 4.16 shows the difference when Baseline peak ebb flow velocity is subtracted from the Alternative C peak ebb flow velocity. The figure shows peak ebb flow velocity can decrease by 0.3 fps at Basins 1 and 2 and adjacent shoreline; decrease by 0.3 fps at Basins 3 and 4 and at a small area on the ebb shoal; and increase by 0.2 fps at the southern end of Old Crady Bridge. Other velocity increase (red) at the shoreline are attributed to wetting and drying and not due to any basin.

Figure 4.17 shows the difference when Baseline peak flood flow velocity is subtracted from the Alternative D peak flood flow velocity. The figure shows that because Basin 2 is not constructed in Alternative D, the flow through the south tidal channel does not substantially increase and flow distribution between the north and south channels remains similar to the Baseline distribution. Model results show small velocity changes as peak flood flow can decrease by 0.4 fps at Basin 1 and 0.3 fps at Basins 3, 4, 6, and 7. Figure 4.18 shows peak ebb flow velocity can decrease by 0.4 fps at Basin 7; by 0.3 fps at Basin 6; and by 0.3 fps at Basins 4, 3, and 1. The figure also shows Alternative D can increase peak ebb flow velocity by 0.2 fps at the south end of Old Crady Bridge. Other velocity reductions (blue) or velocity increase (red) at the shoreline are attributed to wetting and drying and not due to any basin.

Figure 4.19 shows the difference when Baseline peak flood flow velocity is subtracted from the Alternative E peak flood flow velocity. Like Alternative B, the figure shows Basins 1, 2, and 3 construction can divert more flow from the north tidal channel to the south tidal channel. This increases flow through the south tidal channel and through Basins 1, 2, and 3. Peak flood flow velocity can increase by 0.2 fps at the Basin 1; decrease by 0.5 fps at Basin 2 (just south of SR-A1A Bridge); decrease by 0.2 fps at mid-length of SR-A1A Bridge and Old Crady Bridge; increase by 0.5 fps northwest of Old Crady Bridge; and increase by 0.2 fps along Nassau River south shoreline between Cut-27 and Old Crady Bridge. Model results show the flow diversion to the south tidal channel can reduce peak flood flow velocity by 0.1 fps at the north ends of SR-A1A Bridge and Old Crady Bridge and by 0.4 fps at Basin 4. Unlike Alternative B, Figure 4.20 shows the effect of Basins 1, 2, and 3 can extend further downstream of Basin 1. The figure shows peak ebb flow velocity can decrease by 0.3 fps at Basin 4, Basin 3, Basin 2 and by 0.1 – 0.2 fps at select locations along the bridges; and increase by 0.2 – 0.3 fps at Basins 2 and 1. Other velocity reductions (blue) or velocity increase (red) at the shoreline are attributed to wetting and drying and not due to any basin.

Figure 4.21 shows the difference when Baseline peak flood flow velocity is subtracted from the Alternative F peak flood flow velocity. The figure shows peak flood flow velocity can decrease by about

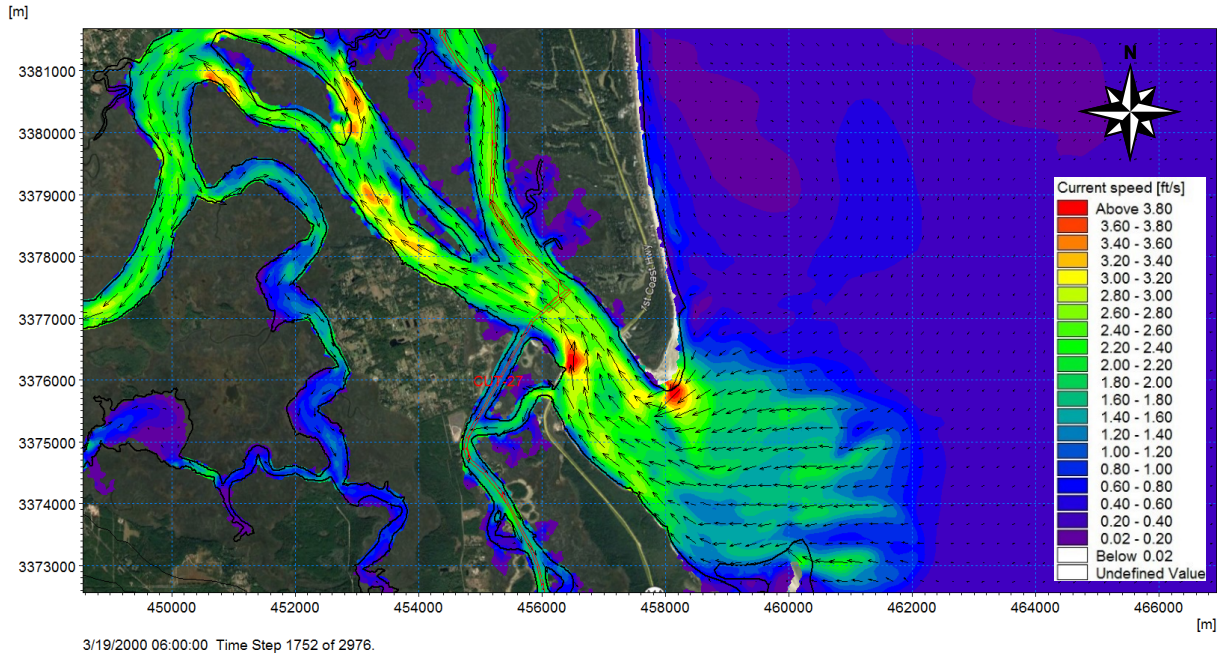
0.3 fps at Basin 4 and by 0.1 fps at Basin 6. Figure 4.22 shows the difference when Baseline peak ebb flow velocity is subtracted from the Alternative F peak ebb flow velocity. The figure shows peak ebb flow can decrease by 0.3 fps at Basin 4 and by 0.2 – 0.7 fps at Basin 6 and increase by 0.4 fps in a small portion of Cut-27B. Other velocity reductions (blue) or velocity increase (red) at the shoreline are attributed to wetting and drying and not due to any basin.

Overall, peak flood and peak ebb flow velocity differences are too small to affect navigation safety and too small to increase shoreline erosion. More importantly, as Figure 4.11 to Figure 4.22 show flow differences at peak flood and ebb when flow velocities are maximum, flow differences between basin alternatives and Baseline conditions for the other phases of the tidal cycle will likely be less than those shown for peak flood and ebb.

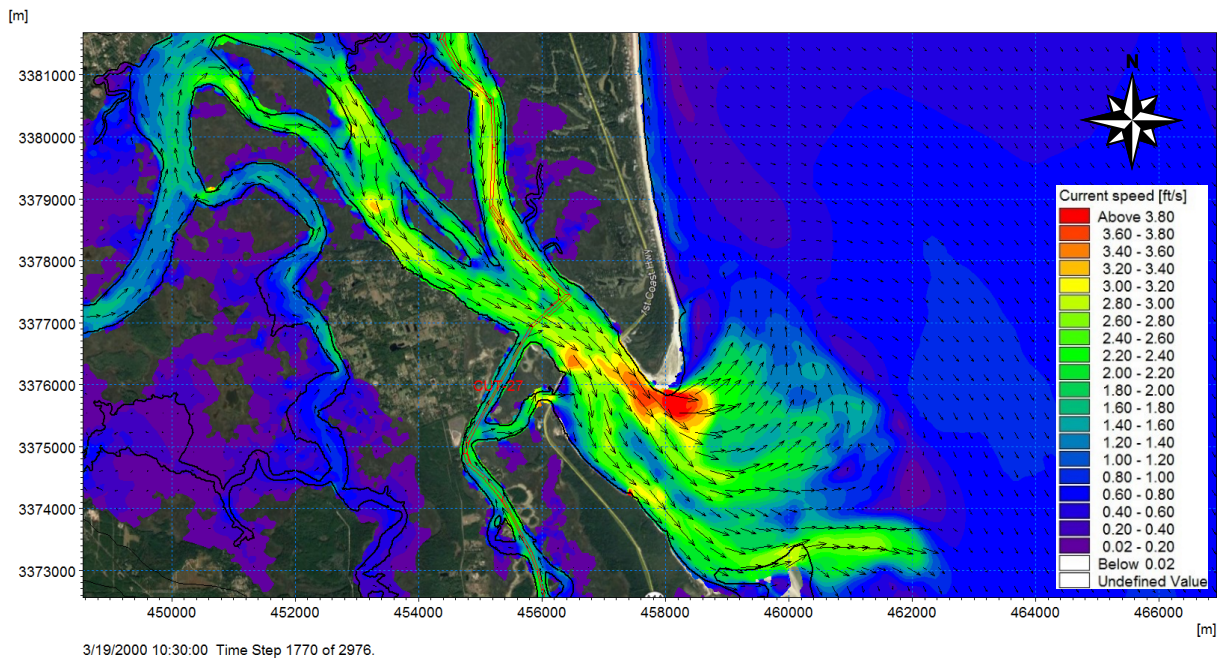
#### *4.6.2 Peak Wave Heights*

Figure 4.23 shows the modeled propagation of peak waves from the east. The 8.8-ft and 9-second easterly incident waves decrease in height and start breaking on the ebb shoal. Wave height decreases substantially on the ebb shoal from 6.3 ft at the shoal edge to 1.7 ft at the mouth of Nassau River. Some of the wave energy propagates through Nassau River but barely reaches Old Crady Bridge. Waves diffract around the southern tip of Amelia Island to propagate at sharply decreased energy along the north shoreline of the river. Model results show only small amounts of the incident wave energy propagate pass Old Crady Bridge where incident wave heights measure 0.3 ft. As Baseline wave heights are about 0.3 ft at the AIWW and 1.5 ft at the Basin 1 location, changes in wave heights due to the basin constructions will be smaller than the Baseline wave heights and therefore not substantial enough to adversely impact navigation safety and shoreline erosion.

Based on Figure 4.11 to Figure 4.23, model results show Alternative A would likely have the least hydraulic impact; Alternative F will likely have the second least hydraulic impact; Alternative D will likely have the third least hydraulic impact; and Alternative C will likely have the fourth least hydraulic impact. Alternatives B and E can divert more flood flows from the north tidal channel to the south tidal channel and will likely impact larger areas. Model results show Alternative B will likely have the fifth least hydraulic impact and Alternative E will likely have the largest hydraulic impact among the alternatives. However, for all alternatives, velocity differences from Baseline conditions are too small to affect navigation safety and too small to increase shoreline erosion.



**Figure 4.9** Modeled Baseline Peak Flood Velocity



**Figure 4.10** Modeled Baseline Peak Ebb Velocity



**Figure 4.11** Difference in Modeled Alternative A and Baseline Peak Flood Velocities



**Figure 4.12** Difference in Modeled Alternative A and Baseline Peak Ebb Velocities

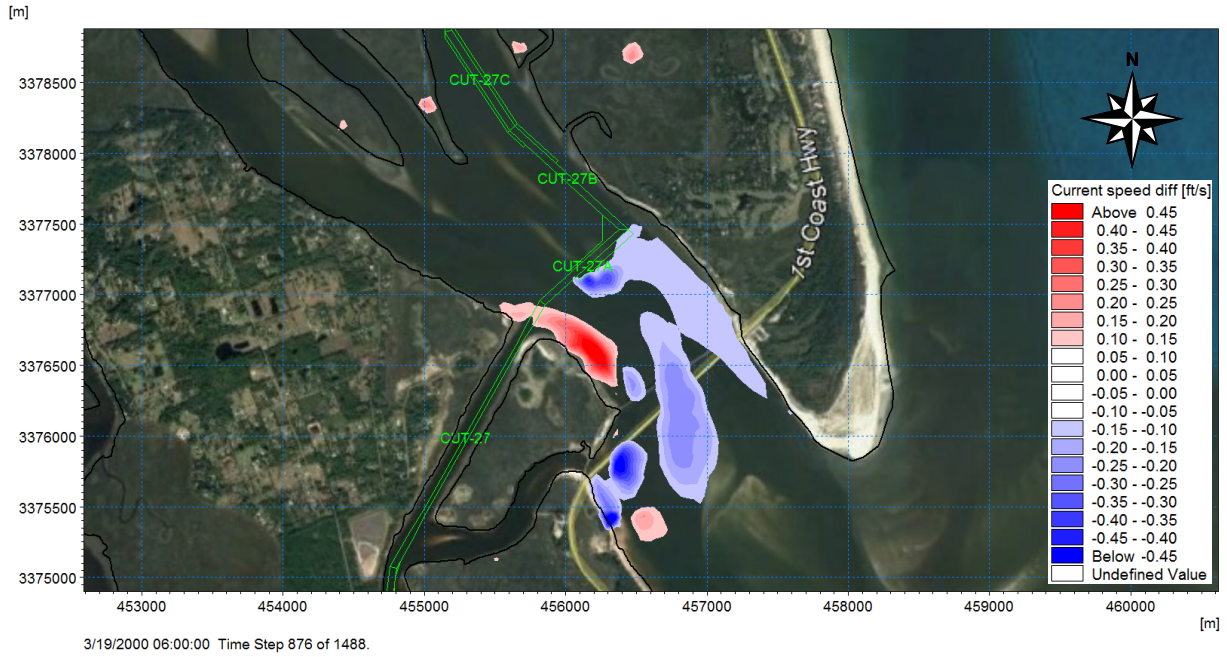


**Figure 4.13** Difference in Modeled Alternative B and Baseline Peak Flood Velocities



**Figure 4.14** Difference in Modeled Alternative B and Baseline Peak Ebb Velocities



**Figure 4.15** Difference in Modeled Alternative C and Baseline Peak Flood Velocities



**Figure 4.16** Difference in Modeled Alternative C and Baseline Peak Ebb Velocities



**Figure 4.17** Difference in Modeled Alternative D and Baseline Peak Flood Velocities



**Figure 4.18** Difference in Modeled Alternative D and Baseline Peak Ebb Velocities

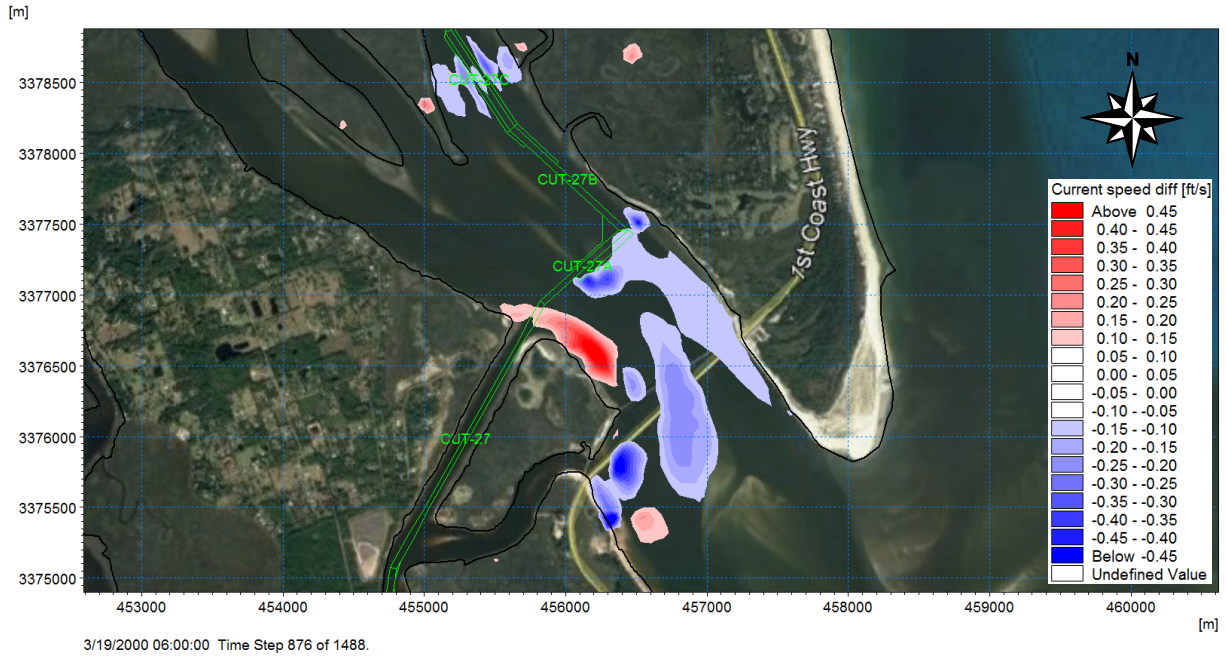


**Figure 4.19** Difference in Modeled Alternative E and Baseline Peak Flood Velocities

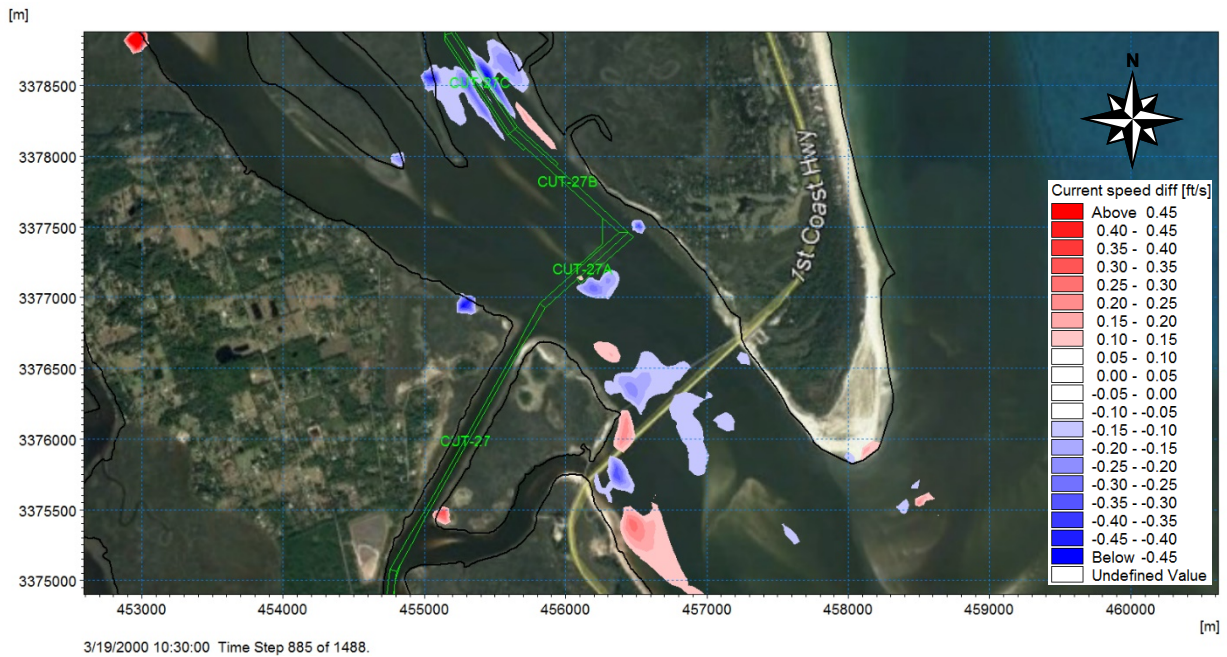


**Figure 4.20** Difference in Modeled Alternative E and Baseline Peak Ebb Velocities



**Figure 4.21** Difference in Modeled Alternative F and Baseline Peak Flood Velocities



**Figure 4.22** Difference in Modeled Alternative F and Baseline Peak Ebb Velocities

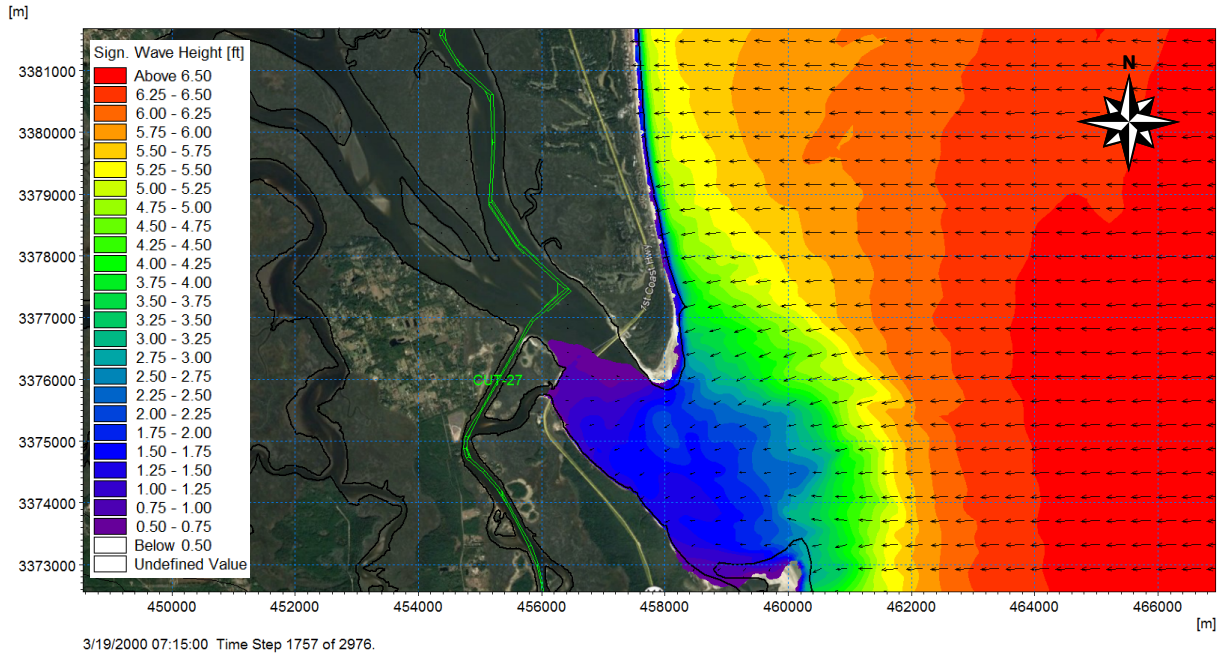


**Figure 4.23** Baseline Modeled Peak Wave Heights and Directions

## **5.0 DREDGING, DESIGN, AND PERMITTING CONSIDERATIONS**

This section provides brief description of recommendation for dredging methods, engineering design, and permitting.

### **5.1 Dredging Method**

Previous dredging events in the Sawpit Creek area and AIWW have used cutterhead suction dredge. Unless new geotechnical data suggests otherwise, this study recommends cutterhead suction dredge for the basin construction.

### **5.2 Engineering Design and Submerged Aquatic Vegetation Survey Considerations**

Preliminary engineering design will require an updated bathymetric survey that focuses at locations of the proposed basins to determine bed elevations changes since completion of the USACE-SAJ January – April 2019 bathymetric surveys along AIWW Cuts 24, 25, 26, 27, 27A, and 27C. The survey will consist of ground elevations at 100-foot intervals. The bathymetric survey can use multi-beam, single-beam, and/or hand-held RTK/GPS survey instruments as needed to collect survey data for deep-water areas as well as shallow shoaled areas. In areas deemed impractical for multi-beam sounding technology, the bathymetric survey can use a combination of single-beam sounding methods, RTK GPS, total station and/or standard poling techniques.

Following collection of detailed bathymetric data in the proposed sediment basin area, preliminary engineering design includes development of a three-dimensional AutoCAD-based digital terrain model of the project area. The digital terrain model can generate a dredge template that includes plan area, cross sections, and total required dredging volume by individual basins.

Preliminary engineering includes review of core boring data from nearby locations to learn likely subsurface soil layer characteristics. Final recommendations for dredging methods and final numerical modeling will require sediment characteristics near the locations of the proposed basins.

In support of permitting, preliminary engineering design also includes preparation of permit drawings for the various site elements. If appropriate, the permit set can include photo-based sheets depicting the project areas. The drawings will provide plan, cross section, and detail views of the proposed dredging project and the associated beach and/or upland disposal.

Prior to final engineering design, long-term modeling of the shoaling rates can provide better guidance on the long-term shoaling rates in the channels and basins. The long-term numerical modeling can better account for change in basin sediment trapping efficiency as the basin fills up and include more variance (seasonal flows and extreme surge events) in the driving forces for sediment transport, erosion, and deposition.

Preparers of engineering design should coordinate with FIND's designated environmental specialist subcontractor, as necessary, during the natural resources surveying process. Preliminary engineering design can provide FIND's subcontractor with an AutoCAD-based digital terrain model of the dredge template (plan area, cross sections, and total required dredging volume by individual basin cut) for the subcontractor's Uniform Mitigation Assessment Method (UMAM) and seagrass impact calculations, if necessary.

## 5.3 Permitting Considerations

### 5.3.1 Overview

The dredging project will require State (FDEP) and federal (USACE) authorizations. The project goal of reducing the annual maintenance dredging activity in the project area, the lack of submerged resources, the low level of watershed development, the ongoing dredging activity for maintenance of the AIWW channel, and established disposal options for dredged material (adjacent beaches or FIND Dredged Material Management areas) should simplify the permitting process.

A permit process begins with drafting separate state and federal applications. While there is overlap, the FDEP and USACE have different regulatory interests and the applications are focused on those interests. When the portions of the application known to be required are in first-draft format, meetings with the agencies are conducted to obtain guidance regarding project specific details and other information regarding the permitting process for the proposed project.

The FDEP has a clear written policy regarding review timelines. After receipt of an application package, the FDEP responds within 30 days with a request for additional information (RAI—most common for a project such as proposed basins construction) or notification that the application is complete and is in final processing. RAI letters include a timeline for response—typically 2 – 4 months. The applicant may request an extension of the timeline for a variety of reasons. Once the RAI process is complete, the state has final processing steps that may require an additional 30 – 90 days.

The federal permit application review process is not clock-constrained and cannot be accurately predicted. It is at least partially dependent upon the agency workload and the level of National Environmental Policy Act (NEPA) consultation and documentation required. The federal authorization cannot be processed without the FDEP permit (which fills some of the USACE Clean Water Act requirements) and without completion of consultation with sister agencies. It may require as much as a year or more to obtain a federal permit. Notably, if the USACE constructs the project, no Federal permit will be required, however, a full environmental assessment will need to be performed.

### 5.3.2 Permit Application

Permit applications include preparation and submittal to FDEP and USACE of application forms from each agency with associated attachments detailing the summary information provided in the completed forms and a request for maintenance dredging exemption. Because the basin construction sites are not part of already permitted footprints, this study expects that the FDEP will require an individual Environmental Resources Permit and the USACE will require standard “Dredge and Fill” permit; however, each lead agency will identify the appropriate authorization. These permits require a relatively high level of detail (compared to other authorizations from these agencies) because the site has not previously been permitted for this (or other) activity.

The FDEP application will include several sections for the general project information, supplemental information, and authorization to use state-owned submerged land. For the proposed project, the modeling reports, sediment quality reports, natural resources report, signed and sealed plan drawings, and other technical information will be provided as attachments to the summaries of that information provided in the forms.

The USACE application will include the information provided in the FDEP application, but will also include an alternatives analysis, an assessment of federally protected resources (e.g. essential fish habitat, listed species, and managed species) that may occur in the project area. Depending on the requirements the agency identifies of a particular authorization, the USACE may also offer the application the option of drafting documents that will make the agency task completion more efficient; in particular a cumulative impact analysis, but other documents (such as a formal environmental assessment) may also be requested. The applicant has no formal responsibility to provide these documents, but may make such decisions based on the available budget and the potential difference that drafting such documents may make in the permit application timeline.

### *5.3.3 Pre-Application Meetings*

Once the basic elements of the permit applications have been developed, pre-application meetings with the FDEP and the USACE are necessary to introduce the project, identify an expected permitting approach and authorization format and level of information required, and discuss foreseeable permit application issues. The applicant will solicit agency recommendations concerning the content and format of the application materials and obtain guidance from each lead agency necessary to provide a complete permit applications packages for review. During the meeting with the USACE, the agency can identify what regional or programmatic permits can be used to streamline the permitting process and provide an overview of the NEPA consultation process they will undertake.

FIND's agent can prepare a preapplication package, coordinate the meeting schedules, and write meeting summaries. FIND's participation in the meetings is encouraged to provide the agencies with the best project understanding and most complete identification of applicant issues and constraints.

### *5.3.4 Responses to request for Additional Information (RAI)*

After initial review of the maintenance exemption and general permit verification requests, the FDEP and USACE will likely issue one or more RAIs requesting additional information necessary for the agency to have an application package sufficiently complete to issue a public comment notice. An RAI typically contains questions that require additional clarification or other information regarding the proposed work. The technical staff that prepared the initial application provide all RAI responses to the permit applicant for review before submittal to the FDEP and USACE. Depending on the question, the technical staff may also strategize with the applicant to identify the best response for the applicant.

Once the USACE has received public comments provided during the public comment period and subsequently during NEPA consultations with sister federal agencies, the USACE may receive information request and pass those requests along to the applicant for responses.

## **5.4 Other Considerations**

The South Amelia Shore Stabilization Association and Nassau County have applied for an FDEP Joint Coastal Permit and USACE Department of the Army Permit to dredge as much as 4.140 million cy from a primary and supplemental borrow areas for beach nourishment along the southern shoreline of Amelia Island from monuments R-59 to R-79. The borrow areas lie on the Nassau Sound ebb shoal along the southern 3.6 mi of the Amelia Island shoreline. The 200-acre primary borrow area and 138-acre supplemental borrow area are estimated to yield 2.870 million cy and 2.160 million cy, respectively. Olsen Associates, Inc. (Olsen Associates, 2019) expects the primary borrow area to shoal during the first few years of the beach nourishment interval of 9 – 10 years.

If these borrow areas on the Nassau Sound ebb shoal are constructed, the engineering design of the proposed Sawpit Creek area sediment basins should take into consideration the existence of these borrow areas.

## 6.0 CONCLUSIONS AND RECOMMENDATIONS

This study successfully validated a two-dimensional hydrodynamic model through comparisons of modeled water level and flow velocity at select locations in the project area. This study also developed a two-dimensional wave model and applied wave model parameters recommended from literature to calculate wave-generated currents that mainly drive longshore transport. The study also developed a two-dimensional depth-averaged particle tracking model that used established data and equations in literature to estimate sediments properties, settling rate, and critical shear stress for erosion. The particle tracking model provided the means to locate sediment transport pathways, deposition areas, and proposed in-channel shoaling reduction sediment basins. This study also developed a two-dimensional sediment transport model to estimate total sediment transport from bed load and suspended sediment transport. The sediment transport model included a morphological model to estimate shoaling rates (deposition and erosion) in channels and proposed basins.

Comparisons of inshore morphological model results with observed historical sedimentation patterns shows the modeled sedimentation patterns are consistent with observed historical sedimentation patterns. These sedimentation patterns include (a) large deposition along Fort George River; (b) large sediment transport from the Nassau Sound ebb shoal through Nassau River, Amelia River, and the AIWW; (c) AIWW shoaling between Cut-24 to Cut-27M; and (d) very large shoaling rates at Cut-27A and Cut-27C. The general good agreement between modeled and observed sedimentation patterns at inshore and nearshore locations makes the sediment transport and morphological model validated to transport sediment from nearby inshore areas to the areas of interest near Sawpit Creek and the AIWW.

### 6.1 Conclusions

Historically, the USACE-SAJ conducts maintenance dredging at Cut-27A and nearby cuts on average once every six years to maintain the authorized AIWW navigation depth of -12 ft-MLLW. Comparisons of the model simulations for Baseline and the Alternatives A – F provide longer dredging intervals of 9 years (Alternative A), 11 years (Alternative B), 9 years (Alternative C), 10 years (Alternative D), 10 years (Alternative E), and 9 years (Alternative F). This study evaluated the Baseline and Alternatives A – F equivalent uniform annual cost using a project life of 45 – 55 years (i.e., multiples of dredging intervals); the new federal annual interest rate of 2.750% for 2020; and an assumption that the next dredging event occurs in 2024. Compared to the Baseline maintenance dredging annual cost (i.e., the current annualized dredging cost), the cost analysis ranks Alternative A first for offering the largest savings of \$788,000/year; Alternative F second for offering savings of \$720,000/year; Alternative C third for offering savings of \$569,000/year; Alternative D fourth for offering savings of \$491,000/year; Alternative B fifth for offering savings of \$294,000/year; and Alternative E sixth for offering small savings of \$14,000/year. This study does not recommend Alternative E for further consideration because it provides only a small estimated annual savings which is well within uncertainties in dredge volume calculations and dredge maintenance cost estimation.

Model results show Alternative A would likely have the least hydraulic impact; Alternative F will likely have the second least hydraulic impact; Alternative C will likely have the third least hydraulic impact; and Alternative D will likely have the fourth least hydraulic impact. Alternatives B and E can divert more flood flows from the north tidal channel to the south tidal channel and will likely impact larger areas. Model results show Alternative B will likely have the fifth least hydraulic impact and Alternative E will likely have the largest hydraulic impact among the alternatives. However, for all

alternatives, velocity differences from Baseline conditions are too small to affect navigation safety and too small to increase shoreline erosion.

Table 6.1 summarizes the rankings of Alternatives A – F based on their performance to reduce in-channel shoaling, cost savings, and extent of hydraulic impact. Alternatives with small impacted areas were ranked high. Overall, this study selects Alternative F over Alternative A because, unlike Alternative A, it reduces in-channel shoaling not only at Cut-27A but also at Cut-27C.

**Table 6.1** Summary of Ranking of Alternatives for In-Channel Shoaling Reduction

Alternatives	Basis for Ranking			Overall Ranking
	Performance	Cost Savings	Hydraulic Impact	
Alternative F	3	2	2	1
Alternative A	4	1	1	2
Alternative D	1	4	4	3
Alternative C	5	3	3	4
Alternative B	6	5	5	5
Alternative E	2	6	6	6

## 6.2 Recommendations

Based on the model simulations performed and analyses of model results, this study makes the below recommendations.

1. The conclusions in this report support proceeding with the permitting, engineering, and design of Basins 4, 5, and 6 of Alternative F.
2. Design of Basins 4, 5, and 6 should include finding more efficient in-channel shoaling-reduction performance through adjustments of basin sizes.
3. The engineering design for the final channel and basin modifications should evaluate long-term (e.g., year-long) shoaling rate variation for better estimation of the variation of the sediment trapping performance of channels and basins and to better account for more potential variations of waves and water levels.
4. The engineering design should also account for the construction of future borrow areas on the Nassau Sound ebb shoal that maybe constructed to provide beach material for the Amelia Island southern shoreline beach nourishment.
5. Future bathymetric surveys should include the areas of Basins 4, 5, and 6 to establish baseline shoaling rates at these locations.

## REFERENCES

Berenbrock, C. and Tranmer, A.W. 2008. *Simulation of Flow, Sediment Transport, and Sediment Mobility of the Lower Coeur d'Alene River, Idaho*, U.S. Geological Survey Scientific Investigations Report 2008-5093, 164 p.

Danish Hydraulic Institute (DHI). 2019. *MIKE 21 Flow Model FM Hydrodynamic Module User Guide*. Hørsholm, Denmark.

Olsen Associates, Inc. 2019. *Hydrodynamics and Sediment Transport Analyses with Delft3D, Phase II Report, Alternatives*.

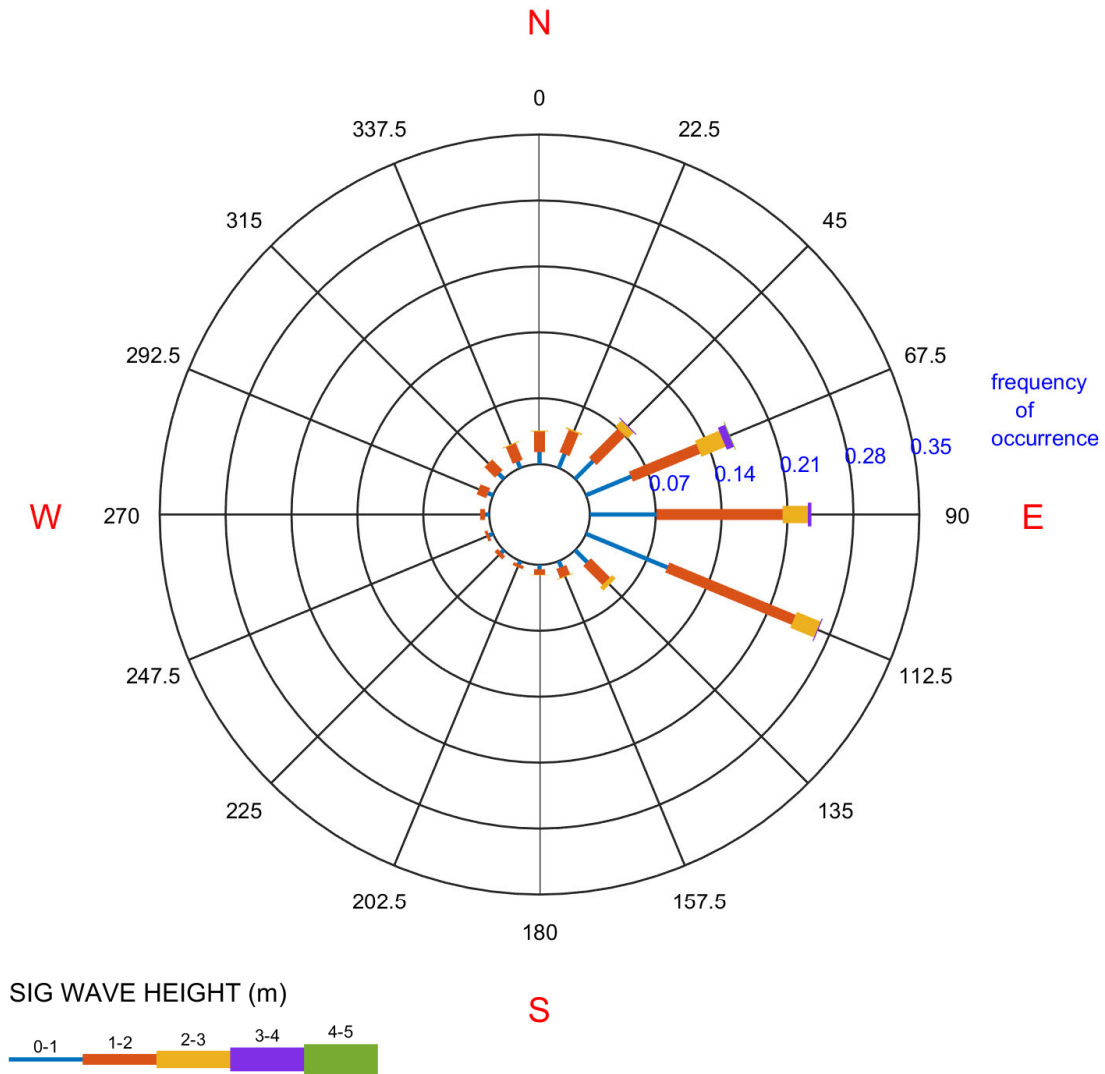
**APPENDIX A**

**WIS Stations 63402 Monthly Hindcasted Wave Rose for 1980 – 2017**



Atlantic WIS Station 63402  
ALL Jans: 1980 - 2017  
Long: -81.08° Lat: 30.58° Depth: N/A m  
Total Obs : 28271

**WAVE ROSE**



US Army Engineer Research & Development Center

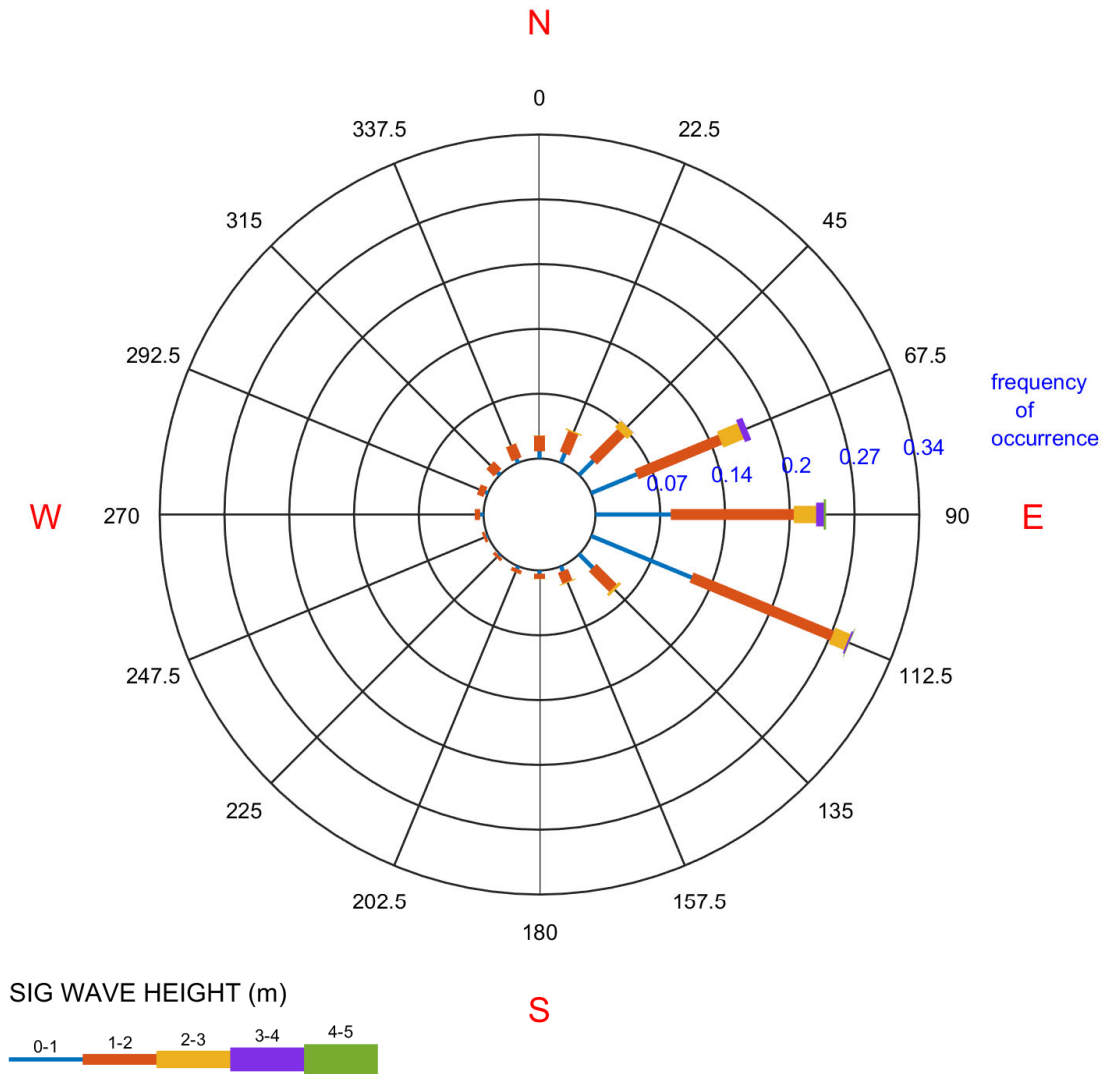
ST63402\_v03

**Figure A.1** Hindcasted Wave Rose at WIS Station 63402 for January (1980 – 2017)  
(Source: U.S. Army Engineer Research and Development Center)



Atlantic WIS Station 63402  
ALL Febs: 1980 - 2017  
Long: -81.08° Lat: 30.58° Depth: N/A m  
Total Obs : 25776

**WAVE ROSE**



US Army Engineer Research & Development Center

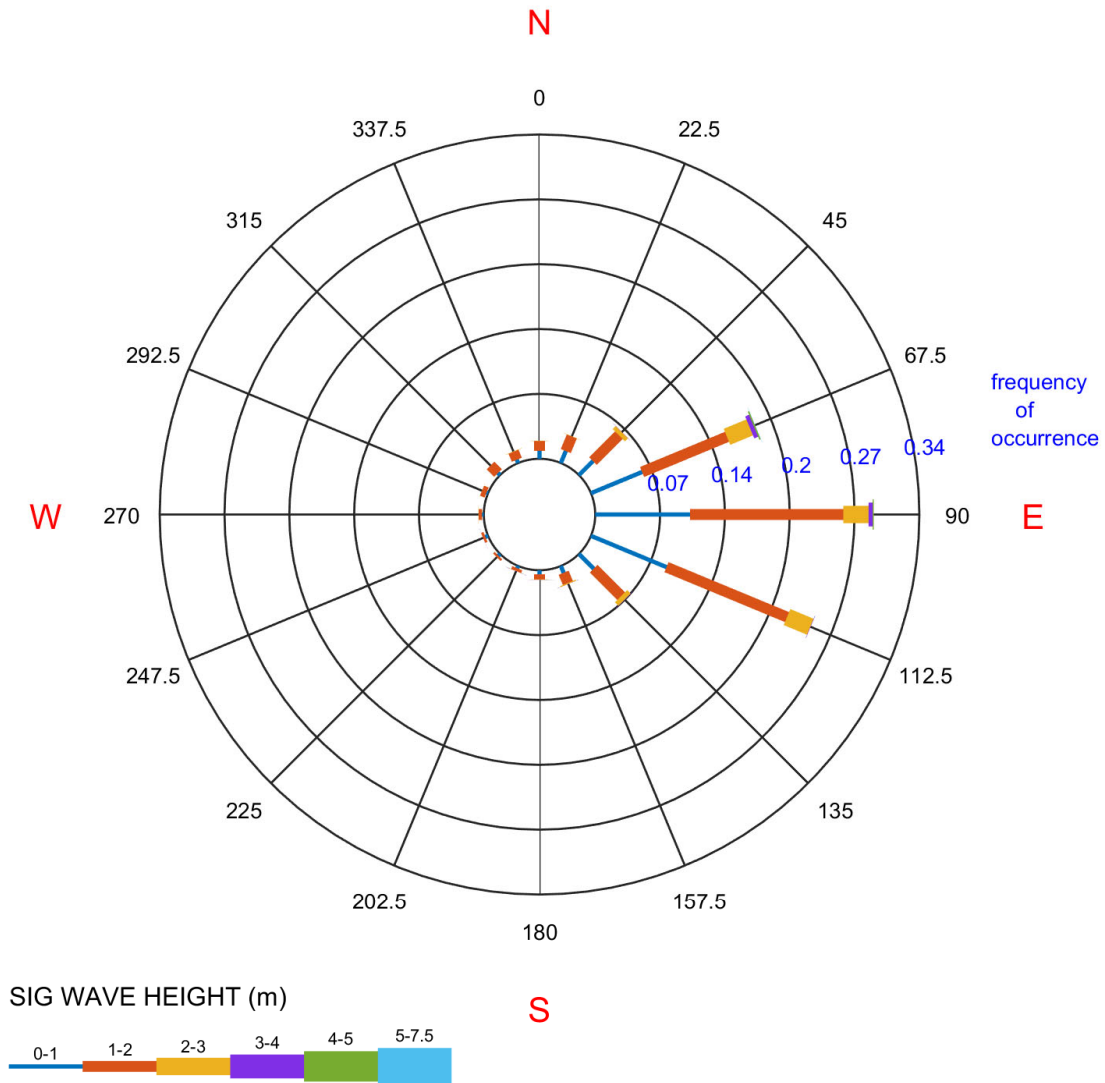
ST63402\_v03

**Figure A.2** Hindcasted Wave Rose at WIS Station 63402 for February (1980 – 2017)  
(Source: U.S. Army Engineer Research and Development Center)



Atlantic WIS Station 63402  
ALL Mars: 1980 - 2017  
Long: -81.08° Lat: 30.58° Depth: N/A m  
Total Obs : 28272

WAVE ROSE



US Army Engineer Research & Development Center

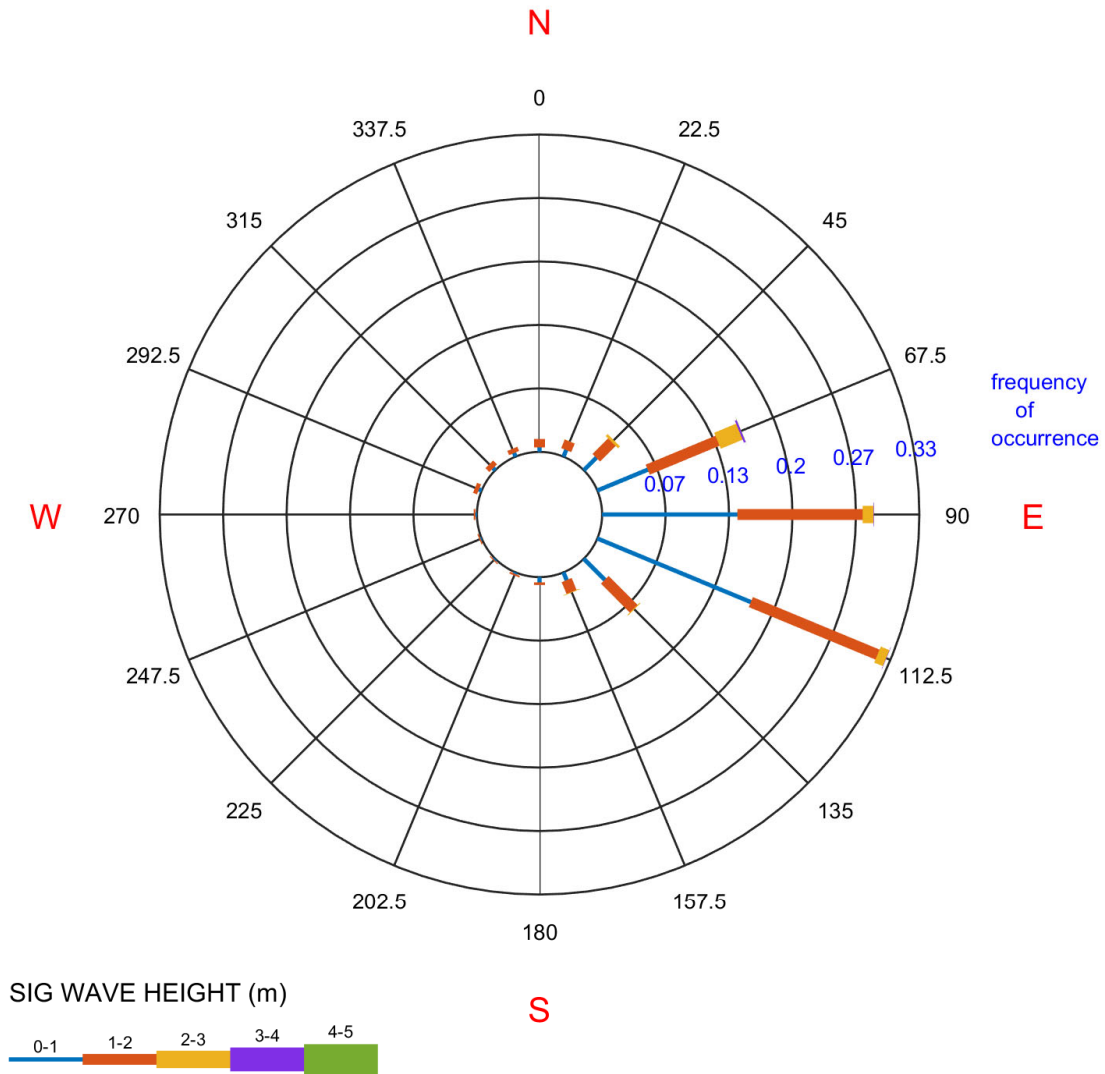
ST63402\_v03

Figure A.3 Hindcasted Wave Rose at WIS Station 63402 for March (1980 – 2017)  
(Source: U.S. Army Engineer Research and Development Center)



Atlantic WIS Station 63402  
ALL Aprs: 1980 - 2017  
Long: -81.08° Lat: 30.58° Depth: N/A m  
Total Obs : 27360

**WAVE ROSE**



US Army Engineer Research & Development Center

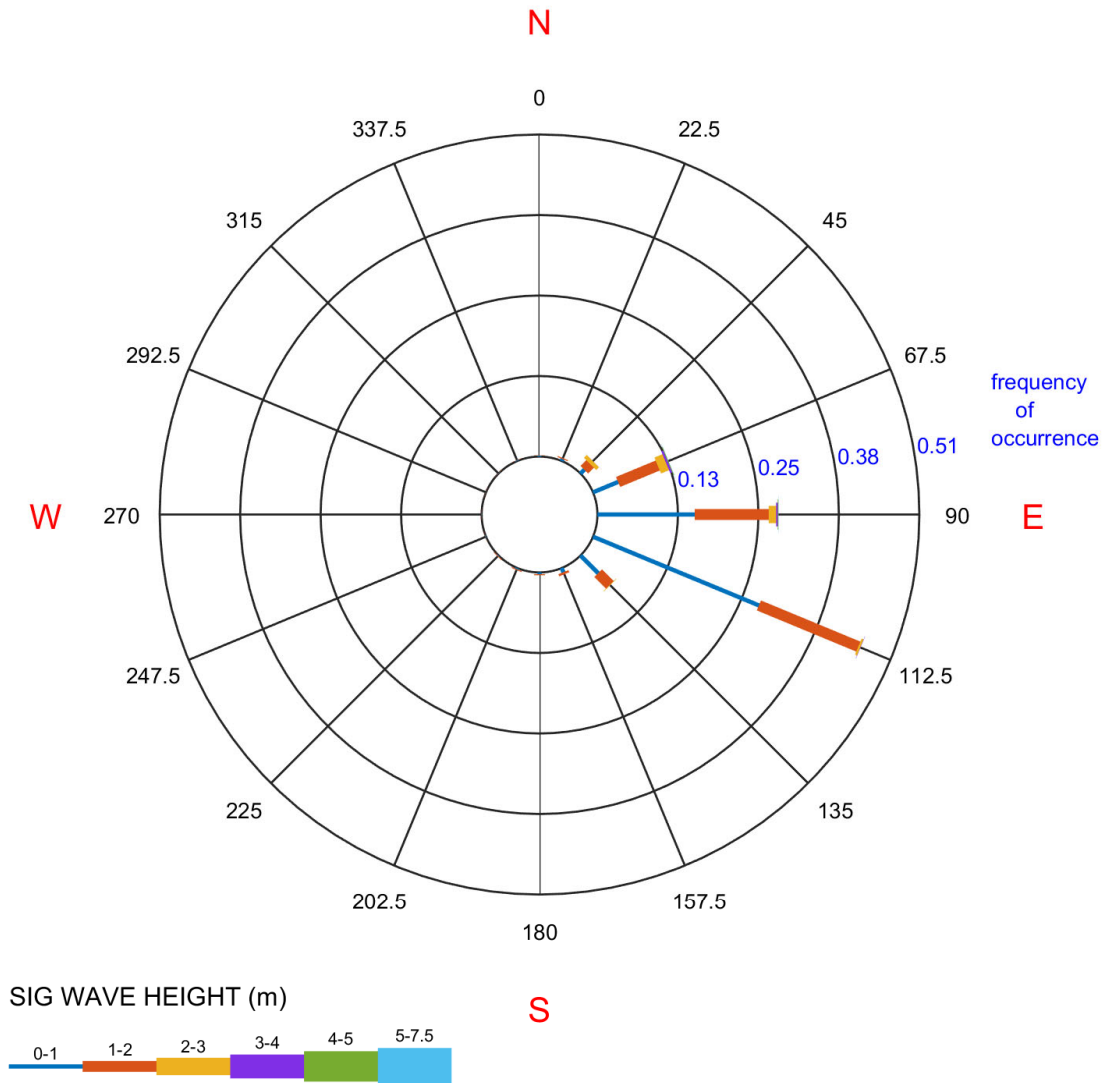
ST63402\_v03

**Figure A.4** Hindcasted Wave Rose at WIS Station 63402 for April (1980 – 2017)  
(Source: U.S. Army Engineer Research and Development Center)



Atlantic WIS Station 63402  
ALL Mays: 1980 - 2017  
Long: -81.08° Lat: 30.58° Depth: N/A m  
Total Obs : 28272

**WAVE ROSE**



US Army Engineer Research & Development Center

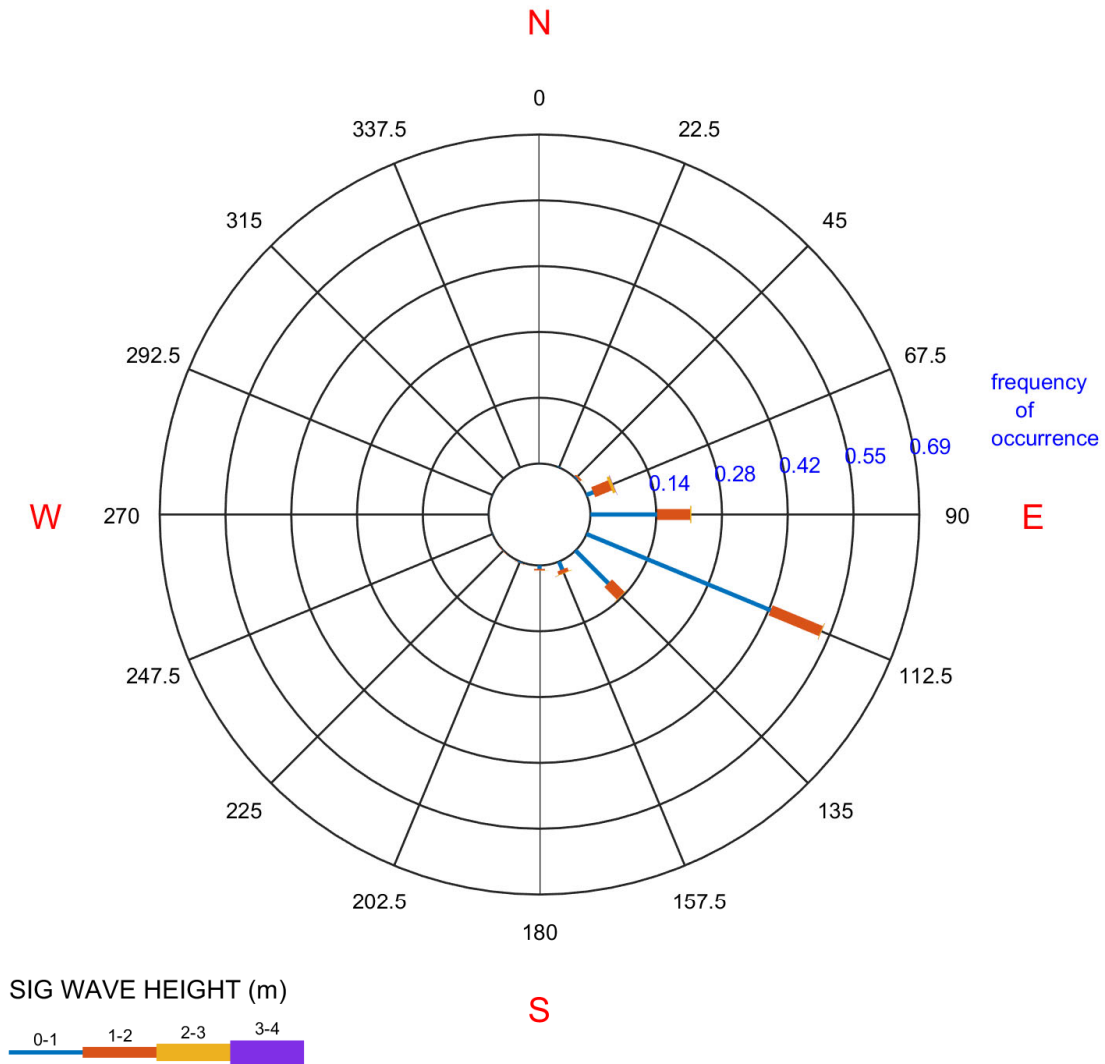
ST63402\_v03

**Figure A.5** Hindcasted Wave Rose at WIS Station 63402 for May (1980 – 2017)  
(Source: U.S. Army Engineer Research and Development Center)



Atlantic WIS Station 63402  
ALL Juns: 1980 - 2017  
Long: -81.08° Lat: 30.58° Depth: N/A m  
Total Obs : 27360

**WAVE ROSE**



US Army Engineer Research & Development Center

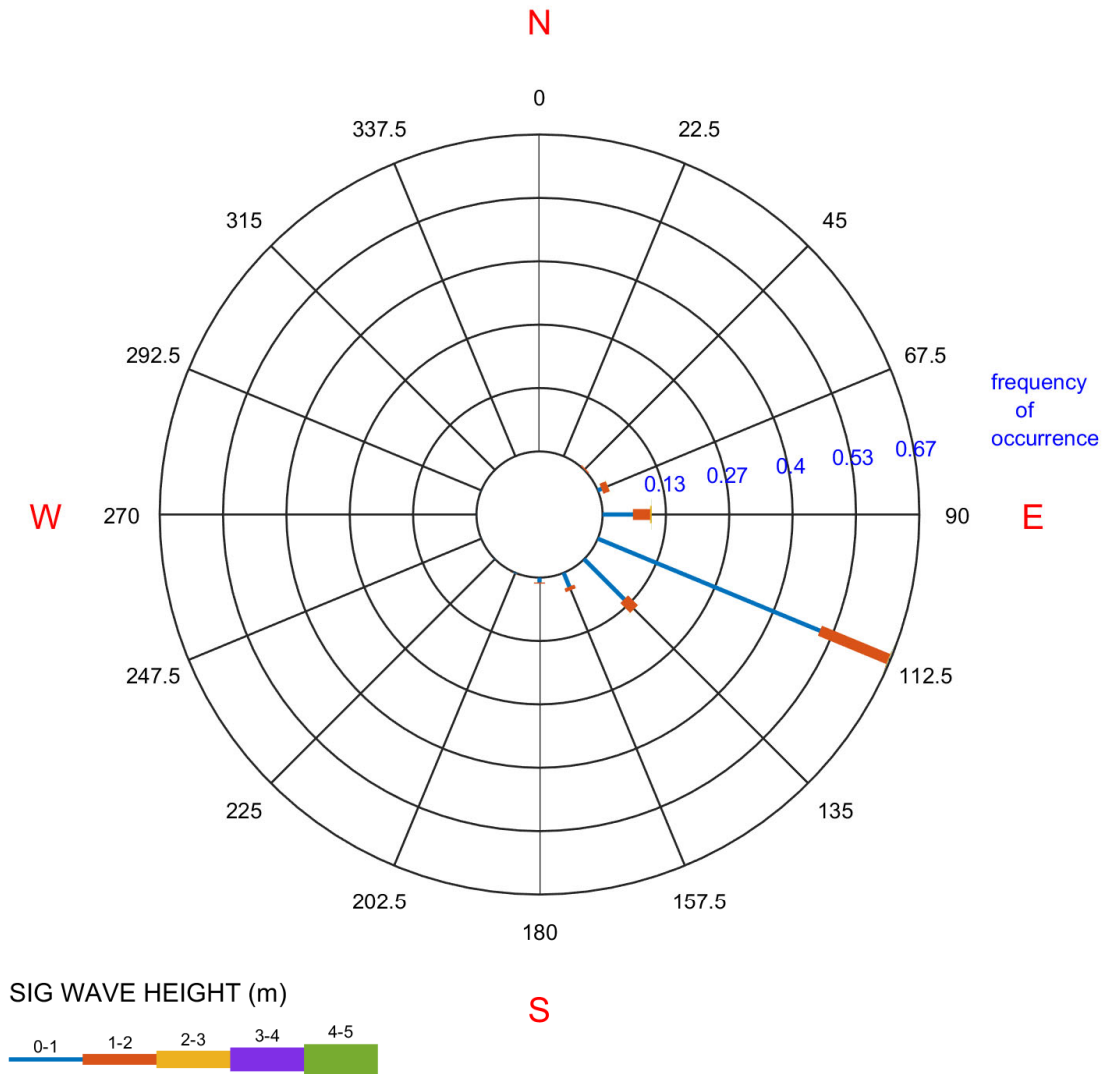
ST63402\_v03

**Figure A.6** Hindcasted Wave Rose at WIS Station 63402 for June (1980 – 2017)  
(Source: U.S. Army Engineer Research and Development Center)



Atlantic WIS Station 63402  
ALL Juls: 1980 - 2017  
Long: -81.08° Lat: 30.58° Depth: N/A m  
Total Obs : 28272

**WAVE ROSE**



US Army Engineer Research & Development Center

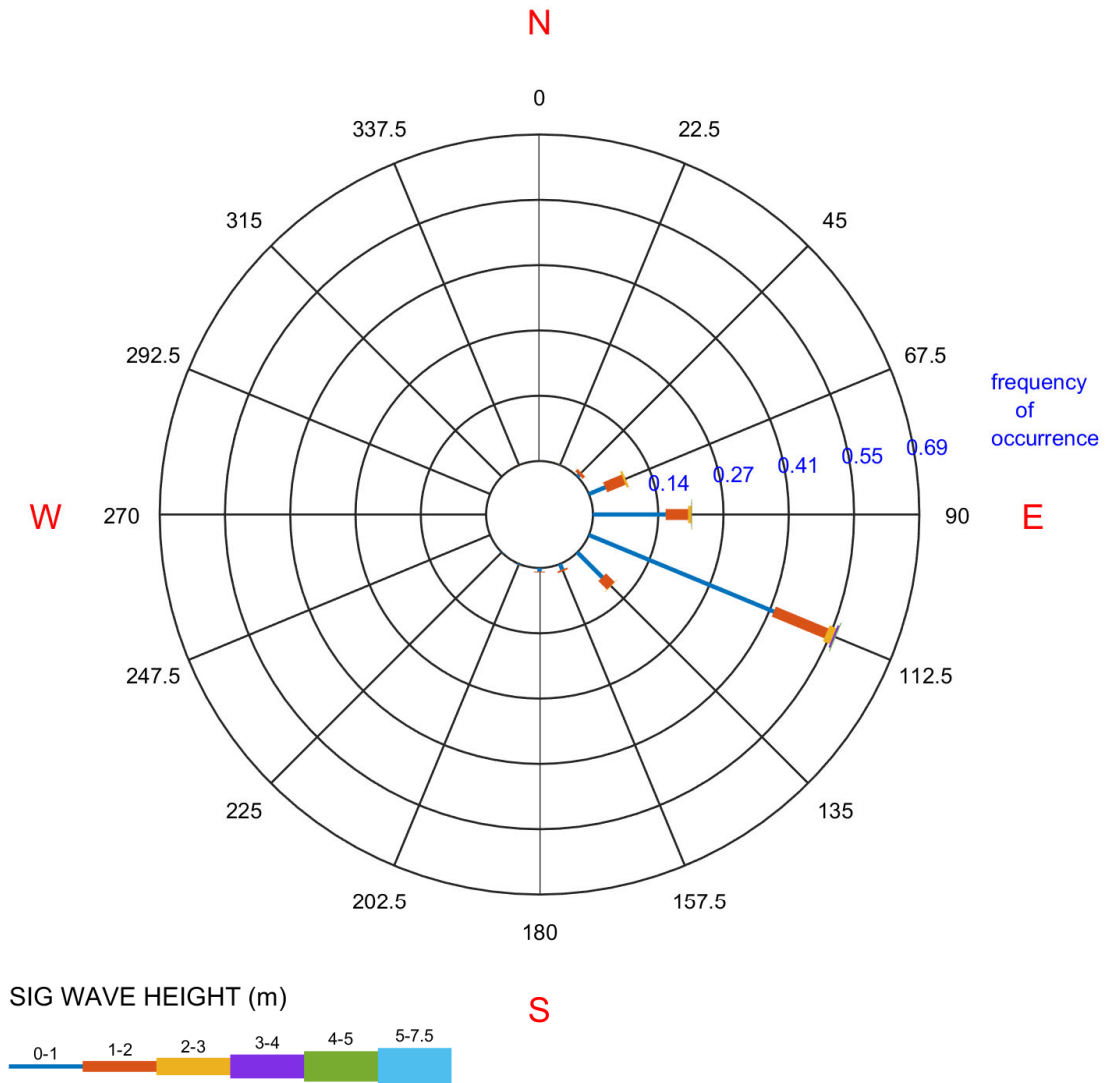
ST63402\_v03

**Figure A.7** Hindcasted Wave Rose at WIS Station 63402 for July (1980 – 2017)  
(Source: U.S. Army Engineer Research and Development Center)



Atlantic WIS Station 63402  
ALL Augs: 1980 - 2017  
Long: -81.08° Lat: 30.58° Depth: N/A m  
Total Obs : 28272

### WAVE ROSE



US Army Engineer Research & Development Center

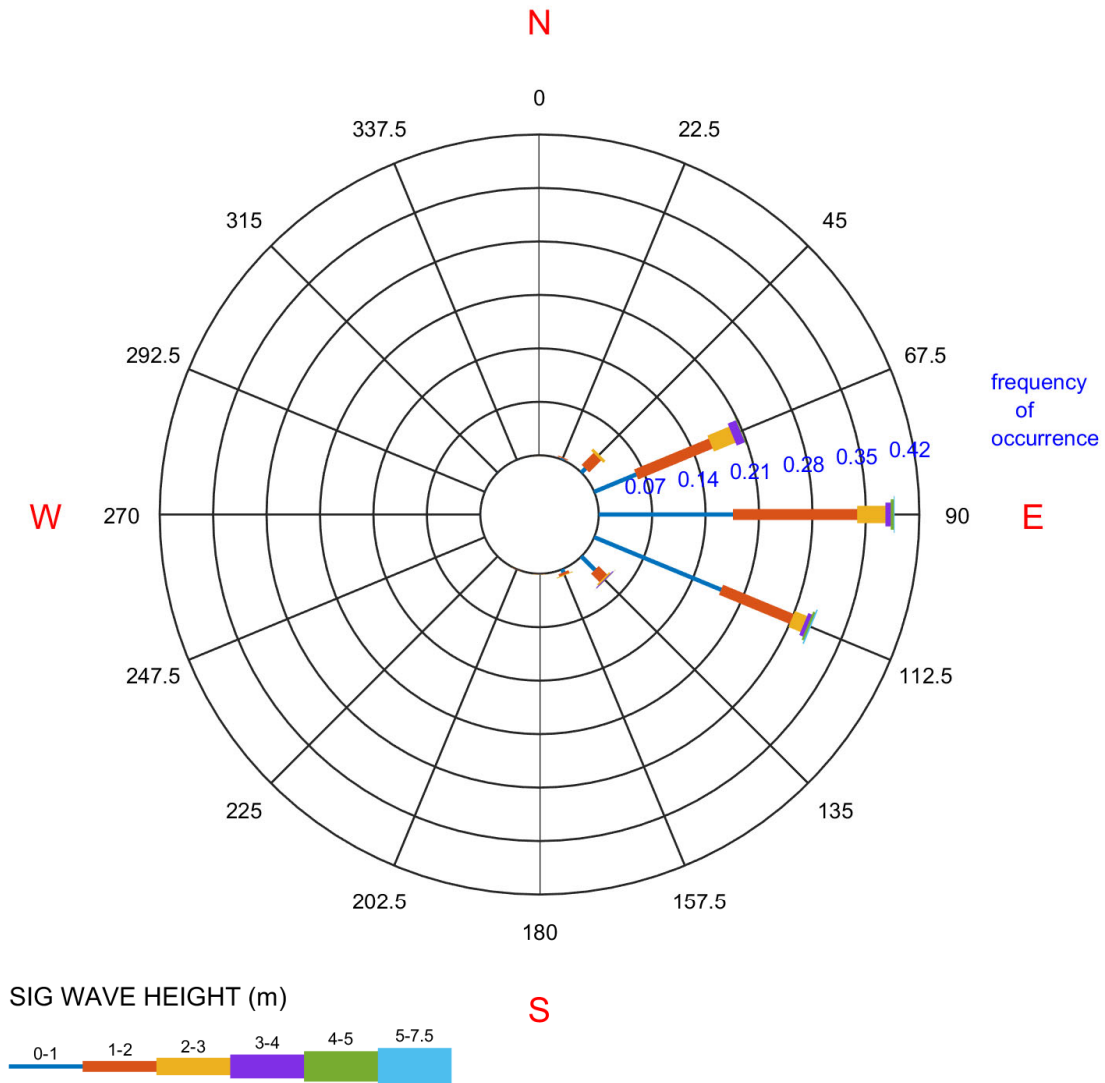
ST63402\_v03

**Figure A.8** Hindcasted Wave Rose at WIS Station 63402 for August (1980 – 2017)  
(Source: U.S. Army Engineer Research and Development Center)



Atlantic WIS Station 63402  
ALL Seps: 1980 - 2017  
Long: -81.08° Lat: 30.58° Depth: N/A m  
Total Obs : 27360

**WAVE ROSE**



US Army Engineer Research & Development Center

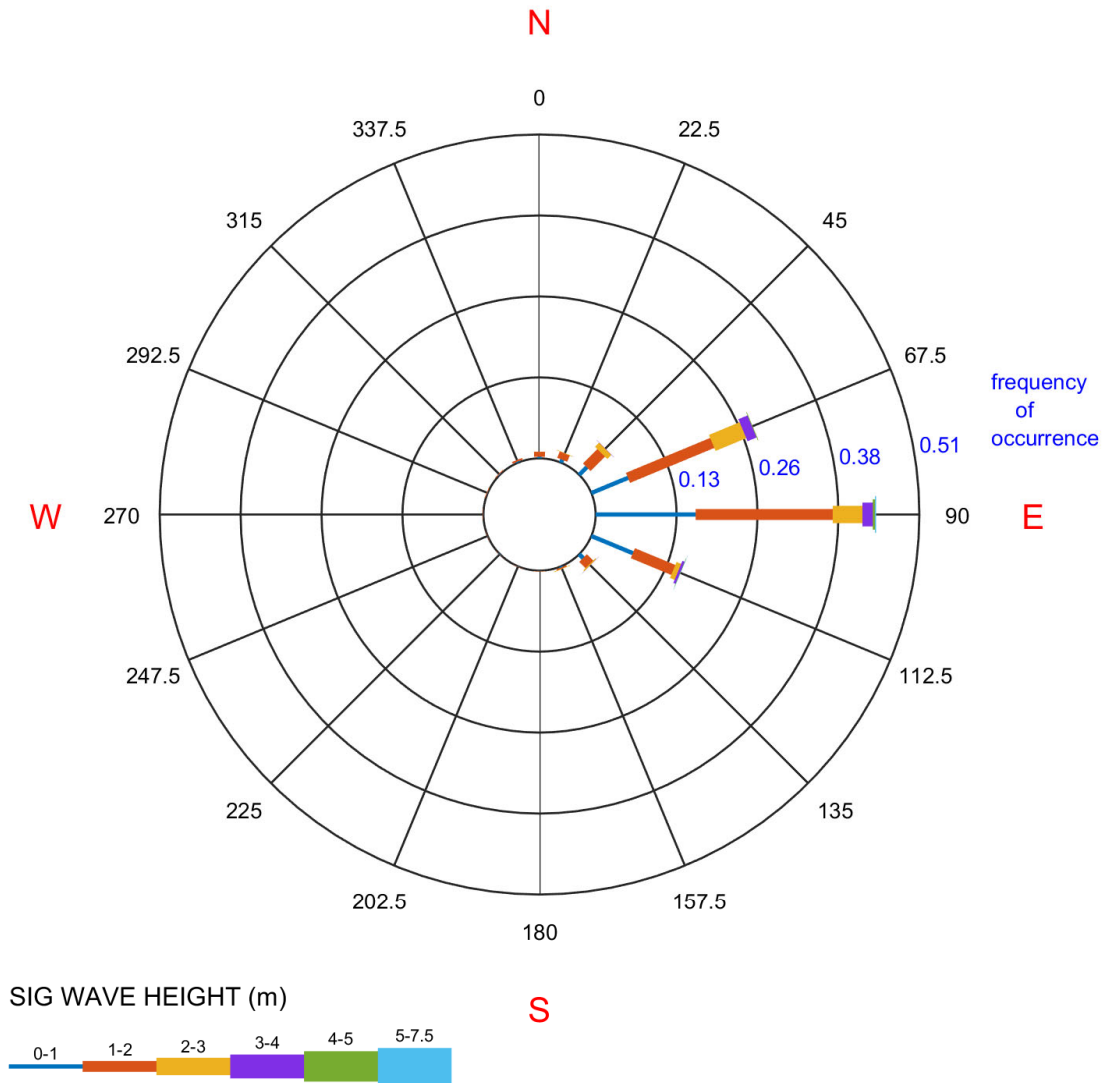
ST63402\_v03

**Figure A.9** Hindcasted Wave Rose at WIS Station 63402 for September (1980 – 2017)  
(Source: U.S. Army Engineer Research and Development Center)



Atlantic WIS Station 63402  
ALL Octs: 1980 - 2017  
Long: -81.08° Lat: 30.58° Depth: N/A m  
Total Obs : 28272

**WAVE ROSE**



US Army Engineer Research & Development Center

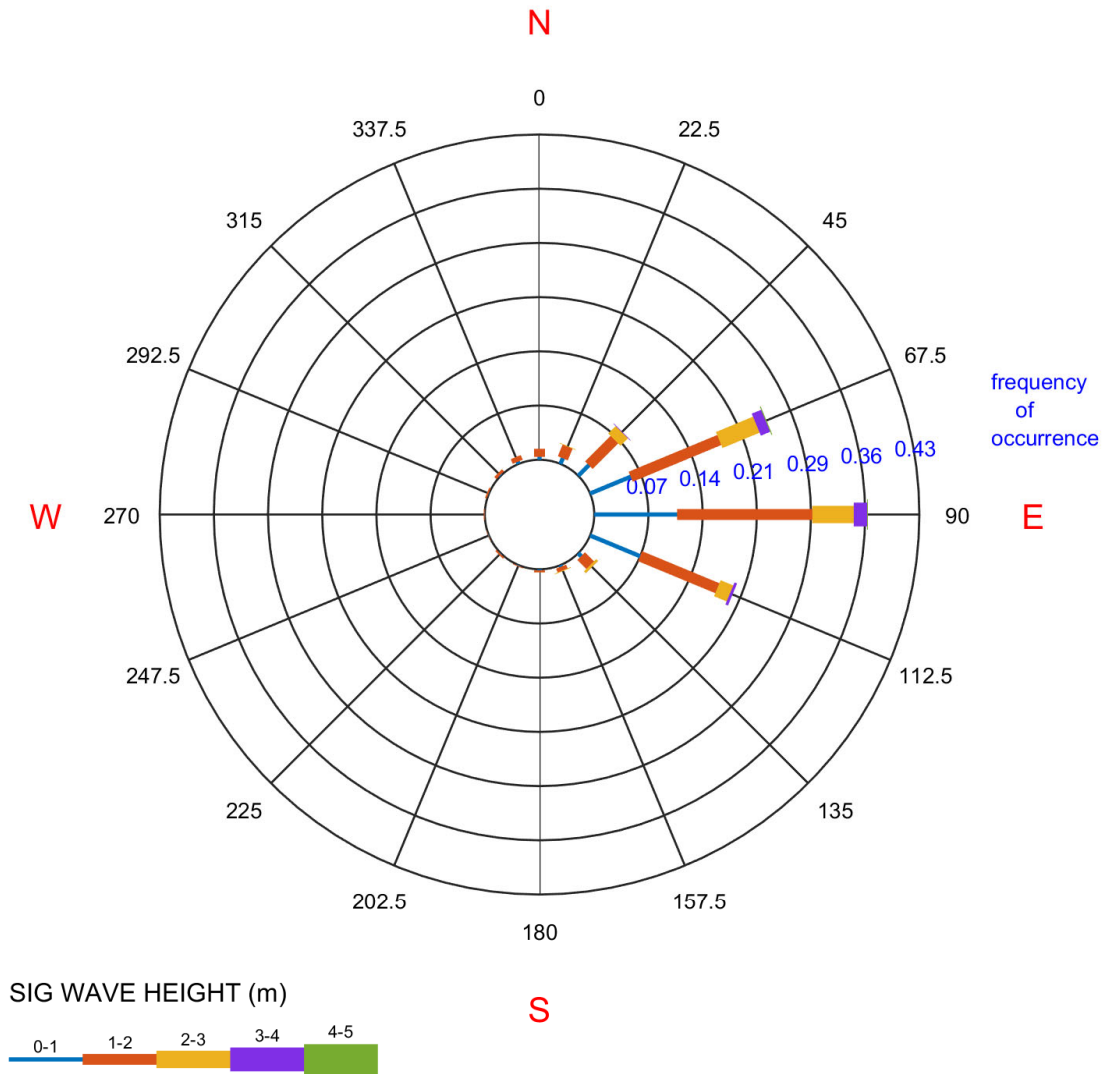
ST63402\_v03

**Figure A.10** Hindcasted Wave Rose at WIS Station 63402 for October (1980 – 2017)  
(Source: U.S. Army Engineer Research and Development Center)



Atlantic WIS Station 63402  
ALL Novs: 1980 - 2017  
Long: -81.08° Lat: 30.58° Depth: N/A m  
Total Obs : 27360

**WAVE ROSE**



US Army Engineer Research & Development Center

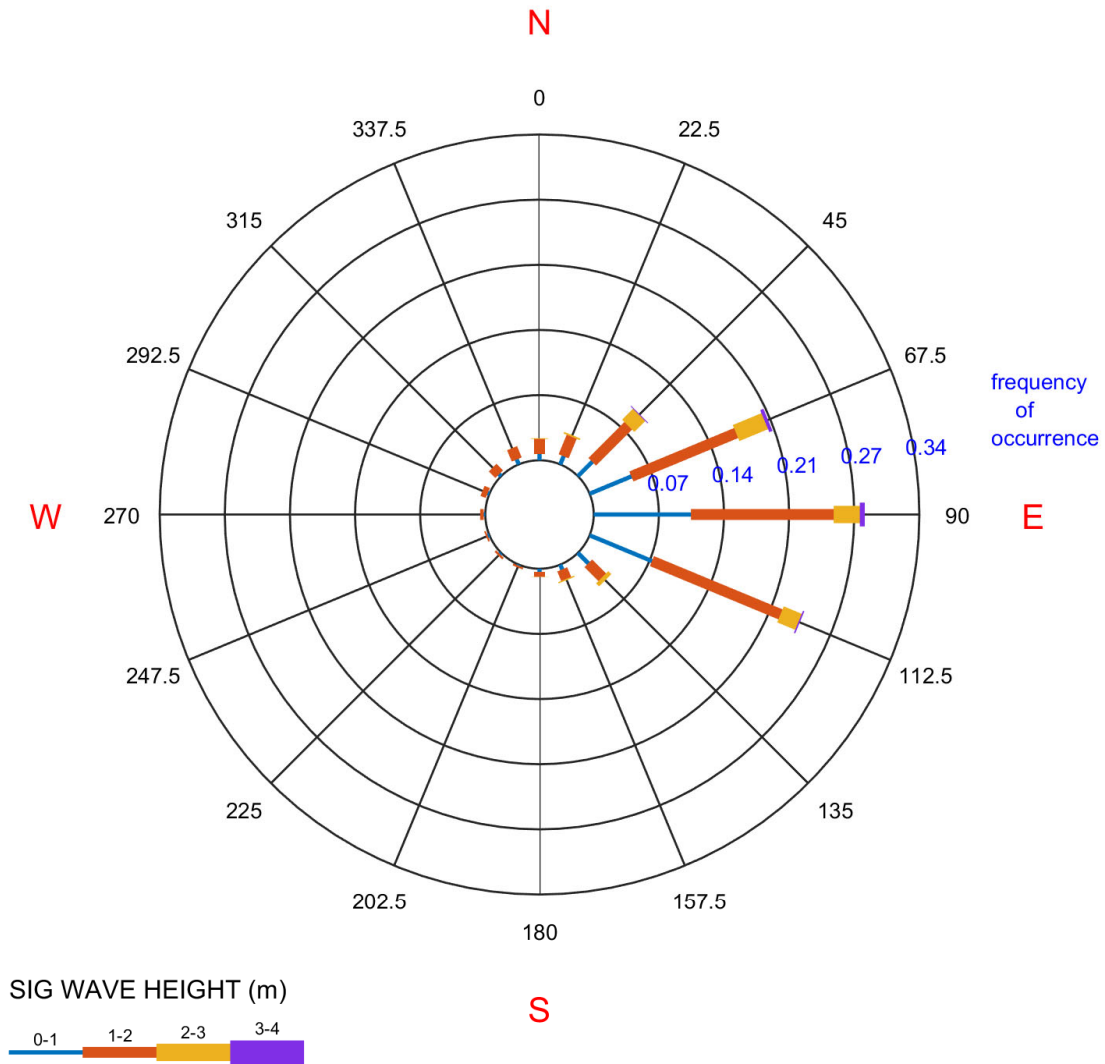
ST63402\_v03

**Figure A.11** Hindcasted Wave Rose at WIS Station 63402 for November (1980 – 2017)  
(Source: U.S. Army Engineer Research and Development Center)



Atlantic WIS Station 63402  
ALL Decs: 1980 - 2017  
Long: -81.08° Lat: 30.58° Depth: N/A m  
Total Obs : 28272

**WAVE ROSE**



US Army Engineer Research & Development Center

ST63402\_v03

**Figure A.12** Hindcasted Wave Rose at WIS Station 63402 for December (1980 – 2017)  
(Source: U.S. Army Engineer Research and Development Center)

**APPENDIX B**

**Measured Depth-Averaged Flow Velocity**

**Table B.1** Measured Depth-Averaged Flow Velocity at Stations V1E and V1W in May 2019

Station	Date/Time	Speed (fps)*	Direction (degree azimuth)
V1E	5/10/2019 8:01	0.61	339.3
V1E	5/10/2019 8:02	0.52	332.8
V1E	5/10/2019 8:03	0.57	325.2
V1E	5/10/2019 8:04	0.37	335.2
V1E	5/10/2019 8:05	0.58	318.4
V1E	5/10/2019 8:06	0.61	325.3
V1E	5/10/2019 8:51	1.04	323.6
V1E	5/10/2019 8:52	0.96	328.6
V1E	5/10/2019 8:53	1.06	314.2
V1E	5/10/2019 8:54	1.03	319.1
V1E	5/10/2019 8:55	1.07	324.4
V1E	5/10/2019 8:56	1.17	320.5
V1E	5/10/2019 9:43	1.49	327.0
V1E	5/10/2019 9:44	1.52	335.6
V1E	5/10/2019 9:45	1.50	330.7
V1E	5/10/2019 9:46	1.70	331.2
V1E	5/10/2019 9:47	1.52	330.8
V1E	5/10/2019 10:57	1.34	326.2
V1E	5/10/2019 10:58	1.26	323.8
V1E	5/10/2019 10:59	1.08	326.0
V1E	5/10/2019 11:00	1.34	327.4
V1E	5/10/2019 11:01	1.23	327.9
V1E	5/10/2019 11:52	1.43	330.7
V1E	5/10/2019 11:53	1.46	339.8
V1E	5/10/2019 11:54	1.43	342.9
V1E	5/10/2019 11:55	1.43	334.4
V1E	5/10/2019 11:56	1.59	335.9
V1E	5/10/2019 13:11	0.27	302.8
V1E	5/10/2019 13:12	0.22	276.5
V1E	5/10/2019 13:13	0.19	271.4
V1E	5/10/2019 13:14	-0.30	266.7
V1E	5/10/2019 13:15	-0.27	253.3
V1E	5/10/2019 14:09	-0.78	149.6
V1E	5/10/2019 14:10	-0.84	132.0
V1E	5/10/2019 14:11	-0.88	186.3
V1E	5/10/2019 14:12	-0.87	188.0
V1E	5/10/2019 14:13	-1.17	174.9
V1E	5/10/2019 15:26	-0.81	128.0
V1E	5/10/2019 15:27	-0.94	166.5
V1E	5/10/2019 15:28	-0.87	157.2

V1E	5/10/2019 15:29	-0.84	125.3
V1E	5/10/2019 15:30	-0.89	108.5
V1E	5/17/2019 15:02	0.75	344.6
V1E	5/17/2019 15:03	-0.59	221.2
V1E	5/17/2019 15:04	0.94	281.0
V1E	5/17/2019 15:05	0.27	327.0
V1W	5/17/2019 8:47	-2.02	154.7
V1W	5/17/2019 8:48	-1.92	150.3
V1W	5/17/2019 8:49	-1.90	156.5
V1W	5/17/2019 8:50	-2.02	157.0
V1W	5/17/2019 8:51	-2.04	154.6
V1W	5/17/2019 8:52	-2.00	157.7
V1W	5/17/2019 9:44	-2.09	162.2
V1W	5/17/2019 9:45	-2.16	163.5
V1W	5/17/2019 9:46	-2.04	163.5
V1W	5/17/2019 9:47	-2.01	167.1
V1W	5/17/2019 9:48	-2.09	162.7
V1W	5/17/2019 9:49	-2.01	162.9
V1W	5/17/2019 10:33	-2.11	163.9
V1W	5/17/2019 10:34	-2.35	163.7
V1W	5/17/2019 10:35	-2.36	165.9
V1W	5/17/2019 10:36	-2.02	163.3
V1W	5/17/2019 10:37	-2.13	160.0
V1W	5/17/2019 10:38	-2.24	162.3
V1W	5/17/2019 10:39	-2.22	160.4
V1W	5/17/2019 11:56	-1.68	158.9
V1W	5/17/2019 11:57	-1.79	157.6
V1W	5/17/2019 11:58	-1.63	158.4
V1W	5/17/2019 11:59	-1.58	156.3
V1W	5/17/2019 12:00	-1.61	156.5
V1W	5/17/2019 12:01	-1.67	156.9
V1W	5/17/2019 12:50	-1.44	159.7
V1W	5/17/2019 12:51	-1.20	154.9
V1W	5/17/2019 12:52	-1.20	152.4
V1W	5/17/2019 12:53	-1.11	153.4
V1W	5/17/2019 12:54	-1.21	148.5
V1W	5/17/2019 12:55	-1.18	163.7
V1W	5/17/2019 12:56	-1.31	150.8

Note: \* Negative speed is southward.

**Table B.2** Measured Depth-Averaged Flow Velocity at Stations V2E and V2W in May 2019

Station	Date/Time	Speed (fps)	Direction (degree azimuth)
---------	-----------	-------------	----------------------------

V2E	5/17/2019 9:03	1.71	325.4
V2E	5/17/2019 9:04	1.66	321.6
V2E	5/17/2019 9:05	1.60	326.3
V2E	5/17/2019 9:06	1.72	327.4
V2E	5/17/2019 9:07	1.70	326.4
V2E	5/17/2019 9:08	1.60	320.5
V2E	5/17/2019 9:09	1.69	325.5
V2E	5/17/2019 9:59	2.37	325.6
V2E	5/17/2019 10:00	2.25	321.6
V2E	5/17/2019 10:01	2.35	323.4
V2E	5/17/2019 10:02	2.25	323.6
V2E	5/17/2019 10:03	2.29	321.4
V2E	5/17/2019 10:04	2.40	324.6
V2E	5/17/2019 10:49	2.30	328.5
V2E	5/17/2019 10:50	2.31	327.4
V2E	5/17/2019 10:51	2.11	323.5
V2E	5/17/2019 10:52	2.18	327.9
V2E	5/17/2019 10:53	2.09	323.8
V2E	5/17/2019 10:54	2.16	326.6
V2E	5/17/2019 10:55	1.95	319.4
V2E	5/17/2019 12:13	1.25	322.9
V2E	5/17/2019 12:14	1.22	327.9
V2E	5/17/2019 12:15	1.30	319.9
V2E	5/17/2019 12:16	1.03	326.8
V2E	5/17/2019 12:17	1.29	319.0
V2E	5/17/2019 12:18	1.20	320.6
V2E	5/17/2019 13:09	0.72	311.4
V2E	5/17/2019 13:10	0.76	318.1
V2E	5/17/2019 13:11	0.83	312.2
V2E	5/17/2019 13:12	0.76	317.7
V2E	5/17/2019 13:13	0.91	324.7
V2E	5/17/2019 13:14	0.70	316.3
V2E	5/17/2019 13:15	0.80	327.6
V2E	5/17/2019 14:28	0.14	285.7
V2E	5/17/2019 14:29	0.09	295.7
V2E	5/17/2019 14:30	0.07	282.0
V2E	5/17/2019 14:31	0.22	324.4
V2E	5/17/2019 14:32	-0.15	268.5
V2E	5/17/2019 14:33	0.26	327.4
V2E	5/17/2019 15:17	-0.53	153.4
V2E	5/17/2019 15:18	-0.65	149.8
V2E	5/17/2019 15:19	-0.83	155.7

V2E	5/17/2019 15:20	-0.45	165.4
V2E	5/17/2019 15:21	-0.58	166.2
V2E	5/17/2019 15:22	-0.60	161.2
V2W	5/17/2019 8:02	-0.38	115.9
V2W	5/17/2019 8:03	-0.48	126.7
V2W	5/17/2019 8:04	-0.47	128.4
V2W	5/17/2019 8:05	-0.35	120.1
V2W	5/17/2019 8:06	-0.42	118.1

Note: \* Negative speed is southward.

**Table B.3** Measured Depth-Averaged Flow Velocity at Stations V3E and V3W in May 2019

Station	Date/Time	Speed (fps)	Direction (degree azimuth)
V3E	5/10/2019 8:35	-0.19	170.0
V3E	5/10/2019 8:36	-0.41	185.6
V3E	5/10/2019 8:37	-0.27	253.9
V3E	5/10/2019 8:38	0.10	292.4
V3E	5/10/2019 8:39	-0.31	212.6
V3E	5/10/2019 9:22	-0.54	206.1
V3E	5/10/2019 9:23	-0.40	209.8
V3E	5/10/2019 9:24	-0.45	192.4
V3E	5/10/2019 9:25	-0.62	200.7
V3E	5/10/2019 9:26	-0.61	213.4
V3E	5/10/2019 13:47	-0.31	239.8
V3E	5/10/2019 13:48	-0.31	233.9
V3E	5/10/2019 13:49	-0.27	226.3
V3E	5/10/2019 13:50	-0.20	242.1
V3E	5/10/2019 13:51	-0.32	251.6
V3E	5/10/2019 15:07	1.30	3.1
V3E	5/10/2019 15:08	1.17	5.0
V3E	5/10/2019 15:09	1.22	359.0
V3E	5/10/2019 15:10	1.37	5.4
V3E	5/10/2019 15:11	1.32	4.1
V3E	5/10/2019 15:53	1.41	9.0
V3E	5/10/2019 15:54	1.49	8.5
V3E	5/10/2019 15:55	1.59	9.5
V3E	5/10/2019 15:56	1.49	9.7
V3E	5/10/2019 15:57	1.35	3.1
V3E	5/17/2019 9:20	1.24	7.6
V3E	5/17/2019 9:21	1.34	7.5
V3E	5/17/2019 9:22	1.30	3.5

V3E	5/17/2019 9:23	1.42	10.4
V3E	5/17/2019 9:24	1.24	7.1
V3E	5/17/2019 9:25	1.31	8.0
V3E	5/17/2019 10:14	2.10	10.0
V3E	5/17/2019 10:15	1.94	9.5
V3E	5/17/2019 10:16	1.81	9.4
V3E	5/17/2019 10:17	1.82	12.0
V3E	5/17/2019 10:18	1.71	10.5
V3E	5/17/2019 10:19	1.75	9.7
V3E	5/17/2019 11:05	1.49	5.2
V3E	5/17/2019 11:06	1.50	3.5
V3E	5/17/2019 11:07	1.49	4.0
V3E	5/17/2019 11:08	1.41	10.0
V3E	5/17/2019 11:09	1.32	11.2
V3E	5/17/2019 11:10	1.46	6.9
V3E	5/17/2019 12:27	1.21	0.5
V3E	5/17/2019 12:28	1.08	8.6
V3E	5/17/2019 12:29	1.10	5.7
V3E	5/17/2019 12:30	1.11	10.9
V3E	5/17/2019 12:31	0.95	6.3
V3E	5/17/2019 12:32	0.89	11.9
V3E	5/17/2019 13:26	0.61	359.7
V3E	5/17/2019 13:27	0.67	359.9
V3E	5/17/2019 13:28	0.67	352.6
V3E	5/17/2019 13:29	0.52	4.3
V3E	5/17/2019 13:30	0.67	8.2
V3E	5/17/2019 13:31	0.65	17.6
V3E	5/17/2019 14:41	0.38	358.5
V3E	5/17/2019 14:42	0.40	346.1
V3E	5/17/2019 14:43	0.39	349.2
V3E	5/17/2019 14:44	0.47	343.3
V3E	5/17/2019 14:45	0.48	353.8
V3E	5/17/2019 14:46	0.37	343.1
V3E	5/17/2019 15:33	-0.57	211.1
V3E	5/17/2019 15:34	-0.68	210.9
V3E	5/17/2019 15:35	-0.72	203.6
V3E	5/17/2019 15:36	-0.55	213.6
V3E	5/17/2019 15:37	-0.66	201.3
V3E	5/17/2019 15:38	-0.77	200.2
V3E	5/17/2019 15:39	-0.75	199.6
V3W	5/10/2019 10:20	-1.03	164.3
V3W	5/10/2019 10:21	-1.12	173.6

V3W	5/10/2019 10:22	-1.26	167.3
V3W	5/10/2019 10:23	-1.29	172.2
V3W	5/10/2019 10:24	-1.43	169.9
V3W	5/10/2019 11:32	-1.36	177.7
V3W	5/10/2019 11:33	-1.26	170.6
V3W	5/10/2019 11:34	-1.30	173.7
V3W	5/10/2019 11:35	-1.39	170.9
V3W	5/10/2019 11:36	-1.27	178.5
V3W	5/10/2019 12:40	-0.86	177.6
V3W	5/10/2019 12:41	-0.82	133.3
V3W	5/10/2019 12:42	-0.73	90.4
V3W	5/10/2019 12:43	-0.80	112.8
V3W	5/10/2019 12:44	-0.68	117.7
V3W	5/17/2019 8:26	-0.32	159.4
V3W	5/17/2019 8:27	-0.34	154.9
V3W	5/17/2019 8:28	-0.27	145.7
V3W	5/17/2019 8:29	-0.34	140.1
V3W	5/17/2019 8:30	-0.40	150.5
V3W	5/17/2019 8:31	-0.25	134.1
V3W	5/17/2019 8:32	-0.41	133.0

Note: \* Negative speed is southward.

**APPENDIX C**

**Coordinates of Proposed Basins Bottom Corners**

**Table C.1** Proposed Basins Bottom Corner Coordinates

Corner	Basin 1		Basin 2	
	North Latitude (°)	West Longitude (°)	North Latitude (°)	West Longitude (°)
1	30.510755	-81.453462	30.512500	-81.454539
2	30.511228	-81.453804	30.513179	-81.454967
3	30.511675	-81.454086	30.513715	-81.454835
4	30.512057	-81.454393	30.515042	-81.454049
5	30.512500	-81.454539	30.516421	-81.453652
6	30.512741	-81.454051	30.517383	-81.453615
7	30.513064	-81.453528	30.519113	-81.454522
8	30.513226	-81.452883	30.519367	-81.454069
9	30.513358	-81.452324	30.519698	-81.453715
10	30.512878	-81.452420	30.519661	-81.453073
11	30.512411	-81.452791	30.519703	-81.452513
12	30.512095	-81.453195	30.519324	-81.452188
13	30.511649	-81.452916	30.519294	-81.452738
14	30.511208	-81.452633	30.519335	-81.453383
15	30.512741	-81.454051	30.518989	-81.453659
16			30.518676	-81.453288
17			30.518573	-81.452717
18			30.518149	-81.452464
19			30.517699	-81.452285
20			30.516999	-81.451713
21			30.516025	-81.451782
22			30.515543	-81.451885
23			30.515066	-81.452028
24			30.513358	-81.452324
25			30.513064	-81.453528
Corner	Basin 3		Basin 4	
	North Latitude (°)	West Longitude (°)	North Latitude (°)	West Longitude (°)
1	30.519113	-81.454522	30.525109	-81.458612
2	30.520367	-81.455285	30.525718	-81.457837
3	30.521381	-81.456335	30.525447	-81.457552
4	30.522557	-81.454076	30.528432	-81.453678
5	30.520515	-81.452056	30.526035	-81.451480
6	30.519661	-81.453073	30.522634	-81.456286
7	30.519698	-81.453715		
8	30.519367	-81.454069		
Corner	Basin 5		Basin 6	

	North Latitude (°)	West Longitude (°)	North Latitude (°)	West Longitude (°)
1	30.525402	-81.458954	30.529192	-81.456330
2	30.526424	-81.460031	30.533488	-81.461931
3	30.529630	-81.455925	30.533595	-81.462247
4	30.527963	-81.455922	30.533858	-81.462292
5	30.526126	-81.458263	30.534760	-81.463405
6	30.526027	-81.458160	30.539300	-81.466933
7			30.540043	-81.467507
8			30.540802	-81.467968
9			30.540889	-81.467622
10			30.534870	-81.462992
11			30.533946	-81.461763
12			30.534076	-81.461621
13			30.529630	-81.455925
Corner	Basin 7			
	North Latitude (°)	West Longitude (°)		
1	30.528461	-81.453716		
2	30.532910	-81.459414		
3	30.533041	-81.459278		
4	30.535410	-81.462262		
5	30.541712	-81.467110		
6	30.541950	-81.466879		
7	30.541867	-81.466632		
8	30.541617	-81.466569		
9	30.541428	-81.466364		
10	30.537938	-81.463675		
11	30.535727	-81.461981		
12	30.535507	-81.461777		
13	30.533632	-81.459274		
14	30.533200	-81.458871		
15	30.532956	-81.458801		
16	30.532822	-81.458548		
17	30.531585	-81.457198		
18	30.531385	-81.456440		
19	30.530688	-81.455460		
20	30.530525	-81.455035		
21	30.530264	-81.454750		
22	30.529925	-81.454641		
23	30.529748	-81.454315		
24	30.529159	-81.453278		

25	30.528830	-81.453148		
----	-----------	------------	--	--